Division of Pharmaceutical Chemistry and Technology
Faculty of Pharmacy
University of Helsinki
Finland

Effect of Surface Chemistry on the Immune Responses and Cellular Interactions of Porous Silicon Nanoparticles

by

Mohammad-Ali Shahbazi

ACADEMIC DISSERTATION

To be presented, with the permission of the Faculty of Pharmacy of the University of Helsinki, for public examination in Lecture Hall 2 at B-building (Latokartanonkaari 7, Helsinki), on February 13th 2015, at 12:00 noon.

Helsinki 2015

Supervisors

Docent Dr. Hélder A. Santos
Division of Pharmaceutical Chemistry and Technology
Faculty of Pharmacy
University of Helsinki
Finland

Professor and Dean Dr. Jouni Hirvonen
Division of Pharmaceutical Chemistry and Technology
Faculty of Pharmacy
University of Helsinki
Finland

Reviewers

Docent Dr. Jessica Rosenholm
Laboratory for Physical Chemistry
Åbo Akademi University
Finland

Professor Dr. Ennio Tasciotti
Department of Nanomedicine
Houston Methodist Research Institute
USA

Opponent

Professor Dr. Ijeoma Uchegbu
University College of London
School of Pharmacy
UK

ISBN 978-951-51-0555-4 (Paperback)
ISBN 978-951-51-0556-1 (PDF)
ISSN

Helsinki University Printing House
Helsinki 2015

Abstract

Porous silicon nanoparticles (PSi NPs) have recently drawn increasing interest for therapeutic applications due to their easily modifiable surface, large pore volumes, high surface area, nontoxic nature, and high biocompatibility. Nevertheless, there is no comprehensive understanding about the role of the surface chemistry of these NPs on the biological interactions and the therapeutic effect of the PSi-based nanosystems. Therefore, extensive attempts are still needed for the development of optimal PSi-based therapeutics.

The first step for evaluating the biological activity of the NPs was to investigate the potential toxic effects. Accordingly, the immunotoxicity and hemocompatibility of the PSi NPs with different surface chemistries were assessed at different concentrations on the immune cells and red blood cells, since these are the first biological cells in contact with the NPs after intravenous injection. PSi NPs with positively charged amine functional groups showed higher toxicity compared to negatively charged particles. The toxicity of the negatively charged particles was also highly dependent on the hydrophobic nature of the NPs. Moreover, RBC hemolysis and imaging assay revealed a significant correlation between the PSi NP surface chemistry and hemotoxicity.

To further understand the impact of the surface chemistry on the immunological effects of the PSi NPs, the immunostimulatory responses induced by a non-toxic concentration of the PSi NPs were evaluated by measuring the maturation of dendritic cells, T cell proliferation and cytokine secretion. Overall, the results suggested that all the PSi NPs containing higher amounts of nitrogen or oxygen on the outermost surface layer have lower immunostimulatory effects than the PSi NPs with higher amounts of C–H structures on the NPs' surface.

Combination cancer therapy by the PSi NPs was then studied by evaluating the synergistic therapeutic effects of the nanosystems. Sorafenib-loaded PSi NPs were biofunctionalized with anti-CD326 monoclonal antibody on their surface. The targeted PSi NPs showed a sustained drug release and increased interactions with the breast cancer cells expressing the CD326 antigen on their surface. These NPs also showed higher antiproliferation effect on the CD326 positive cancer cells compared to the pure drug and sorafenib-loaded PSi NPs, suggesting CD326 as an appropriate receptor for the antibody-mediated drug delivery. In addition, anti-CD326 antibody acted as an immunotherapeutic agent by inducing antibody-dependent cellular cytotoxicity and enhancing the interactions of immune cells with cancer cells for the subsequent phagocytosis and cytokine secretion.

Next, the development of a stable PSi NP with low toxicity, high cellular internalization, efficient endosomal escape, and optimal drug release profile was tested by using a layer-by-layer method to covalently conjugate polyethyleneimine and poly(methyl vinyl ether-co-maleic acid) copolymers on the surface of the PSi NPs, forming a zwitterionic nanocomposite. The surface smoothness and hydrophilicity of the polymer functionalized NPs improved considerably the colloidal and plasma stability of the NPs. Moreover, the double layer conjugation sustained the drug release from the PSi NPs and improved the cytotoxicity profile of the drug-loaded PSi NPs.

In conclusion, this work showed that the surface modification of the PSi NPs with different chemical groups, antibodies and polymers can affect the toxicological profiles, the cellular interactions and the therapeutic effects of the NPs by modifying the charge, stability, hydrophilicity, the drug release kinetics and targeting properties of the PSi NPs.

Acknowledgements

The laboratory work in this study was carried out at the Division of Pharmaceutical Chemistry and Technology, Faculty of Pharmacy, University of Helsinki during the years 2012–2014.

I would like to extend my sincere gratitude to my supervisor, Docent Dr. Hélder A. Santos, for his patient guidance, enthusiastic encouragement, friendship, and support. I would like to also appreciate his positive attitude towards life and science that made me realize how lucky I have been to pursue my endeavor in Finland. Without his scientific support and kindness this dissertation would have not been possible.

I am also extremely grateful to my supervisor, Professor and Dean Dr. Jouni Hirvonen, for all his trust, his unwavering scientific support, enthusiastic attitude towards science, and providing me this wonderful opportunity to earn my doctoral degree.

Special thanks go to all my co-authors, for their invaluable scientific input and fruitful discussions. I would also like to thank particularly to Docent Dr. Jarno Salonen, Dr. Mehrdad Hamidi and Ermei Mäkilä for their endless, important suggestions and remarks, and their permanent collaboration and productive discussions during this research program despite their already heavy loads of responsibilities.

I would like to express my sincere appreciation to my friends Neha Shrestha, Patrick Almeida, Francisca Araújo, Mónica Ferreira, Barbara Herranz, Alexandra Correia, Dr. Hongbo Zhang, Dr. Dongfei Liu, Chang-Fang Wang, Dr. Vimalkumar Balasubramanian and Martti Kaasalainen for their after-hours company, help, and the pleasant scientific environment they provided for me. I greatly cherish their friendship and hope that to be everlasting.

I would like to express my sincere gratitude to Docent Dr. Jessica Rosenholm and Professor Dr. Ennio Tasciotti for reviewing this thesis and making constructive comments for its improvement.

I would like to extend my deepest thanks to all my colleagues at the Division of Pharmaceutical Chemistry and Technology, particularly to the Santos' lab, for the pleasant working atmosphere, unreserved sharing of knowledge and letting me share a part of my life with them.

I wish to thank my parents and sisters for their trust, support and encouragement throughout my life. My deepest appreciation is expressed to them for their love, understanding, and inspiration. Without their blessings and encouragement, I would have not been able to finish this work.

The Research Fund from the Ministry of Health and Medical Education, Iran, the European Research Council under the European Union's Seventh Framework Programme (FP/2007-2013, grant no. 310892), and the Finnish Center for International Mobility (CIMO, grant no. TM-12-8201) are acknowledged.

I also would like to thank to my beautiful daughter, Anna, who joined us when I was doing the last experiments of my PhD work, for giving me unlimited happiness and pleasure.

Last but not least, I want to thank my wife, Fatemeh, for her unconditional love, motivation, and constant encouragements that helped me through the hard times of this

program and let me accomplish my academic and career goals. She was always there cheering me up and stood by me through all the good and bad times. I hope we can spend more pleasant moments together and enjoy our lovely life.

Helsinki, February 2015

Mohammad-Ali Shahbazi

Contents

Abstract i
Acknowledgements iii
Contents v
List of original publications vii
Abbreviations viii
1 Introduction 1
2 Review of the literature 4
2.1 Immunotherapy and immunotherapeutic approaches 4
2.1.1 Role of the cytokines in immunoactivation 5
2.1.2 Role of the DCs in immunoactivation 7
2.1.3 Role of the T cells in immunoactivation 8
2.1.4 Role of the B cells and antibodies in immunoactivation 9
2.2 Nanotechnology and immunotherapy 10
2.2.1 Adjuvant effect of the NPs on DCs 11
2.2.2 DC targeting using NPs 12
2.2.3 Immunotherapeutic nanovehicles 13
2.3 Interactions between cells and NPs 14
2.3.1 The impact of the NP size on the cellular interactions 15
2.3.2 The impact of the NP's surface charge on the cellular interactions 16
2.3.3 The impact of NP hydrophobicity and surface chemistry on the cellular interactions 17
2.3.4 Correlation of the NPs' properties and the cellular cytotoxicity 18
2.4 Porous silicon (PSi) nanoparticles 19
2.4.1 Drug loading methods in the PSi particles 21
2.4.2 PSi NPs for drug delivery 22
2.4.3 Immunotherapeutic applications of PSi particles 25
2.4.4 Cellular uptake and trafficking 26
3 Aims of the study 28
4 Experimental 29
4.1 Fabrication and characterization of the PSi NPs 29
4.1.1 Preparation of the UnTHCPSi-polyethylenimine (Un-P) NPs (II and IV) 30
4.1.2 Preparation of the APSTCPSi-poly(methyl vinyl ether-alt-maleic acid) (APM) NPs (II and V) 30
4.1.3 Preparation of anti-CD326 antibody-conjugated UnTHCPSi NPs (III) 30
4.1.4 Formation of UnTHCPSi-PEI-PMVE-MA (Un-P-P) nanocomposites (IV) 31
4.1.5 Characterization of the PSi NPs (I–V) 31
4.1.6 Drug loading and release (III and IV) 32
4.2 Cellular toxicity experiments 33
4.2.1 Cell lines and culture (I–V) 33
4.2.2 Reactive oxygen species (ROS) assay (I) 33
4.2.3 ATP activity (I and III–V) 34
4.2.4 Genotoxicity analysis (I) 34
4.2.5 Hemocompatibility studies (I) 34
4.2.6 *In vivo* biochemical and histopathological experiments (I) 35
4.3 Immunostimulation experiments 36
4.3.1 Dendritic cells (DCs) maturation (II) 36

4.3.2 T cell proliferation and differentiation (II) 36
4.3.3 Cytokine secretion (II and III) 37
4.3.4 ADCC-mediated immunotherapeutic effect (III) 37
4.4 Cellular association and intracellular distribution 38
4.4.1 Confocal microscopy and flow cytometry experiments (III–V) 38
4.4.2 TEM imaging (III–V) 38
4.4.3 *In vitro* anti-cell proliferative experiments (III–IV) 39
5 Results and discussion **40**
5.1 Effect of the surface chemistry on the biocompatibility of the PSi NPs (I) 40
5.1.1 Analysis of the immunotoxicity mechanism of the PSi NPs 40
5.1.2 Hemocompatibility 43
5.1.3 in vivo histopathological and biochemical biocompatibility 44
5.2 Effect of surface chemistry of the PSi NPs on the immunostimulatory responses (II) 46
5.2.1 Inducing DC maturation and stimulation by PSi NPs 46
5.2.2 Cytokine secretion and T cell responses 48
5.3 Antibody functionalized PSi NPs for targeted cancer chemo-immunotherapy (III) 50
5.3.1 Ab-mediated cell–NP interactions 50
5.3.2 Immunotherapeutic potential of Ab-functionalized UnTHCPSi NPs 52
5.3.3 Drug release and anticancer effect 54
5.4 Surface polymeric engineering of the PSi NPs for the cellular interaction enhancement (IV and V) 56
5.4.1 Stability, cellular association and endosomal escape 56
5.4.2 Drug loading, release study and antiproliferation effect 60
6 Conclusions **63**
References **64**

List of original publications

This thesis is based on the following publications, which are referred to in the text by their respective roman numerals (**I–V**):

I **Shahbazi M.A.,** Hamidi. M., Mäkilä E., Zhang H., Almeida P., Kaasalainen M., Salonen J., Hirvonen J., Santos H.A., 2013. The mechanisms of surface chemistry effects of mesoporous silicon nanoparticles on immunotoxicity and biocompatibility. Biomaterials, 34: 7776–7789.

II **Shahbazi M.A.,** Fernández T.D., Mäkilä E., Guével X.L., Mayorga C., Kaasalainen M., Salonen J., Hirvonen J., Santos H.A., 2014. Surface chemistry dependent immunostimulative potential of porous silicon nanoplatforms. Biomaterials, 35: 9224–9235.

III **Shahbazi M.A.,** Shrestha N., Mäkilä E., Araújo F., Correia A., Ramos T., Sarmento B., Salonen J., Hirvonen J., Santos H.A., 2014. A prospective cancer chemo-immunotherapy approach mediated by synergistic CD326 targeted porous silicon nanovectors. Nano Research, DOI 10.1007/s12274-014-0635-4.

IV **Shahbazi M.A.,** Almeida P., Mäkilä E., Kaasalainen M., Salonen J., Hirvonen J., Santos H.A., 2014. Augmented cellular trafficking and endosomal escape of porous silicon nanoparticles via zwitterionic bilayer polymer surface engineering. Biomaterials, 35: 7488–7500.

V **Shahbazi M.A.,** Almeida P., Mäkilä E., Correia A., Ferreira M., Kaasalainen M., Salonen J., Hirvonen J., Santos H.A., 2014. Poly(methyl vinyl ether-alt-maleic acid) functionalized porous silicon nanoparticles for enhanced stability and cellular internalization. Macromolecular Rapid Communication, 35: 624–629.

 In publication **II**, the first two authors contributed equally to the work.

Abbreviations

APSTCPSi	(3-aminopropyl)triethoxysilane-functionalized thermally carbonized porous silicon
Ab	Antibodies
ADCC	Antibody-dependent cell-mediated cytotoxicity
APCs	Antigen presenting cells
APM	APSTCPSi-PMVE-MA
AST	Aspartate transaminase
ATR-FTIR	Attenuated total reflectance Fourier transform infrared
BCR	B cell receptor
BMDCs	Bone marrow-derived dendritic cells
BrdU	5-bromo-20-deoxyuridine
CDC	Complement dependent cytotoxicity
CFSE	Carboxyfluorescein succinimidyl ester
CTL	Cytotoxic T lymphocytes
DCF-DA	2´,7´-dichlorodihydrofluorescein diacetate
DCs	Dendritic cells
DMEM	Dulbecco's modified Eagle's medium
EDC	1-ethyl-3-[3-dimethylaminopropyl] carbodiimide hydrochloride
EDTA	Ethylenediaminetetraacetic acid
ELISA	Enzyme-linked immunosorbent assay
EtOH	Ethanol
FA	Folic acid
FBS	Fetal bovine serum
GhA	Ghrelin antagonist
GLP-1	Glucagon like peptide-1
GM-CSF	Granulocyte-macrophage colony-stimulating factor
H&E	Hematoxylin and eosin
HA	Hyaluronic acid
HBSS	Hank's balanced salt solution
HEPES	(4-(2-hydroxyethyl)-1-piperazineethanesulfonic acid)
HF	Hydrofluoric acid
HLA	Human leukocyte antigens
HPLC	High-performance liquid chromatography
IFN	Interferon
IgG	Immunoglobulin G
ILs	Interleukins
imDCs	Immature DC
LDH	Lactate dehydrogenase
LPS	Lipopolysaccharide
MAC	Membrane attack complex
MDDCs	Monocyte-derived dendritic cells

MDGI	Mammary-derived growth inhibitor
MES	2-(N-morpholino) ethanesulfonic acid
MHC	Major histocompatibility complex
MPL	Presenting monophosphoryl lipid A
MTII	Melanotan II
MTX	Methotrexate
Na	Sodium
NF-κB	Nuclear factor–κB
NHS	*N*-hydroxysuccinimide
NPs	Nanoparticles
PBL	Peripheral blood lymphocytes
PBMCs	Peripheral blood mononuclear cells
PBS	Phosphate buffered saline
PdI	Polydispersity index
PEG	Poly(ethyleneglycol)
PEI	Polyethyleneimine
PLGA	poly(lactic-co-glycolic acid)
PMVE-MA	Poly(methyl vinyl ether-alt-maleic acid)
PMVE-MAh	Poly(methyl vinyl ether-alt-maleic anhydrate)
PSi	Porous silicon
RBCs	Red blood cells
RNOS	Reactive nitric oxide species
ROS	Reactive oxygen species
RPMI 1640	Rosewell Park Memorial Institute 1640
RT	Room temperature
SEM	Scanning electron microscopy
SFN	Sorafenib
SiRNA	Small interfering RNA
SLN	Solid lipids nanoparticles
TCPSi	Thermally carbonized porous silicon
TCR	T cell receptors
TEM	Transmission electron microscopy
THCPSi	Thermally hydrocarbonized porous silicon
TNF-α	Tumor necrosis factor-alpha
TOPSi	Thermally oxidized porous silicon
Un-Ab	Ab functionalized UnTHCPSi
Un-P	UnTHCPSi-PEI
Un-P-P	UnTHCPSi-PEI-PMVE-MA
UnTHCPSi	Undecylenic acid functionalized thermally hydrocarbonized porous silicon

1 Introduction

It is currently approved that owing to the differences in the surface properties and superior surface-to-volume ratio, nanosized particles are chemically more reactive than the corresponding bulk materials, leading to changes in many of their biological effects such as toxicity and cellular interactions. That is the main reason for the high interest in studying the toxicity and biological interactions of the nanoparticles (NPs), along with the growing utilization potential of the nanoparticulate systems for medical applications [1-3]. These toxicological and biological studies clarify the impact of the NPs at cellular level, and also increase the knowledge regarding the cellular interactions of the NPs and their effects on the proper function of main organs in the body. Moreover, they can provide additional knowledge on the right route of administration to be used, the dose to be administered, the clearance rate of the NPs and also aid to predict the possible therapeutic potency of the developed nanosystems.

Although there is currently abundant understanding regarding the biological effects of different NPs, little is still known about the biological, toxicological and immunological effects of porous silicon (PSi) NPs, nanostructured materials with remarkable advantages, including high surface area and stability, tunable pore size, modifiable shape and size, effective protection of the therapeutic cargos from undesirable degradation, facile surface functionalization, biodegradability and biocompatibility [4]. Since the change in the surface chemistry of the PSi NPs can render new properties to these NPs by affecting on their hydrophilicity, charge and aggregation profile [5], there is a high probability to observe different biological responses, cellular interactions and toxicity for the PSi NPs with various surface functional groups. For example, it is not still well understood whether the toxicity of the PSi NPs with different surface chemistries is originated from: (1) hole formation or instability of ion transport in the cell membranes, (2) direct effect on the mitochondria and ATP depletion, (3) induction of reactive oxygen species (ROS) and/or reactive nitric oxide species (RNOS) production, (4) induction of pro-inflammatory biomolecules release, (5) direct DNA damage, or (6) a combination of all the abovementioned mechanisms.

In addition to possible changes in the toxicological profile of the NPs with different surface chemistries, some studies have shown the impact of the physicochemical properties of the NPs on their applications for immunostimulatory purposes [6, 7]. A wide variety of studies have already reported safe and effective immunotherapeutic nanocarriers [8-11] that are able to activate immune responses via inducing the maturation of antigen presenting cells (APCs; e.g., dendritic cells, DCs), and then, stimulating T cells to stimulate subsequent immunoactivatory responses [12]. To stimulate resting T cells, two activation signals are necessary to be provided by the APCs. The first signal is provided through the presentation of antigens to the T cell receptors (TCRs) via a major histocompatibility complex (MHC)-II molecules on the surface of DCs (antigen-specific). The second one is a co-stimulatory signal provided through the binding of the cognate ligands (CD80/CD86) of DCs to CD28 receptors on the surface of T cells [13]. In many immunotherapeutic studies, the main reason for low immunostimulatory response is the lack of the second signal (CD80/CD86) and the low activity of T cells despite the

recognition of antigens by DCs [14]. To overcome this shortcoming, nano-based immunoadjuvants with the intrinsic ability of co-stimulatory ligand activation are proposed for the delivery of antigens or other immunostimulating molecules, or even inducing nonspecific immunotherapy without targeting a certain cell or antigen [12]. Several factors, such as size, concentration, charge, and hydrophobicity, have been shown to have a strong effect on the immunological responses of different NPs [7, 8, 15]. However, there is still lack of knowledge about the physicochemical factors affecting the immune responses of the PSi NPs, making it crucial to explore the immunological responses of these NPs.

In addition to the impact of the surface functional groups on the toxicity and immunological responses, the NP's surface modification with biomolecules can render new benefits, such as targeting, immunostimulation or dual therapy to the NPs for the treatment of deadly diseases like cancer. For example, combination therapy by an anticancer drug together with biological molecules, such as monoclonal antibodies (Ab), is a promising revolutionary approach for the suppression of tumor growth [16]. To date, many different types of targeting ligands including carbohydrates, Abs, peptides, and small organic molecules have been successfully conjugated to various forms of nanocarriers [17]. Nonetheless, the surface modification with Abs has been studied most extensively because of their ability to render targeting properties to the NPs, to enhance the cellular uptake [18], to improve the site specific drug release and to activate several immunological pathways, such as antibody-dependent cell-mediated cytotoxicity (ADCC) and complement dependent cytotoxicity (CDC), leading to synergistically increased anticancer effects [19]. However, there are some major challenges concerning the ability to conjugate targeting moieties to the NPs with high efficiency, low complexity and avoiding alterations in their biological activity. In recent years, non-covalent techniques, such as adsorption by electrostatic and hydrophobic interactions [20] or strong biotin-avidin binding [21], have been mostly reported. Although the adsorption is a very straightforward and innocuous process owing to the absence of toxic reagents, the ligand is prone to suffer from competitive displacement by endogenic proteins in the bloodstream [22]. Also, there is a major concern regarding the clinical use of biotin-avidin complexes due to the probable immunogenicity [23]. Accordingly, applying efficient covalent attachment techniques remains crucial in the production of stable and efficient biomolecule conjugated NPs.

Besides the surface modification with biomolecules to increase the cellular interactions of NPs and enhance the therapeutic effect, polymer surface functionalization has also attracted a lot of interest for therapeutic applications by adjusting the colloidal and plasma stability, cellular interactions and drug release profiles of the NPs. In addition, polymers used on the surface of the NPs can increase the bloodstream circulation time, improve the NPs' stability, enhance endosomal escape, and reduce the toxicity of the NPs [24, 25]. Since the PSi NPs still suffer from poor cellular interactions and high localization of the internalized NPs in the lysosomal compartments [26], surface polymeric functionalization can be an efficient strategy for increasing their uptake into the cells and localization within the cytoplasm with the aim to improve the potential use of these NPs for drug delivery.

This dissertation focuses on understanding the impact of the surface modification of PSi NPs and its effects at the cellular level on the toxicity and immune responses. In addition, this work demonstrates how the surface functionalization of the PSi NPs with biomolecules and polymers can affect the physicochemical properties of these NPs and render them new properties for specific applications, like targeting and cancer therapy.

2 Review of the literature

2.1 Immunotherapy and immunotherapeutic approaches

Immunotherapy is a therapeutic method that uses the body's own defence mechanisms to fight against the physiological abnormalities by reinforcing or suppressing the immune system. Nowadays, this method has attracted a lot of attention for the treatment of various diseases [13, 27], for example, by applying different synthetic or natural immunogenic materials.

The three most popular strategies for the therapeutic immunostimulation include application of immunoadjuvant materials for non-specific immunoactivation, application of monoclonal antibodies, and vaccination [28-31]. Non-specific immunotherapies can be given as a single therapy or at the same time with another treatment, such as chemo- or radiation therapy in the case of cancer treatment. Interferons and interleukins (ILs) are the most common non-specific immunotherapies capable of activating different immunological pathways [32]. Monoclonal antibodies (Ab) are another type of compounds used in immunotherapy, produced in the body upon detecting antigens (e.g., viruses, bacteria, fungi and parasites) by the immune system [33]. Therapeutic Ab can act through a number of mechanisms, such as ADCC effect, blocking the function of the targeted molecules, inducing apoptosis in the cells expressing target antigen, and increasing the phagocytosis of the target cells by macrophages or by modulating the signalling pathways of the target cells [29, 30, 33]. In addition to immunotherapy, monoclonal Ab can be also applied for targeted treatment and diagnosis [34, 35]. For example, radioactive molecules can be directly conjugated to the monoclonal Ab and deliver low doses of radiation specifically to the cancer tissue while leaving the healthy cells unharmed. Ibritumomab tiuxetan (Zevalin) and tositumomab (Bexxar) are the main examples of targeted radio-immunotherapeutic formulations [36] (Figure 1A). Moreover, cancer chemotherapeutic molecules can be attached to the monoclonal Ab and specifically kill cancer cells without damaging the healthy cells. Brentuximab vedotin (Figure 1B) is one example of such a system applied for the treatment of Hodgkin's and non-Hodgkin's lymphoma [37].

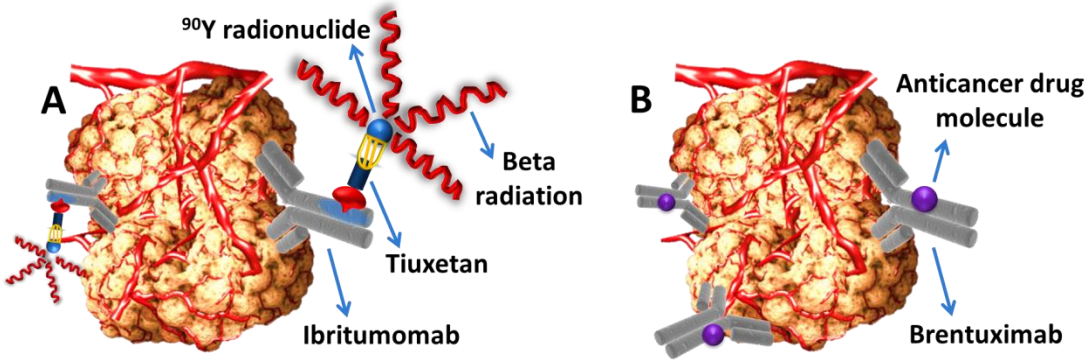

Figure 1 *Antibody mediated radiotherapy (A) and chemotherapy (B) of cancer tissue.*

Vaccination is another approach to help the body in fighting against diseases [31]. Vaccines contain an agent that resembles a disease-causing microorganism and are able to improve the immunity against a particular disease. While traditional vaccines are often made from dead or weakened forms of the microbe or their toxins, nowadays the investigation is more focused on the development of new vaccines made from surface proteins and DNA of the immunogenic microorganisms or cells. The immune system can recognize the immunogenic molecule, keep a record of it, and more easily recognize and destroy any of the microorganisms containing the immunogenic molecule if the body encounters with it later on [38].

In all the abovementioned immunotherapeutic strategies, cytokines, dendritic cells (DCs), T cells and B cells play a pivotal role for inducing proper immune responses, therefore it is very important to understand the function of all these immunomediators in immunotherapy, as it will be discussed below.

2.1.1 Role of the cytokines in immunoactivation

Cytokines are a category of small proteins that act as mediators to regulate the homeostasis of the immune system and also allow the immune cells to communicate with each other in order to generate a response against a target antigen [39, 40]. Although the communication of the immune system usually occurs via direct interactions between the immune cells, cytokine secretion causes the rapid propagation of immuno–cellular interactions in an efficient and multifaceted manner. Accordingly, over the last few decades, the growing interest in exploiting the immune system to fight against various diseases has been accompanied by the increased efforts for using the vast signalling networks of cytokines to improve the therapeutic immune responses [41, 42]. For example, numerous studies have already shown the ability of cytokines to directly stimulate the immune effector cells at the tumor tissue and to enhance the recognition of tumor cells by cytotoxic effector cells [39]. In recent years, a number of cytokines, such as IL-12, IL-15, IL-7, IL-18, IL-21, and granulocyte-macrophage colony-stimulating factor (GM-CSF), have entered clinical trials for the cancer treatment [39, 43]. In addition, some cytokines, such as IL-2 and interferon (IFN)-α have achieved FDA approvals for the treatment of metastatic melanoma and stage III melanoma, respectively [39]. Moreover, ongoing pre-clinical studies have shown promoted anti-tumor immunity through the neutralization of immuno-suppressive cytokines, such as IL-10 and TGF-β [44, 45]. Despite all the abovementioned findings regarding the role of various cytokines in the immunotherapeutic applications, the extensive pleiotropism (the ability of cytokines to act on different types of immune cells to mediate diverse or opposing effects), redundancy of cytokine signalling, the dual immuno-activation and suppression function of some cytokines, and the effect of cytokines on each other are still big challenges towards the development of proper cytokine based formulations for therapeutic applications. For example, one of the primary limitations for IL-2 mediated therapy is the dual potent function of IL-2 on the activation of the T effector cells and the T regulatory compartments [46-49]. Therefore, it is of paramount importance to understand the mechanistic effect of various cytokines for the development of cytokine

based non-specific immunotherapeutic formulations. Table 1 presents the general properties of some of the most important cytokines.

Table 1. *General properties of cytokines* [39-42, 50, 51].

Cytokine	Primary Cell Source	Target Cells	Biological Function
IL-1	Macrophages[1] B cells Monocytes[2] DCs	T cells B cells NK cells	Co-stimulation Cell activation Inflammation Maturation Proliferation
IL-2	T cells Natural killer (NK) cells[3]	T cells NK cells B cells Monocytes	Cell growth/activation differentiation of T cell response
IL-4	T cells Macrophages	T cells B cells	Th2 differentiation Cell growth/activation IgE isotype switching
IL-6	Macrophages T cells B cells	T cells B cells	Co-stimulation Cell growth/ activation Acute phase reactant Antibody secretion
IL-10	Monocytes Th2 cells Macrophages	Macrophages T cells B cells	Inhibits antigen presenting cells Inhibits cytokine production
IL-12	DCs B cells T cells Macrophages	T cells NK cells	Th1 differentiation

[1]Macrophages are responsible for the phagocytosis of microbes, foreign substances, cellular debris, and cancer cells. [2]Monocytes are responsible for replenishing resident macrophages under normal states and quick moving to the sites of infections to proliferate and differentiate into DCs and macrophages. [3]NK cells are effector lymphocytes that control different types of microbial infections and tumors by limiting their spread and subsequent tissue damage. NK cells contain special proteins such as perforin and proteases known as granzymes in their cytoplasm. Perforin releases in the close vicinity to a cell slated for killing and cause pore formation in the cell membranes, allowing the granzymes to enter inside the cells and induce apoptosis.

2.1.2 Role of the DCs in immunoactivation

DCs are the antigen-presenting cells of the immune system, residing in the peripheral tissues and acting as the sentinels of the body through patrolling in search of antigens. Before exposure to an antigen, they are in an immature state, characterized by a low surface expression of co-stimulatory molecules and major histocompatibility complex (MHC) class I and II molecules [52] (Figure 2). The immature DCs can recognize and uptake both exogenous and endogenous antigens. While the exogenous antigenic peptides can be processed and presented in the form of MHC class II complexes on the surface of DCs, endogenous antigens can cleave into peptides by proteosomes and be presented via the MHC class I.

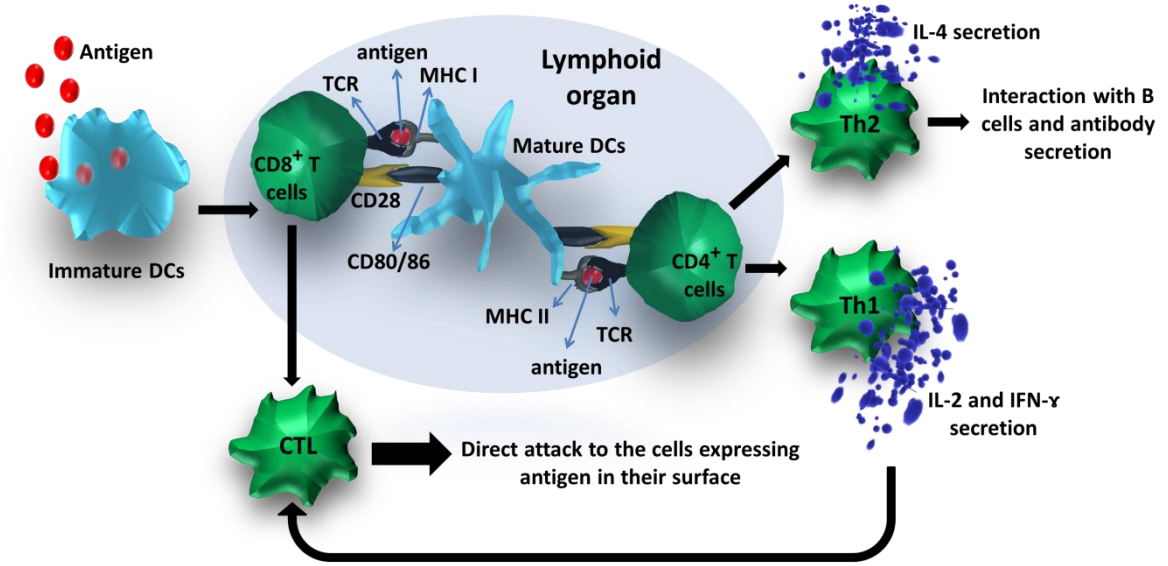

Figure 2 *The induction of immunostimulation via antigen presenting capability of the DCs. Antigens are taken-up by immature DCs in the peripheral tissues. During DC maturation, they migrate to draining lymph nodes to present the antigen in combination with a co-stimulatory signal to the T cells and activate them. Finally, the activated antigen-specific T cells differentiate, proliferate, and migrate out of the lymphoid organ to destroy the antigenic cells.*

For DC-based cancer immunotherapy, the DCs should be able to recognize tumor antigens, and then undergo a maturation process [52], which is a cascade of biological pathways to potentiate the DCs for antigen presentation and initiation of further immunological responses. During maturation, DCs migrate to the lymphoid organs and up-regulated co-stimulatory molecules (e.g., CD80, CD83 CD86, and CD40) on their surface in the lymph node. Then, the DCs interact with T cells to activate them for further stimulation of the immune system (Figure 2). Generally, two signals are essential for T cell activation: (1) the interaction of the MHC–antigen complex with the TCR, and (2) the interaction of the activated co-stimulatory signals on the surface of DCs with the CD28 receptors of the T cells. Next, depending on the type of T cell interacted with the DCs, different immune response mechanisms can be activated. For example, the activation of $CD8^+$ T cells results in the production of cytotoxic T lymphocytes (CTL), while $CD4^+$ T

cells differentiate into Th1 or Th2 cells depending on the environmental factors that skew the cellular differentiation [53]. Finally, the activated T cells circulate through the body and destroy the antigen expressing cells through different pathways as shown in the Figure 2.

Several studies have shown the importance of DC maturation for the induction of immunological responses against cancer cells [52, 54-57]. It has been suggested that the superiority of mature DCs in inducing the T cell activation is not only correlated to the high expression of co-stimulatory molecules and MHC subclasses, but also owing to the higher migratory capacity of the cells to draining lymph nodes compared to the immature DCs [58], because most of the DCs interact with the T cells in the peripheral lymphoid organs. It has also been recently shown that intradermal injection of immunostimulative molecules leads to a higher DC migration into the draining lymph nodes and subsequent T cell activation [52].

2.1.3 Role of the T cells in immunoactivation

T cells move through all tissues, scanning for MHC–antigen complexes that, as mentioned above, specifically activate their TCRs and lead to the proliferation and differentiation of T cells. Currently, one of the greatest challenges in the field of immunotherapy is the identification of appropriate antigens, particularly in diseases like cancer, because there are self-antigens shared by tumour cells and normal tissues [59].

Both activated $CD4^+$ and $CD8^+$ T cells have separately demonstrated therapeutic immunostimulatory effects for different diseases, particularly in cancer; however, their combination works much better, as the $CD4^+$ T cells are the most important producers of cytokines, which provide help for the proper function of $CD8^+$ T cells [60]. Nevertheless, one of these two pathways, $CD4^+$ and $CD8^+$ T cells, is activated more than the other in different diseases. For example, since the antigens of cancer cells are mostly presented by the MHC I subclass, the roles of $CD8^+$ T cells and CTLs in anti-tumour immunity are often investigated in much greater detail than the $CD4^+$ T cells [61]. However, the available MHC II positive APCs can increase the production of cytokines, such as interferon gamma, which has an inhibitory effect on tumour vasculature and also promotes the proper functionality of CTLs [62] to directly attack and kill cancer cells via apoptosis inductions. The main mechanism through which the CTLs induce cell apoptosis is by the calcium-dependent release of lytic granules upon recognition of antigen on the surfaces of target cells [63]. These granules are kind of lysosomes with two distinct classes of cytotoxic effector protein, namely perforin and granzyme. Although these proteins are stored in an active form in the lytic granules, they do not act before being released from the CTLs. Upon perforin is released, it polymerizes to form transmembrane pores in target cell membranes, allowing granzymes to move into the target cells and act as digestive enzymes to increase the cytotoxicity induction in the target cells. Hence, both perforin and granzymes are required for effective cell killing [64, 65]. Finally, the phagocytic cells ingest dead cells by recognizing the change in their phosphatidylserine, which is normally located only in the inner leaflet of the cell membrane [66]. The mechanism through which CTLs destroy target cells is shown in Figure 3.

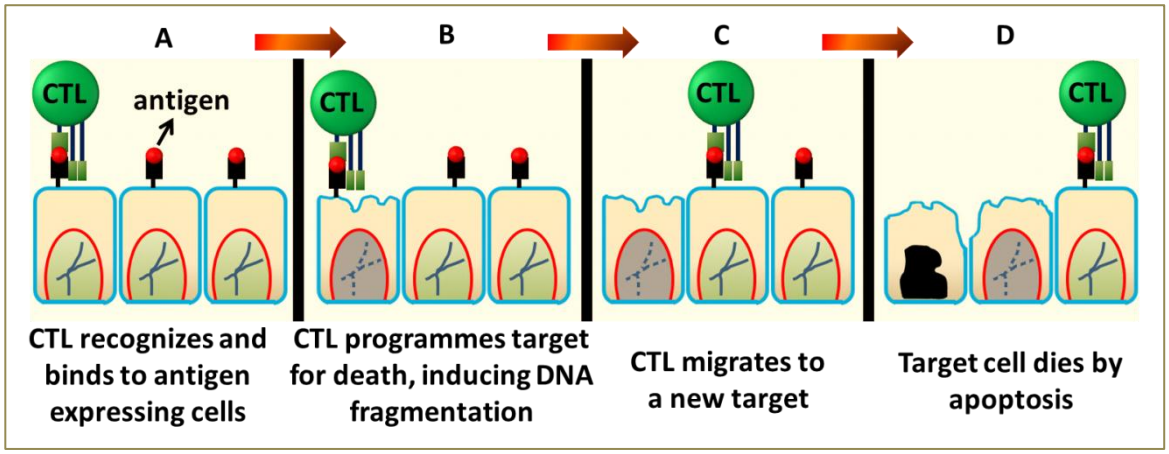

Figure 3 *Programmed apoptosis induction process by CTLs. To kill target cells, CTLs should recognize peptide–MHC complexes on a target cell. CTLs can recycle to kill multiple targets. In the first step (A), CTL binds to healthy target cells with a normal nucleus. Then, the release of cytotoxic proteins sheds the membrane vesicles and induces DNA fragmentation (B); however, the integrity of the cell membrane is still retained. Then, CTL moves to another healthy cell to induce the same mechanism (C). In the last stage (D), the nucleus is destroyed and the cell loses most of its membrane and cytoplasm through the shedding of vesicles.*

2.1.4 Role of the B cells and antibodies in immunoactivation

B cells are a type of lymphocytes with the principal functions of producing Abs against antigens, performing the role of antigen-presenting, and developing into memory B cells after activation by antigen interaction [67, 68]. Although human body makes millions of different types of B cells each day, they do not produce Ab until they become activated [69, 70]. The B cells possess B cell receptors (BCRs) on their surface that can bind to their cognate antigens, and then differentiate into plasma B cells and/or memory B cells upon receiving the second signal from the interaction with T helper cells. While plasma B cells are able to produce and secrete large amounts of Ab against target cells, memory B cells form activated B cells that are specific to the antigen encountered during the primary immune response. These cells remain in the body for a long time and can quickly respond by Ab secretion following the second exposure to the same antigen [71-73].

Abs are immunoglobulins produced to specifically react with the antigens that have provoked their production. Abs possess two distinct functional sections, including the fragment of antigen binding (Fab) and the constant fragment (Fc). Although Abs have been widely used over the last few years for cancer therapy, it is not completely clear how the cancer specific Abs work [74, 75]. One of the main proposed mechanisms of a monoclonal Ab is the disruption of signalling pathways involved in the maintenance of the cancer cells. Other tumor-specific immune responses, such as ADCC and CDC, also play an important role in the Ab-based immunity [74-79]. In ADCC, an effector immune cell (e.g., natural killer cells, macrophages, neutrophils, and eosinophils) actively lyses the target cells, whose membrane-surface antigens are bound by specific antibodies, via the release of cytokines such as IFN and cytotoxic granules containing perforin and granzymes, inducing apoptosis and cell death [80-82]. In CDC, the C1q binds the Ab and

triggers the formation of the membrane attack complex (MAC) at the surface of the target cell, which induces the death at the target cells [83, 84]. Figure 4 shows the schematic illustration of the abovementioned mechanisms.

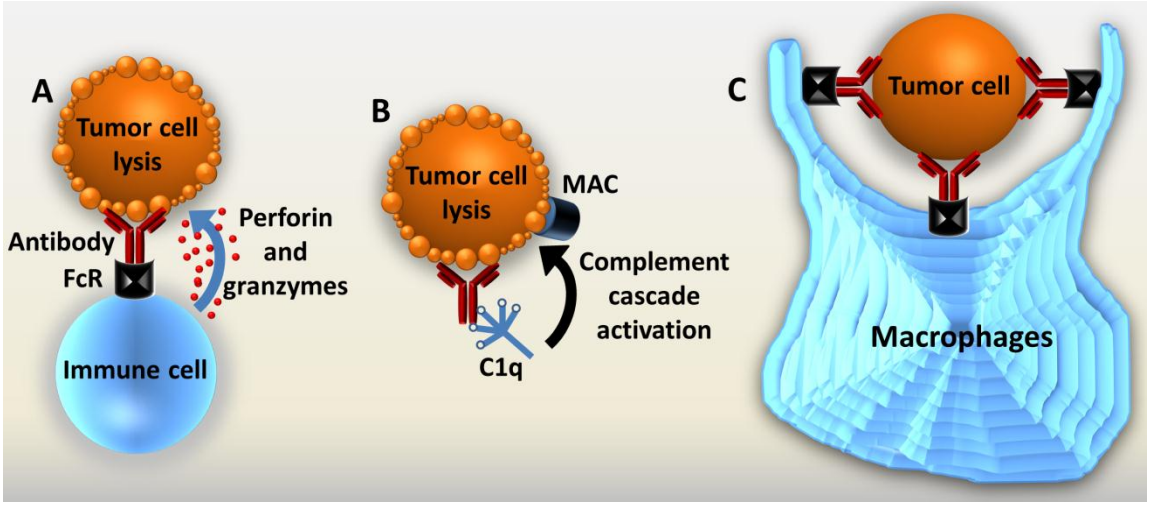

Figure 4 *Antitumor mechanisms mediated by Ab. ADCC (A), CDC (B), and phagocytosis (C) all lead to tumor cell death. Adopted from ref. [19].*

2.2 Nanotechnology and immunotherapy

The main shortcomings of current immunostimulatory materials are related to the lack of DC targeting and short time of immunostimulation, as the concentration of the immunogenic molecules decreases in the body over a short period of time. Current immunoactivating molecules mainly elicit Immunoglobulin G (IgG) isotype Ab and suffer from inducing the secretion of a wide range of Ab isotypes [10]. Therefore, immunotherapeutic protections induced by the available immunostimulative biomolecules are not long-lasting, and thus, new strategies are required to more efficiently activate the immune system against different diseases.

In general, the ideal properties of a good immunotherapeutic formulation include the capability of eliciting the desired immune responses after a single dose, absence of a booster dose, high safety, simple and affordable preparation process, easy administration and scaling-up process, no premature drug release, and high physicochemical stability of the immunogenic agents and excipients throughout the process, storage and administration [12]. To combine all these properties in one formulation, NPs have been suggested as versatile systems capable of improving the biological effects of the immunostimulatory molecules via different mechanisms. The immunostimulative biomolecules can be either encapsulated within or conjugated on the surface of the NPs [31, 85]. The former method can maximize the exposure time of immunostimulative compounds to the immune system by sustaining the release of the encapsulated molecules. However, it causes lower extent of immunity compared to the NPs that have immunostimulative molecules adsorbed on their surface with the aim to induce rapid and short immune responses.

Below, the adjuvanticity of the NPs as well as the current progresses in the development of nanovaccines, particularly those with high potential to be used in the clinic, are addressed and discussed.

2.2.1 Adjuvant effect of the NPs on DCs

Adjuvants are immunogenic compounds with the ability to accelerate and extend the response of immunostimulative biomolecules. Currently, alum salts are the most widely used immune adjuvants [86], owing to their potential in triggering the so-called "inflammasome" mechanism in the cells that leads to the release of danger signals and subsequent secretion of proinflammatory biomolecules, resulting in the activation of the immune system [87]. Despite the popularity of immunogenic alum salts over the last few decades, they suffer from major limitations, such as adverse local reactions, degradation during freeze-drying, lack of inducing cellular immune responses, and necessity of multi-dosing to reach long lasting protection [86]. These limitations have encouraged scientists to work on the development of new vaccine delivery systems with the potential of attenuating the restrictions of current immunoadjuvants and vaccines.

Although a wide variety of adjuvants have been recently developed, only few of them are used for therapeutic purposes in humans, because of their high toxicity, low stability and severe side effects [88]. Hence, the scientific community is trying to replace these adjuvants with the new generation of nanomaterials that are able to show intrinsic immuno-adjuvanticity and also to act as carriers for the delivery of stabilized vaccine antigens and immunotherapeutic biomolecules [89]. This strategy provides an opportunity for simultaneous humoral and cell-mediated immunity induction, which can lead to improved therapeutic effects [90, 91]. NPs may also assist the interaction of the delivered antigens with APCs, enhancing the antigen-based immune responses [89, 92]. Moreover, co-encapsulation of anticancer drug molecules or imaging agents with immunostimulative biomolecules can be obtained for multifunctional purposes. Accordingly, nanovaccines have recently attracted a lot of interest owing to their unique properties to overcome the limitations of immuno-therapeutics, including inherent instability of biomacromolecules, low interaction with APCs, and lack of cross-presentation to T lymphocytes [89, 92].

The impact of NPs on the maturation of DCs is usually examined by studying the expression of co-stimulatory molecules and MHC classes I and II bioreceptor molecules, the production of cytokines, and the downstream signalling pathways [13]. For example, the effects of poly(lactic-co-glycolic acid) (PLGA) NPs on the maturation of DCs were examined in mice spleen [93] and showed a dose-dependent expression of co-stimulatory molecules such as CD80, CD86, CD40, and MHC class I, enhancement of the inflammatory cytokines and chemokines, such as tumor necrosis factor-α (TNF- α) and interleukin-6 (IL-6), as well as increase in the activity of mitogen-activated protein kinase and nuclear factor–κB (NF-κB) signalling pathways. The activation of DCs with ovalbumin loaded mannosylated dendrimers also showed a distinct increase in CD40, CD80, and CD86 expression [94].

2.2.2 DC targeting using NPs

NPs are more favourable than microparticles for DC targeting because of the inverse relationship between the efficiency of uptake by DCs and the particle size [92]. In addition, positively charged NPs are more desirable as they can highly interact with the cells via binding to the negatively charged surface of the cells [95, 96]. After the internalization of NPs into the DCs, loaded immunostimulants can be released in endosomes, degrade, and eventually bind to the MHC II molecules on the surface of the DCs to present the antigenic molecules to the $CD4^+$ T cells [97]. If the NPs escape from the endosome and release their immunostimulative antigens in the cytoplasm, antigens degrade to small peptides by the proteosomes, and finally, form a complex with the MHC I in order to be recognized by the $CD8^+$ T cells [97, 98].

Targeting of DCs can be achieved via passive and active processes. The efficiency of the nanovaccines to passively target DCs is strongly dependent on the surface charge, size, hydrophilicity, hydrophobicity, and the interactions with the plasma proteins and cell-surface receptors [99]. It has been shown that NPs with a size higher than 500 nm are taken-up less efficiently by the DCs [100], and mainly ingested by macrophages [86, 101]. In addition, a pre-clinical study performed in mice suggested that the NP size of 40–50 nm was optimal for nanovaccines [8]; however, NPs up to 300 nm have already shown potent induction of the $CD4^+$ and $CD8^+$ T cell responses [8, 102-105]. Positively charged particles are taken-up more efficiently *in vitro* by the DCs than those with a negative or neutral charge [100]. However, some *in vivo* studies have revealed no significant difference in the immunostimulatory effect between the positively and negatively charged particles, indicating the dependency of the surface charge effect on the model system used [106]. Some studies have also demonstrated that particles with positive surface charge can immobilize the nanovaccines in negatively charged components presented in the extracellular matrix of the cells through electrostatic interactions [107], and inhibit the immunostimulative responses owing to the reduced tissue penetration. Hydrophobicity has also been reported as one of the key factors affecting the opsonisation of NPs [108] and also DC activation [109].

Since the DCs express many cell surface receptors, such as CD11c [110], mannose [111, 112], DEC-205 [110], DC-SIGN [113, 114], Langerin [115], clec9A [116], and DCIR2 [117], actively targeted cellular endocytosis of the NPs can be also facilitated via surface modification of the NPs with ligands that target these receptors on the surface of the DCs [118]. It has already been demonstrated that the conjugation of such targeting moieties on the surface of NPs enhances their uptake by the DCs and increase DC maturation as evidenced by the enhanced secretion of cytokine and up-regulation of CD83 and CD86 surface maturation markers [119]. For efficient active DC targeting, nonspecific interaction by other plasma constituents and other cells in the bloodstream can be reduced by introducing a hydrophilic biomaterial consisting of poly(ethyleneglycol) (PEG) onto the surface of the particles [108]. The type of the target receptor can have a substantial effect on the immunological response of nano-immunotherapeutics. A study by Dudziak and coworkers demonstrated that targeting antigens to DEC-205 results mainly in cross-presentation of antigen to the CD8 T cells, whereas antigens targeted to DCIR2 are preferentially presented via MHC class II molecules to the CD4 T cells [117]. This

difference is explained by the fact that these CLRs are expressed on distinct DC subsets that differ in their functional properties and antigen processing capacity.

2.2.3 Immunotherapeutic nanovehicles

Immunotherapy with nanomaterials is a relatively new interdisciplinary field holding great promise by combining materials science, chemistry and immunology. It is currently known that immunostimulatory products with large hydrophobic structures are more immunostimulative than hydrophilic compounds; therefore, it is proposed that microbially derived adjuvants can be replaced with hydrophobic nanomaterials. These nanosystems can also simultaneously serve as delivery vehicles for the immunostimulative molecules [120], with the aim to facilitate single-dose vaccination and eliminate the need for booster shots through sustaining the release of immunotherapeutic payload and potentiating its effect via the intrinsic adjuvanticity of the particles. In addition, most of the NPs applied in immunotherapy possess high safety, and the time and rate of degradation for antigen release is controllable [121]. Owing to these benefits, it can be possible to avoid the need for surgical removal of cancer tissues and circumvent the disadvantages of conventional anticancer formulations by combining chemo- and immuno-therapy approaches using such nanostructures.

One of the common methods for nano-immunotherapy is antigen encapsulation inside nanostructures, offering distinct advantages to the therapy, such as reduced dose of antigen, efficient uptake and processing by APCs, as well as increased stability during storage [122, 123]. Although the entrapment of immunogenic biomolecules within the particles is offered as the best possible protective strategy, the main drawback of this method is the unavailability of the loaded antigens upon administration because of the slow drug release profile [124]. In addition, the loaded bio-immunogenics can physically or chemically degrade during the loading process [125]. Accordingly, the absorption or conjugation of antigen on the surface of the polymers has been suggested; however, this method also suffers from low stability and rapid degradation [9, 126].

One of the benefits of nanovaccines is that the morphology, size distribution, entrapment efficiency, release kinetics and other physicochemical properties that affect the obtained immune responses can be controllable, leading to the successful development of promising vaccines [127]. In addition, the systemic severe side effects of high dose administration of the immunostimulants, such as toll-like receptor ligands [128], can be minimized using NPs. NPs can also reduce the needed dose and limit the non-specific immune responses [129]. Nevertheless, several hurdles, such as reproducibility, stability during production, and method for non-thermal sterilization, are needed to be taken into account [130, 131]. For example, the reproducibility of the formulation can be affected by the variation in the size of the NPs that in turn can modify the immunogenic property of the final product [8].

Polysaccharides [132], poly(lactic acid) [133], polyanhydrides [134], PLGA [135] and polyphosphazene [136], are among the most widely studied nanomaterials prepared for immunostimulative purposes. Different techniques have been employed to prepare nano-immunotherapeutics using the abovementioned polymers, including spray drying,

emulsification/solvent evaporation, and coacervation [9, 12]. All of these methods can produce polymeric NPs with a large surface area that improve the interaction between immune cells and immunostimulative payload [99], leading to the enhanced uptake of antigens by DCs and improved immune responses [137].

The main reason for the great interest in immunostimulatory potential of the above-mentioned NPs is the superior biocompatibility, versatile chemistry, high protection of the loaded biomolecules, high loading efficiency, efficient endocytosis and high presentation of the immunogenic molecules [132-136, 138]. For example, some of these nanocarriers have shown endosomal escape properties, potentiating the proteosome-dependent processing of the immunogenic payload and cross-presentation through MHC class I [137, 139]. Another benefit of these NPs is the ability to control the release pattern of the loaded immunostimulative compound and to act as an adjuvant and increase the therapeutic effect of the formulation [11, 12, 140]. For example, Gómez *et al*. [141] have demonstrated the ability of poly(methyl vinyl ether-alt-maleic anhydrate) (PMVE-MAh) nanocarriers for vaccination using OVA as a model antigen. The results showed higher humoral immunity (IgG titers) in response to the OVA-loaded NPs compared to the alum, showing the potential of PMVE-MAh for antigen delivery and improving immune responses. In addition, N-trimethyl chitosan has been proposed as a proper nano-immunoadjuvant for the delivery of influenza subunit antigen [142]. All these examples show high potential of NPs to act synergistically for improving the immunostimulative effect of antigens and other immunogenic molecules. However, using NPs as immunoadjuvants for the delivery of immunostimulative biomolecules still suffers from several major drawbacks, including the problems for scaling-up the system, expensive preparation processes, and limitations for producing sterile products [143]. Accordingly, despite the great versatility and promising features observed for the potential of such therapeutic systems, intensive research studies are still needed in order to develop nano-formulations that can be produced in large scale and applied in the clinic.

2.3 Interactions between cells and NPs

One of the main hallmarks of the cell membranes is the ability to selectively control the transport of ions and molecules into and out of the intracellular structure, and to also protect the cell compartments from the extracellular environment. Accordingly, to be internalized inside the cells, NPs have to surmount the cell membrane. Generally, large molecules, such as proteins, viruses and also NPs can transport into and out of the cell membrane by endocytosis and exocytosis. Depending on the property of the transported particle, such as size, shape, surface charge and surface chemistry [144], different types of endocytosis pathways, which vary in the involved internalization machinery, cargo properties and the size of the transport vesicle (Figure 5), may mediate the cellular uptake. For example, it is currently approved that while large particles penetrate into the cells via phagocytosis, the cellular uptake of small particles occurs via different non-phagocytic mechanisms (Figure 5) [145]. Owing to the importance of the NPs' physicochemical properties on their interaction with the cells, some of these characteristics are discussed in the next subsections.

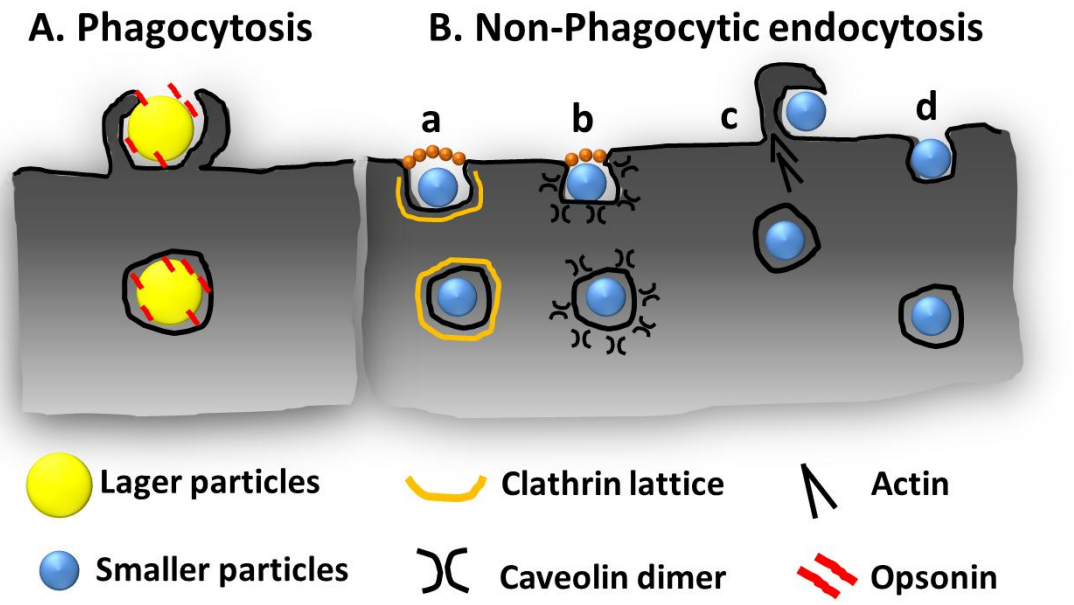

Figure 5 *The cellular internalization pathways of NPs and respective size limitations. (A) Larger NPs are internalized via phagocytosis. (B) Smaller particles can interact with the cells and be internalized through several mechanisms, such as clathrin-mediated endocytosis (a), caveolar-mediated endocytosis (b), macropinocytosis (c), and clathrin-independent and caveolin-independent endocytosis (d). Adopted from Ref.[145].*

2.3.1 The impact of the NP size on the cellular interactions

The size of NPs plays an important role in their cellular distribution, phagocytosis, and circulation half-life [145-147]. One of the benefits of the NPs is their ability to enter into the cells via endocytosis because of their similarity to many biomolecules in terms of size [148]. This internalization can be via the engagement of caveolin or clathrin pits, or other pathways independent of these proteins. For example, Hökstra *et al*. [149] studied the effect of the NP size on the internalization mechanism in nonphagocytic B16 cells and showed that while the internalization of NPs smaller than 200 nm was mediated through active clathrin-coated pits, caveolae-mediated pathway became dominant for NPs with a size of 500 nm. It has been currently accepted that NP size can also affect the uptake efficiency, and the subcellular distribution of the particles. For example, a size-dependent uptake has been observed for iron oxide [150], mesoporous silica [151], and gold [152] NPs.

NPs may also internalize into cells via passive uptake. For the cells lacking the endocytosis machinery (e.g., red blood cells; RBCs), passive transport is the only pathway for particle internalization. Hence, a quantitative understanding of the NP-membrane interaction is an important prerequisite for designing NPs with intentionally improved or suppressed cellular uptake. Table 2 shows some examples of studies that have revealed the paramount importance of the NPs' size on their biological behavior.

Table 2. *Examples of studies performed to clarify the role of the NPs' size in the cellular uptake.*

Active cellular uptake					
NP	**Size (nm)**	**Cell line**	**Techniques**	**Main conclusion**	**Ref.**
Au	2–100	SK-BR-3	CLSM[1]	40–50 nm: highest effect	[153]
TiO_2	5–80	A549	TEM[2], Light scattering μ-Raman	Uptake depends on overall size with hard corona	[154]
Iron oxide	8–65	RAW 264.7	ICP-AES[3]	37 nm: greatest uptake	[150]
Porous silica ($PSiO_2$)	30–280	HeLa	ICP-MS[4], CLSM	50 nm: maximum cellular uptake	[151]
SiO_2	32–83	Caco-2	CLSM	32 nm: enter nucleus and migrate faster	[155]
Polymer	50–300 150–500	Caco-2, HT-29 SMMC-7221	CLSM Fluorimetry	100 nm: maximum uptake Large NPs with high net charge uptake more efficient	[156] [157]
Passive cellular uptake					
$PSiO_2$	100–300	RBCs	TEM	Silanol groups affecting the hemolytic properties of MSNs	[158]
$PSiO_2$	100–600	RBCs	CLSM, TEM	Surface chemistry and particle size affect cellular uptake	[159]

[1]CLSM: Confocal laser scanning microscopy. [2]TEM: transmission electron microscopy. [3]ICP-AES: Inductively coupled plasma atomic emission spectroscopy. [4]ICP-MS: Inductively coupled plasma mass spectrometry.

2.3.2 The impact of the NP's surface charge on the cellular interactions

The surface charge of the NPs is one of the main properties that can significantly affect opsonization, phagocytosis, NPs' stability, cellular interactions, bloodstream circulation time and biodistribution of the NPs [108, 145]. The NP uptake by cells can be explained as a two-step process that starts by the NP binding to the cell membrane, and then, the internalization of the NPs via several mechanisms like pinocytosis, non-specific or receptor-mediated endocytosis [145, 160]. The attachment of the NPs to the cell membrane is highly affected by the surface charge of the NPs, as demonstrated and highlighted by a high number of *in vitro* and *in vivo* studies [157, 161, 162], showing different effects of the NPs' surface charge (e.g., positive, neutral or negative) on the cellular interactions of various NPs. For example, it has been demonstrated that the NPs such as silica nanotubes [163], quantum dots [164], iron oxide [165], and hydroxyapatite

[166] with positive zeta-potentials can be uptaken more compared to their counterparts with negative zeta-potential. This is possibly due to the stronger and higher contact of the positively charged NPs with the negatively charged cell membrane via electrostatic interactions, leading to a concentration- and time-dependent internalization of the NPs. Moreover, the screening of the intracellular distribution has indicated that some positively charged NPs possess endosomal escape ability after being internalized into cells, whereas neutrally and negatively charged NPs prefer the lysosomal co-localization [145]. A plausible explanation for this phenomenon is that the abundant positive charge of the NPs can cause the concurrent influx of chloride ions into the lysosome for the maintenance of neutral charge, leading to the physical rupture of the lysosomal membrane because of the osmotic swelling – a phenomenon known as the 'proton-sponge' effect. This behavior can increase the perinuclear localization of the positively charged NPs and enhance the drug concentration around the nucleus [167]. In contrast, some other studies have shown that the surface negatively charged NPs have more affinity for the cell membrane and can attach to the cationic sites of the cell membrane in the form of clusters because of their repulsion from the large negatively charged domains of the cell surface; thereby, there is a high capture of these particles by the cells compared to the ones with positive zeta-potentials [168, 169]. As a result of the different results reported in the abovementioned studies, there is a high probability that such findings may be due to the differences on the properties of the tested NPs, such as surface hydrophobicity, particle size, composition, or the cell type used, and not only owing to the surface charge of the respective NPs.

2.3.3 The impact of NP hydrophobicity and surface chemistry on the cellular interactions

Since the NPs' surface is in direct contact with the cells, the chemical composition at the surface of the NPs is very important in terms of the amount and the route of the NP uptake [170]. In addition, the surface properties of the NPs are the main factor affecting the type and number of biomacromolecules (e.g., proteins) adsorbed onto the surface of the NPs through hydrophobic/hydrophilic and/or electrostatic interactions. The surface composition of the NPs can also determine the thickness of the adsorbed bio-layer [171]. It has been reported that the hydrophobic NPs have a high affinity for the lipid bilayer of the cells, therefore their uptake is more facilitated compared to the hydrophilic particles [145]. Accordingly, the surface of the NPs can be modified with the aim to favor cellular interactions and improve internalization. For example, the surface conjugation of meso-2,3- dimercaptosuccinic acid of gold nanoshells has been shown to increase the cellular uptake in comparison to unmodified gold nanoshells [172]. It has also been found that the cellular uptake of PLGA coated with Vitamin E D-α-tocopheryl polyethylene glycol 1000 succinate is 1.4-fold higher than the PLGA NPs coated with polyvinyl acetate [173]. The 1-palmitoyl-2-oleoyl-sn-glycero-3-phospho-(1'-rac-glycerol) (POPG)-coated gold NPs have also demonstrated faster and greater uptake than PEGylated gold NPs in MCF-7 cells, mainly owing to the structural similarities between the cell membrane and POPG, which has led to strong interactions between the NPs and the cell surface [174]. In addition, it has been shown that the surface modification of the NPs with targeting

polymers can increase the interaction of NPs with the cells overexpressing the target receptors with high affinity. For example, Almeida *et al.* [175] have reported the covalent conjugation of an amide-modified hyaluronic acid (HA^+) derived polymer on the surface of undecylenic acid functionalized thermally hydrocarbonized PSi (UnTHCPSi) NPs for improving the cellular interactions and internalization due to the capability of the conjugated HA^+ NPs to bind to the CD44 receptors expressed on the surface membrane of the breast cancer cells. These NPs also showed very low polydispersibility, improved colloidal stability and high biocompatibility.

2.3.4 Correlation of the NPs' properties and the cellular cytotoxicity

Nanomaterials possess distinctive properties relative to bulk materials (e.g., high surface area-to-volume ratio) that can endow them with special mechanisms of toxicity. The cytotoxicity of the NPs has been described to be dependent on many factors, such as NP morphology, size, hydrophobicity, surface roughness, porosity, surface charge, concentration, and cell type used [1, 176]. For example, NPs' size plays a crucial role in the body's response to the NPs as well as in the biodistribution and elimination of the NPs after intravenous administration [177]. The NP's size may also modify the pathways of the endocytosis and cellular uptake [149]. One of the main reasons for the considerable impact of the NP size is the exponential enhancement in the surface area-to-volume ratio as the size of the NPs decreases, leading to the more surface reactivity of the nanomaterials [149]. *In vitro* investigation of the non-phagocytic cellular uptake of latex spheres have demonstrated slower endocytosis of larger spheres (>200 nm) compared to smaller ones (50 and 100 nm) [149]. It was also shown in non-phagocytic cells that the size reduction correlates with enhanced toxicity. *In vitro* studies have shown higher cytotoxicity of nanosized mesoporous silica and silicon, ZnO, Ag, Ni, dolomite, and polystyrene compared to the respective microparticles [178]. Interestingly, microparticles have shown stronger interaction with phagocytic cells, such as monocytes and macrophages, than NPs. For example, higher cellular damage has been reported for silica microparticles than for NPs in immune cells [3].

Regarding the correlation of the NP's morphology and cellular toxicity, it is generally accepted that fiber-shaped NPs of a given material are more cytotoxic than spherical particles. For example, carbon nanotubes have revealed greater toxicity than fullerenes [178]. While NP's hydrophobicity and surface charge are often strongly linked to each other, at the same surface charge a higher hydrophobicity leads to more cytotoxic responses compared to the respective hydrophilic particles [179]. Degradability of the material is also a determinant parameter for acute and long-term cytotoxicity. The main problem with non-degradable materials is their accumulation in organs or inside cells where they can cause damaging effects, similar to that of lysosomal storage diseases [180]. Biodegradable materials may also lead to unexpected cytotoxicity owing to the release of toxic degradation products to the biological milieu [2].

Despite all recent progresses in nanotoxicology, this is still a relatively new and challenging field as different factors may work synergistically to cause toxicity. Currently, plenty of reports have focused on the acute toxicity of nanomaterials and less attention has

been paid to long-term toxicity. In this context, the screening of chronic exposure is critical to understand the toxicology of nanomaterials *in vivo* [181].

The toxicity of nanomaterials can occur through different mechanisms. One of the main mechanisms of nanotoxicity is free radical formation and subsequent induction of oxidative stress, causing damage to biological components through oxidation of proteins, lipids and DNA [182]. Oxidative stress can also cause inflammation through upregulation of kinases involved in inflammation, activator protein-1, and redox sensitive transcription factors (e.g., NF-κB) [182, 183]. Intracellularly, the interactions of the nanomaterials with the cell nucleus and mitochondria are considered as key sources of cellular damage. As reviewed by Unfried *et al*. [184], many types of NPs, such as block copolymer micelles, silver-coated gold NPs, carbon nanotubes, and fullerenes, are able to be localized inside the mitochondria, and induce ROS formation and apoptosis. Other mechanisms for cellular toxicity induction include cell-cycle arrest, nuclear DNA damage, and mutagenesis [1]. Additionally, since nanosized materials are inherently quite complex, many unpredicted interactions may arise with biological components. Therefore, appropriately validated analytical methods and carefully designed experimentations are needed to clarify the mechanisms of toxicity so that nanoparticles can be safely used in biomedical applications.

2.4 Porous silicon (PSi) nanoparticles

Over the last decade, the application of PSi NPs in medicine has been highlighted because of the immense advances in the preparation protocol, surface modification, ability of controlling the physicochemical properties of the particles, as well as understanding the biological interactions of this material [185, 186]. The most remarkable characteristics of the PSi nanomaterials are their high surface-to-volume ratio, large surface area (300 to 700–1000 m^2/g) and pore volume (0.9 cm^3/g), possessing a stable and rigid framework with high chemical, mechanical and thermal stability, high biocompatibility, biodegradability, and easy scale-up properties [187]. These advantageous benefits have made the PSi NPs promising reservoirs for drug delivery applications with the aim to overcome the drawbacks of conventional pharmaceutical formulations. Another advantage of the PSi particles is the ability of controlling their pore size to achieve controlled release kinetics [26, 188-190]. In addition, it is facile to modify the surface of the PSi NPs with different functional groups with the aim to provide an opportunity for further modification with biomolecules or polymeric materials to tailor drug release, to target a specific tissue and to enhance cellular interactions [191, 192].

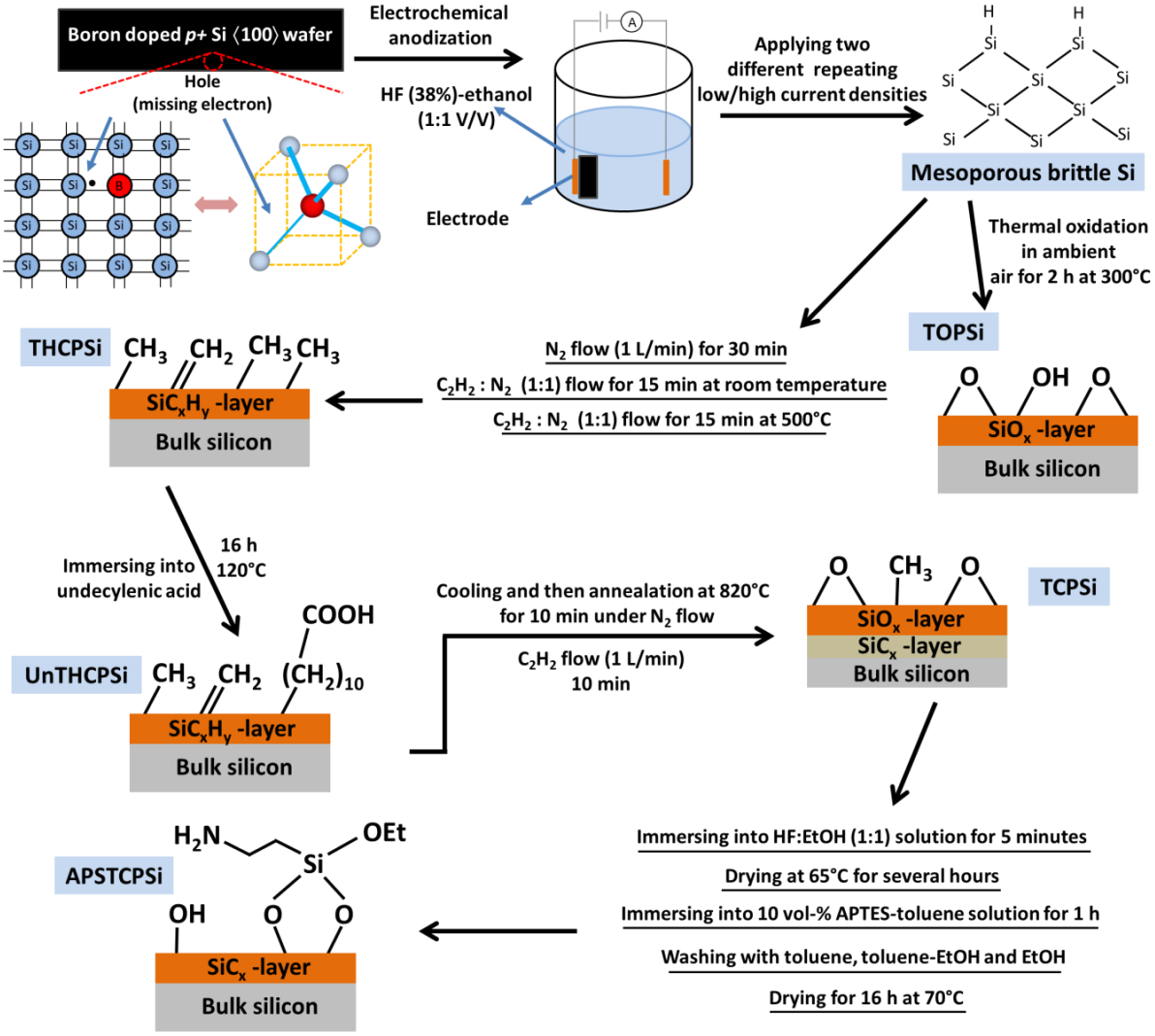

Figure 6 *The protocol applied for the preparation of PSi NPs with different surface chemistries [186, 188, 193-195]. HF: hydrofluoric acid, EtOH: ethanol, TOPSi: Thermally oxidized PSi, THCPSi: Thermally hydrocarbonized PSi, UnTHCPSi: undecylenic acid functionalized thermally hydrocarbonized PSi, TCPSi: Thermally carbonized PSi, APSTCPSi: (3-aminopropyl)triethoxysilane-functionalized thermally carbonized PSi. The detailed explanation of the protocols can be found in the section 4.1.*

Since the freshly etched boron doped *p*+ Si ⟨100⟩ wafers react very slowly with ambient air, electrochemical anodization is applied to convert the original surface of the PSi to hydrogen terminated (Si-H_x) structures that are very reactive even in the dry ambient air [187]. These reactive hydrogen terminated PSi structures can be functionalized with different chemical groups according to the very well developed protocols set up for their surface modification [186, 188, 193, 194] (Figure 6), leading to the formation of stable PSi NPs with new surface functional groups, hydrophilicity and biological effects [5, 194, 196, 197].

In this section, some significant therapeutic aspects of different PSi drug delivery systems will be discussed and the undeniable impact of these particles in the forthcoming technological progress of nanomedicines will be highlighted.

2.4.1 Drug loading methods in the PSi particles

PSi NPs have been established as versatile platforms for drug delivery applications. By loading drugs into the porous structures of these particles, it is possible to control drug release or deliver the appropriate concentrations of therapeutic molecules to the suitable locations in a controlled manner [190, 198, 199]. The most common methods for loading drugs within the PSi NPs include covalent attachment, physical adsorption into the inner pore walls, solvent evaporation, or drug engulfment by oxidation [200]. In addition to the parameters, such as surface charge, pore size, hydrophilicity/hydrophobicity, surface chemistry, and physicochemical properties of the loaded molecule, loading methods can also affect the drug release profiles of the PSi NPs [4, 186, 200]. Covalent attachment is the most robust method for drug loading into the porous structures. Typically, PSi NPs with functional carboxyl or amine groups on their surface can be directly used for covalent based drug loading; however, PEG linkers can also be used as an alternative approach for successful covalent drug loadings [201]. Different reports have shown the application of this method to attach different molecules, such as proteins and enzymes to the surface of the PSi NPs [202] or to load amino acids and anticancer drugs within the PSi matrix [203]. In the covalent attachment method, the payload release can occur only after the breakage of the covalent bonds or the degradation of the supporting PSi matrix, achieving a prolonged drug release. Since the main drawback of this method is the possible inactivity of the loaded molecule, it is essential to conduct relevant assays to confirm the activity of the drugs following the release process [200].

In contrast to the covalent attachment, drug release can be faster when a physical adsorption method (simple immersion of the PSi NPs in a drug solution) is used for drug loading. Loading of drug compounds such as ibuprofen, griseofulvin, ranitidine, furosemide and bovine serum albumin into the PSi structures has been reported using this loading method [204, 205]. Since the bare PSi particles are negatively charged, they can spontaneously adsorb positively charged molecules and lead to higher drug loading degrees of these compared to the negatively charged drug molecules. The hydrophobicity of the PSi NPs can also be very beneficial for the high adsorption and delivery of hydrophobic molecules, such as dexamethasone [206] and porphyrins [207]. This technique is very desirable as it can be performed without exposing the particles or drugs to harsh chemical conditions during the loading process [201]. Since it is not feasible to reach long term release profiles with this technique, it can be used typically when rapid drug delivery rates are required. However, a recent report has shown that physical loading of an anticancer drug, sorafenib, can lead to a very long lasting drug release from the PSi NPs, demonstrating the impact of the drug's physicochemical property on the drug release kinetics [208]. In addition, targeted delivery of PSi particles physically loaded with drug molecules has also been reported. For example, Gu *et al*. have shown the simultaneous loading of super-paramagnetic iron oxide NPs and the anticancer drug, doxorubicin, within PSi microparticles via simple adsorption to achieve magnetically guided delivery of the drug [209].

The oxidation based method for drug loading rely on a process that results in the shrinkage of the pores after drug loading, because of the extra volume of the oxygen atoms on the surface of the particles, leading to an efficient drug entrapment inside the pores.

Since oxidation increases the surface stability of the PSi particles, this method has been applied for many studies [210]. Figure 7 shows a schematic figure of all the abovementioned methods for the loading of drugs inside the PSi particles.

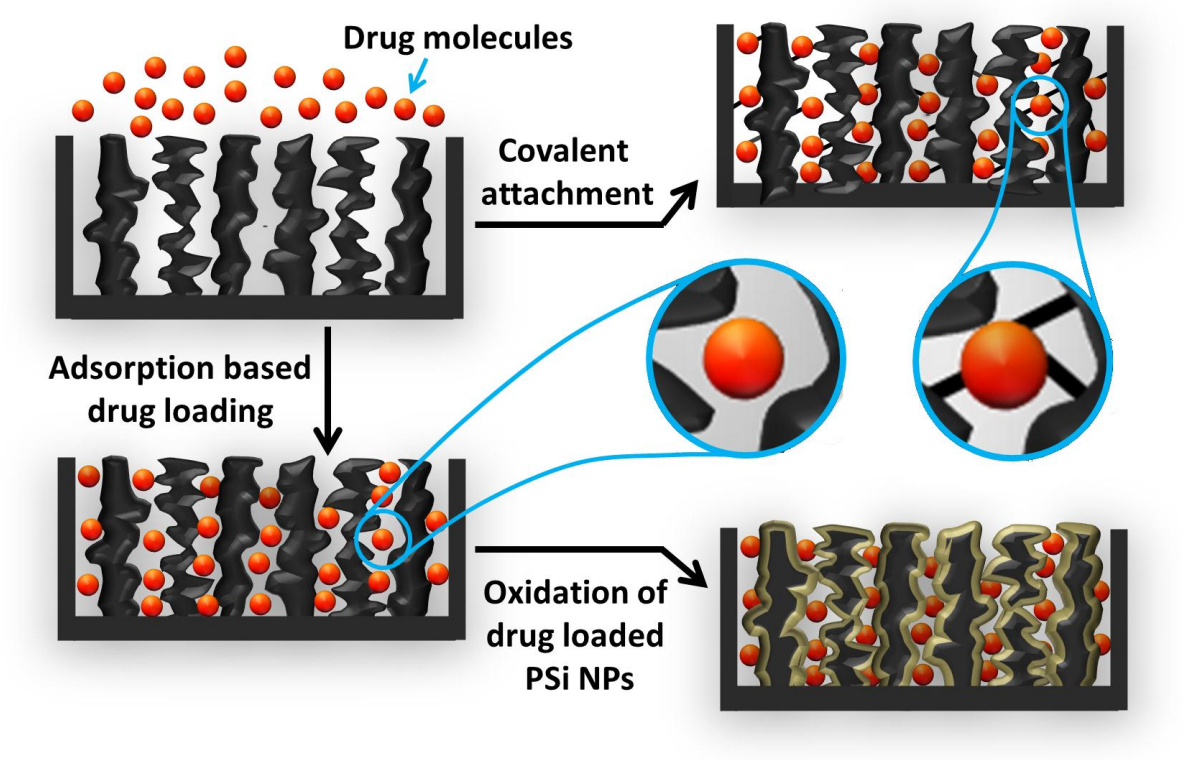

Figure 7 *The most relevant protocols applied for the loading of different drugs into the PSi particles. Drug molecules can be physically loaded, covalently conjugated or locked inside the pores via the oxidation of the PSi because of pore shrinkage resulted from the volume expansion.*

2.4.2 PSi NPs for drug delivery

One of the main challenges of the current drug delivery formulations are the poor solubility properties of the drug molecules, inefficient drug release and rapid clearance of the drug molecules from the body. Accordingly, overcoming all these problems and improving the bioavailability of the drug molecules at the site of interest over a predefined period of time are the main features that a drug delivery system should possess [211, 212]. One of the major focuses of the PSi NPs for drug delivery applications has been devoted to the improvement of the bioavailability by increasing the water solubility of the drugs [185, 187, 204]. When drug molecules are localized inside the pores of PSi, the confined space of PSi NPs avoids the drug to revert back from an amorphous state into its crystalline form, resulting in higher dissolution rates [204]. For example, Bimbo *et al*. [213] have used thermally hydrocarbonized PSi (THCPSi) NPs to load saliphenylhalamide for the inhibition of influenza A virus infection. Since the main drawback of this antiviral drug is the poor water solubility, the possibility to minimize the crystallinity of the drug molecules was investigated by loading the drug inside the THCPSi NPs. Interestingly, the results

showed an efficient inhibition of influenza A infection in human retinal pigment epithelium and Madin-Darby canine kidney cells after the drug was released from the PSi NPs. The enhanced solubility of griseofulvin [186], indomethacin [214] and intraconazole [185] has also been reported.

Since one of the main drawbacks of many anti-cancer drugs is their very poor water solubility, PSi particles have attracted many interests for this area of research. For example, cisplatin loading inside 1,12-undecylenic acid modified PSi particle resulted in significantly higher toxicity than that of free cisplatin in human ovarian cancer cells, owing to the improved solubility [215]. Sustained release of anticancer drugs has been also investigated by PSi particles. In this case, covalent loading of daunorubicin within 1-undecylenic acid modified PSi particles resulted in sustained release of the drug for more than 30 days [216]. To compare the impact of loading methods, the release of doxorubicin after covalent and physical loading into 10-undecylenic acid functionalized PSi particles has been studied [217]. Covalently loaded particles showed drug release once the covalent bond was broken or the PSi was oxidized/degraded, exhibiting no initial burst release and continuous slow release over five days. In contrast, physically adsorbed doxorubicin demonstrated significant burst release in the first 2 h and a complete release within 24 h. This study showed that in addition to the effect of the surface chemistry and pore size of the PSi particles on the drug release rate (by controlling the interactions of drug molecules with the internal and external surface of the particles), drug loading methods have also a significant impact on the drug release profiles.

PSi particles have also been investigated for the sustained delivery of drugs with very short half-lifes and narrow therapeutic windows. For example, the clinical applications of daunorubicin, a model drug suggested for the treatment of proliferative vitreoretinopathy, has been hindered owing to the needs for frequent intravitreal injections over time to obtain sustained treatment. To overcome this problem, several studies have applied PSi particles for long-lasting presence of the drug at the disease site [218, 219]. For example, Hou *et al*. [219] have shown the sustained drug release after a single intravitreal injection of the nanoformulation. They also showed high biosafety of the applied PSi NPs in rabbit eyes [220].

The delivery of protein molecules using PSi NPs is also an emerging area of research. De Rosa *et al.* [221] have used agarose hydrogel matrix to modify the surface of the PSi particles with the aim to avoid repeated administrations of protein drugs (bovine serum albumin was used as a model drug in this study) over a long period of time by enhancing the ability to sustain the drug release, as well as to preserve the molecular stability and the integrity of the loaded protein; thus, influencing the intracellular nucleus delivery, and enhancing the biocompatibility of the formulation. Since the main challenge of current protein formulations is the instability for oral administration because of the enzymatic degradation and poor intestinal penetration, PSi NPs have also been applied to preserve the bioactive structure of the proteins and improve the oral bioavailability of drugs [222]. For example, glucagon like peptide-1 (GLP-1) loaded inside chitosan-coated UnTHCPSi NPs showed sustained drug release and high permeation across the intestinal *in vitro* models, suggesting that these NPs are promising carriers for the oral delivery of GLP-1 [223]. The potential of the THCPSi particles for the oral delivery of melanotan II (MTII, a food intake inhibitor) [224] and ghrelin antagonist (GhA) [225], have also been investigated. The

results showed that while the inhibition of food intake was reduced after 4 h for GhA, GhA loaded particles could retain the food inhibition for up to 18 h. Kovalainen *et al*. [226, 227] have compared loaded and free PYY3-36, a peptide to reduce food intake, in three different PSi NPs, thermally oxidized PSi (TOPSi), THCPSi, and UnTHCPSi NPs. The *in vivo* results showed that while the free PYY3-36 were removed from the bloodstream within 12 h, all the examined PSi NPs were able to extend peptide clearance for up to 96 h [227].

The major obstacle of using oligonucleotides as therapeutic agents is the low intracellular delivery of these negatively charged biomolecules. PSi has been recently suggested as a potential material for the delivery of oligonucleotides [228-230]. Rytkönen *et al*. [230] have used positively charged aminosilane-modified thermally carbonized PSi NPs as oligonucleotide carriers by loading splice correcting oligonucleotides (SCOs) into the pores of PSi. They have shown a drug loading degree of 14.3% (w/w) and 100% loading efficiency within 5 min, achieved by the high electrostatic interactions between particles and oligonucleotides. They demonstrated the successful delivery and release of SCOs inside cells in its biologically active form when formulated together with cell penetrating peptides. Wan *et al*. [192] have also loaded small interfering RNA (siRNA) biomolecules into the PSi NPs to protect them from degradation and increase the cellular uptake. They could load around 7.7 μg of siRNA per mg of PSi NPs in 30 min. This formulation could efficiently induce cell apoptosis and necrosis (33%) by downregulating the target mRNA (~40%) and subsequent protein expression (31%), suggesting that this new delivery system may pave the way towards developing new tumor therapeutic approaches. Zhang *et al.* [231] have also used PSi particles with a pore size in the range of 20–60 nm to modify surface functionality of the pores with PEI and subsequently complex it with siRNA. It was shown that the gradual degradation of the PSi particles under physiological conditions can lead to the sustained release of the spherical PEI/siRNA nanocomplexes. In addition, *in vitro* experiments showed that the siRNA could internalize into the cells and effectively silence the ataxia telangiectasia mutated genes of breast cancer.

To precisely tune the drug release profiles, a so-called "gate-keeping" approach can be applied by attaching a responsive polymer to the surface of the PSi nanostructures [232-235], thus modifying the drug release kinetics. Moreover, coating with non-biologically responsive polymers can modify the drug release rate by altering the diffusion process of the drug through the polymer matrix [236]. Some examples of the coating strategies used for *in vitro* studies of PSi platforms include chitosan to slow down the release of insulin [237], bovine serum albumin capping for sustain release of antibiotic vancomycin [238] and poly(N-Isopropylacrylamide) for temperature responsive release of camptothecin [239]. One of the main considerations for preparing coated PSi particles is using polymers with high biocompatibility and biodegradability. In addition to the significant effect of the polymeric coating on the sustained drug release by providing an obstructive layer on the surface of the particles, the coating layer can also shorten drug release rate by minimizing the oxidization of porous surface layers of the particles, and subsequent degradation [201]. Moreover, polymeric coating can be used for enhanced drug permeability across biological barriers. For example, Shrestha *et al.* [222] have shown ca. 20-fold increase in the permeation of insulin across an *in vitro* intestinal monolayer model compared to the pure

insulin after encapsulation within chitosan coated PSi NPs. In addition to the coating strategy, encapsulation of PSi NPs within other materials can render new properties to the PSi particles. For example, Liu *et al.* [240] have recently fabricated a novel nanocomposite by the encapsulation of THCPSi NPs within solid lipid nanoparticles for drug delivery applications. This formulation showed greatly improved cellular safety of the PSi NPs, highly efficient drug encapsulation, prolonged drug release and very high stability because of the altered surface smoothness of the THCPSi NPs. The incorporation of drug-containing NPs within the PSi particles has been suggested as a promising strategy for pronounced and sustained therapeutic effect. For example, Blanco *et al.* [241] have demonstrated the favorable encapsulation of paclitaxel loaded poly(ethylene glycol)-block-poly(ε-caprolactone) micelles within the pores of PSi particles, resulting in delayed drug release and significant suppression of tumor growth in mice bearing MDA-MB-468 breast cancer cells.

In addition to the all abovementioned drug payloads in PSi NPs, metals or metal oxides particles have also been encapsulated into PSi NPs to generate a potential magnetic resonance imaging contrast agent or to develop theranostic drug delivery systems [242, 243]. All these examples show the high potential of PSi carriers as promising materials for drug delivery applications.

2.4.3 Immunotherapeutic applications of PSi particles

Although nanomaterials have shown promising results for the treatment of various diseases, they still encounter several challenges such as possible toxicity, rapid clearance, low accumulation in the target site, and short-term therapeutic responses, minimizing the best outcome of the therapeutic nanosystems. Therefore, there is a need for using NPs in a different way to get more efficient therapeutic responses. A novel recently suggested approach is immunotherapy through the development of nanoadjuvants and nanovaccines, an alternative strategy to improve the effect of NPs through intentional activation of the immune system to fight against various diseases [13, 89]. PSi NPs are suggested as suitable reservoirs for antigens because of facile loading capability in aqueous media, without the use of organic solvents. For example, *Gu et al.* [21] have used FGK45 (an agonist antibody of CD40) engineered PSi NPs to activate APCs. This immunostimulatory antibody can bind to the receptors of CD40 on the surface of APCs, and subsequently, activate B cells 30–40-fold greater than the stimuli induced by the same concentration of free FGK45. They also observed very low uptake of the bare PSi NPs in the mouse bone marrow-derived DC compared to the FGK loaded counterparts, exhibiting the high ability of the antibody for DC targeting. Marez *et al.* [244] have also shown superior *ex vivo* cellular uptake of the monophosphoryl lipid A (MPL) or lipopolysaccharide (LPS) conjugated PSi microparticles by murine bone marrow-derived DCs and enhanced secretion of immunostimulatory cytokines compared to the free MPL and LPS. It was also shown that enhanced immunostimulation can independently induce anticancer effect and also increase the anti-tumor efficacy of doxorubicin nanoliposomes after the co-administration in mice. For this purpose, Marez *et al.* [245] showed that the injection of PSi-bound MPL results in the enhanced secretion of the Th1 associated cytokines, IFN-γ

and TNF-α, while decreasing the anti-inflammatory cytokine IL-10, leading to the increased tumor suppression effect of low dose doxorubicin nanoliposomes via synergized immunotherapy. Increased DC activation and sustained drug release of the loaded cargo have raised promises for using PSi particles to induce potent protective immunity against the immune system related diseases without the need for repeated doses of the formulation.

2.4.4 Cellular uptake and trafficking

In order to fully understand the interactions of the PSi NPs with the cells, it is crucial to improve the knowledge regarding the biological properties of the cells as well as the subsequent effects of the NPs' physicochemical properties on the cellular compartments [246]. Cell membrane is comprised of proteins, lipids, and receptors, which render a negative charge to the cell surface [26]. Therefore, the surface charge of the PSi NPs is one of the main parameters with a considerable role in the cellular trafficking of the NPs [178]. Other parameters, such as concentration, exposure time, particle size, shape, surface chemistry, and cell type have also a high impact on the cellular uptake of the NPs [247-249]. For example, while it is reported that the cellular uptake of $PSiO_2$ NPs take place via a clathrin-mediated endocytosis, guanidinium- and amine-functionalized $PSiO_2$ NPs have shown clathrin- and caveolae-independent endocytosis [250, 251], and folic acid (FA)-functionalized $PSiO_2$ particles have demonstrated FA receptor-mediated endocytosis [252, 253].

It has been demonstrated that the endocytosis of PSi NPs leads to the formation of a vesicle, which captures the NPs and internalize them into the endosome. Then, the endosome content can either be recycled back to the extracellular environment or transported to the secondary endosomes that fuse with lysosomes [254]. The escape of PSi NPs from the endosomes can lead to drug release in the cytosol, a desirable phenomenon to get high therapeutic efficiency of the nanoformulations. Generally, the positively charged particles can more efficiently escape from the endosomes than the negatively charged NPs, which usually remain trapped within the endosomes [255, 256]. Accordingly, a strategy that can be suggested is using the positively charged polymers with amine groups to create a proton osmotic influx inside the endosome and break-down the endosome via proton sponge effect [257]. For example, Tomoya *et al.* [258] have recently developed cationic polyaspartamide derivatives with a regulated number and spacing of positively charged amino groups in the side chains to improve the cytosolic delivery of siRNA via an endosomal escape mechanism. Mingzhen *et al.* [231] have also developed polyethyleneimine (PEI) modified PSi particles complexed to siRNA with the aim to exert gene silencing effect in human breast cancer cells via the escape of the particles from the late endosomal/lysosomal compartments.

Despite great advances in the delivery of different drugs by various NPs, cancer therapy still suffers from the insufficient therapeutic concentration of the drug at the target cell/tissue owing to the lack of selectivity. Therefore, it is favorable to construct targeted nano-sized particles with a high potential of extravasation [17, 33, 139, 250, 253, 259]. Currently, many research efforts have tried to generate cell targeted NPs with the aim to

selectively guide them to the surface membrane of the cells and trigger receptor-mediated endocytosis [33, 139]. Nevertheless, problems associated to this approach still exist because of the limited attachment sites on the surface of the NPs as well as the possibility of losing the stability during the functionalization steps [26]. Among the astonishing benefits of the PSi NPs, the ability of the surface functionalization with various chemical groups and targeting moieties is one of the most favorable properties reported in the literature, highlighting the potential of these relevant nanoplatforms for a wide range of medical applications [21, 200, 201, 234, 238]. Emilie *et al.* [16] have shown successful conjugation of MLR2, mAb528 and Rituximab antibodies on the surface of PSi NPs for targeting neuroblastoma, glioblastoma and B lymphoma cells, respectively. *Kenji et al.* [191] have also demonstrated the effective targeting of Ly6C Ab decorated PSi nanocarriers to pancreatic cancer cells. They showed the accumulation of intravenously injected nanocarriers at the tumor associated endothelial cells within 15 min. Interestingly, they also observed the accumulation of 9.8 ± 2.3% of Ly6C targeting nanocarriers in the pancreatic tumor as opposed to 0.5 ± 1.8% with non-targeted nanocarriers after 4 h. In all these approaches, it is crucial to retain the binding activity of the targeting ligand by avoiding the denaturation of the protein structure during the procedure used for conjugation or drug loading [260].

In addition to Ab, targeting peptides have also been applied for the active targeting of PSi NPs. Kinnari *et al.* [261] have proposed a tumor homing peptide as a potent targeting ligand to enhance the delivery of PSi NPs to the breast cancer site. They functionalized PSi NPs with a peptide targeting mammary-derived growth inhibitor (MDGI) receptor, which showed ~9-fold higher accumulation in the tumour site compared to the control THCPSi NPs after intravenous injections into nude mice bearing MDGI-expressing tumours.

Since some reports have shown high accumulation of the nanoparticles on the surface of cancer cells, the interest has already been shifted towards strategies to enhance cellular internalization of the NPs after attachment to the surface of cancer cells [262, 263]. In this regard, Wang *et al.* [208] have demonstrated the enhanced cellular uptake of the PSi NPs in EA.hy926 cells after applying a simple and efficient method based on copper-free click chemistry to introduce RGD cell penetrating peptides on the surface of the PSi NPs. With this strategy, a significant increase in the amount of particles localized inside the cells was demonstrated *in vitro*.

In addition to the enhancement of the cellular interactions with the target tissue using the aforementioned strategies, the therapeutic efficacy of drug-delivery PSi carriers depends on the ability of evading the immune system. In this context, Parodi *et al.* [264] have suggested biomimetic hybrids of PSi particles coated with purified cellular membranes of leukocytes for the inhibition of particle opsonization and phagocytosis, enhancing the circulation time of the particle and improving the accumulation in the tumor site through receptor–ligand interactions with endothelial cells.

All the above described strategies and surface modification methods for PSi NPs demonstrate the promising potential of these NPs as the next generation of nanomedicines.

3 Aims of the study

Despite steadily increasing insights on the application of PSi NPs for therapeutic applications, less attention has been paid to the impact of the inherent physicochemical properties of these particles on the biological responses and on the success or failure in the therapeutic applications considered for the developed nanoformulations. Given to the important role of the immune system on the fate of the administered NPs, the aim of this study was to understand the main toxic effects of PSi NPs on different type of cells and also to understand the impact of the chemical structure of PSi on the immunostimulative responses. Furthermore, the development of PSi-based NPs for chemo-immunotherapeutic purposes and increasing cellular trafficking in cancer cells were among the main aims of this dissertation.

The specific objectives of this dissertation were as follows:

1. To assess the impact of the surface chemistry of the PSi NPs with similar size, surface area and pore volume on the immunotoxicity, hemocompatibility, and change in the biochemical parameters and histology of tissues *in vivo* **(I)**.

2. To understand how the non-toxic concentrations of the PSi NPs with different surface chemistries may affect the immune system and work as nano-immunostimulants by the induction of CD80, CD83, CD86, and HLA-DR co-stimulatory ligands activation on DCs, T cell proliferation, T cell differentiation, and cytokine secretion **(II)**.

3. To evaluate the effect of surface monoclonal antibody-functionalization of drug-loaded PSi NPs on the cancer cell targeting, cellular uptake, and simultaneous chemo- and immunotherapy via sustained anticancer drug release, ADCC activation and cytokine secretion **(III)**.

4. To evaluate the impact of the surface polymeric modification of the PSi NPs on the cellular internalization, endosomal escape, drug release, as well as colloidal and plasma stability of the NPs **(IV and V)**.

4 Experimental

4.1 Fabrication and characterization of the PSi NPs

Free-standing multilayer PSi films were electrochemically anodized from monocrystalline, boron doped *p*+ Si ⟨100⟩ wafers with a resistivity of 0.01–0.02 Ω.cm using a 1:1 (v/v) hydrofluoric acid (HF, 38%)–ethanol (EtOH) electrolyte. The multilayer structure was formed by applying a repeating pulsed low/high etching profile, designed to create fracture planes at desired intervals. The multilayer film was lifted off from the substrate by increasing the etching current abruptly to the electropolishing region. The multilayer films were then functionalized with the methods described in Table 3 in order to obtain different surface chemistries, and finally, wet milled with a high energy ball mill to produce the PSi NPs.

Table 3. *Chemical modification methods used for the PSi multilayer films to obtain different surface chemistries.*

Surface chemistry	Chemical modification method	References
TOPSi	The multilayer films were thermally oxidized in ambient air for 2 h at 300°C **(I and II)**.	[186]
THCPSi	Fresh PSi multilayer films were inserted into a quartz tube under N_2 flow (1 L/min) for at least 30 min in order to remove residual moisture and oxygen. An acetylene (C_2H_2) flow (1 L/min) was added to the N_2 flow for 15 min at room temperature (RT) followed by a heat treatment for 15 min at 500°C under the 1:1 (vol.) N_2/C_2H_2 flow. The THCPSi films were allowed to cool back to RT under N_2 flow **(I and II)**.	[194]
UnTHCPSi	UnTHCPSi films were functionalized from THCPSi films by immersing them into undecylenic acid for 16 h at 120°C **(I–IV)**.	[227]
TCPSi[1]	TCPSi films were functionalized from THCPSi films by continuing the carbonization process after the films had cooled back to RT under N_2 flow. C_2H_2 flow (1 L/min) was added for an additional 10 min after which the films were annealed at 820°C for 10 min under N_2 flow. The TCPSi films were allowed to cool back to RT under N_2 flow **(I and II)**.	[197]
APSTCPSi[2]	APSTCPSi films were functionalized from TCPSi films by immersing them into HF:EtOH (1:1, vol.) solution for 5 min and drying them at 65°C for several hours.	[193]

	The HF-activated TCPSi films were immersed into 10 vol-% APTES-toluene solution for 1 h at 25°C. The solution was removed, and the APSTCPSi films were successively washed with toluene, toluene-EtOH and EtOH before drying for 16 h at 70°C **(I, II and V)**.

[1]TCPSi: Thermally carbonized PSi, [2]APSTCPSi: (3-aminopropyl)triethoxysilane-functionalized thermally carbonized PSi

4.1.1 Preparation of the UnTHCPSi-polyethylenimine (Un-P) NPs (II and IV)

To pepare Un-P NPs, the carboxyl groups of UnTHCPSi NPs were covalently conjugated to the amine groups of branched polyethylenimine (PEI; average Mw∼25,000). To successfully accomplish the covalent conjugation, 1.5 mg of UnTHCPSi NPs was dispersed in 4 mL of 10 mM 2-(N-morpholino) ethanesulfonic acid (MES) saline buffer at pH 5.2. Then, 7 and 6 mg of 1-ethyl-3-[3-dimethylaminopropyl] carbodiimide hydrochloride (EDC) and *N*-hydroxysuccinimide (NHS) were added, respectively, and mixed for 2 h to activate the carboxyl groups of the UnTHCPSi NPs. Next, the activated surface of the PSi NPs were exposed to an excess of hyper-branched PEI with a ratio of 1:10 (NPs:polymer) and vigorously stirred (1140 rcf) at RT overnight. The excess of unconjugated polymer was removed by extensively rinsing of the modified particles with MilliQ-water. Finally, the NPs were re-suspended in Hank's balanced salt solution−(4-(2-hydroxyethyl)-1-piperazineethanesulfonic acid) (HBSS−HEPES) buffer (pH 7.4).

4.1.2 Preparation of the APSTCPSi-poly(methyl vinyl ether-alt-maleic acid) (APM) NPs (II and V)

For the chemical conjugation, poly(methyl vinyl ether-alt-maleic anhydrate) (PMVE-MAh; average Mw ∼216,000) was first hydrated and changed to the poly(methyl vinyl ether-alt-maleic acid) (PMVE-MA) by heating at 70 °C for 3 h under stirring speed of 1425 rcf in MES buffer (pH 5.2, 10 mM). Then, 10 mg of the PMVE-MA was dissolved in 6 mL of MES buffer and mixed with 9.6 and 8 mg of EDC and NHS, respectively, for 2 h in the dark to activate the carboxyl groups of the polymer. Finally, the activated polymer chains were exposed to the APSTCPSi NPs with a ratio of 5:1 (polymer:NPs) and vigorously stirred (1140 rcf) at RT overnight. The excess of unconjugated PMVE-MA polymer was rinsed with MilliQ-water and removed before re-suspending APM NPs in HBSS−HEPES buffer (pH 7.4).

4.1.3 Preparation of anti-CD326 antibody-conjugated UnTHCPSi NPs (III)

The covalent conjugation of CD326 antibody (Ab) onto the surface of the UnTHCPSi NPs was performed using EDC/NHS chemistry. Briefly, 100 μg of the NPs was dispersed in 1.5

mL of the 10 mM MES (pH 5.5), followed by the addition of 1.75 mg of EDC and 1 mg of NHS solution. The NP suspension was then left in the dark and under agitation for 2 h using a magnetic stirrer. Next, to remove unreacted EDC and NHS, and to separate the activated UnTHCPSi NPs, centrifugation of the NPs was performed at 21382 rcf for 5 min. 100 µg of the surface activated UnTHCPSi NPs were then suspended in 1 mL of 10 mM MES (pH 6.5) and 10 µg of CD326 Ab was added drop wise and stirred for 1 h. Afterwards, the unconjugated CD326 Ab was removed by centrifugation and the NPs were washed twice with phosphate buffered saline (PBS) buffer.

To identify the amount of Ab-conjugated to the NPs, CD326-FITC Ab (Sigma-Aldrich, Saint Louis, USA) was used in the conjugation procedure and the final sediment and supernatant were collected to measure the amount of conjugated and free Ab by fluorescence using a Varioskan Flash (Thermo Fisher Scientific Inc., USA).

4.1.4 Formation of UnTHCPSi-PEI-PMVE-MA (Un-P-P) nanocomposites (IV)

The preparation of Un-P-P nanocomposites was achieved by the addition of PMVE-MA copolymer onto the Un-P NPs. Briefly, PMVE-MA copolymer was first obtained from PMVE-MAh by dissolving the later one in HBSS–HEPES buffer (pH 5.2) at 70°C for 3 h. Next, PMVE-MA polymer was activated for 2 h by addition of EDC/NHS to the solution, and subsequently, added with a ratio of 1:1 to Un-P NPs dispersed in the same buffer. The obtained polymer-conjugated PSi NPs were washed twice with MilliQ-water by repeated centrifugation at 21382 rcf for 5 min to ensure that no ungrafted polymer or free reagents were present in the final obtained product. The NPs were finally dispersed in HBSS–HEPES buffer (pH 7.4).

4.1.5 Characterization of the PSi NPs (I–V)

The hydrodynamic diameter (Z-average), polydispersity index (PdI) and surface zeta-potential of the bare, polymer-conjugated and Ab-functionalized PSi NPs **(I–V)** were measured using Zetasizer Nano ZS instrument (Malvern Instruments Ltd., UK). For the size measurements, the NPs were dispersed in Milli-Q water prior to loading inside a disposable polystyrene cuvette (SARSTED AG & Co., Germany). The surface zeta-potential of the NPs was measured by using disposable folded capillary cells (DTS1070, Malvern, UK). All measurements were repeated at least three times.

The morphology of the NPs **(II–V)** was also evaluated using a transmission electron microscope (TEM; Jeol JEM-1400, Jeol Ltd., Japan). For this purpose, 2 µL of the NP suspension (50 µg/mL) was dropped on carbon-coated copper TEM grids (150 mesh; Ted PELLA Inc., Redding, CA) and then allowed to dry at RT overnight.

The chemical composition of all the bare, polymer-conjugated and Ab-functionalized PSi NPs were studied by attenuated total reflectance Fourier transform infrared (ATR–FTIR) **(II–V)** using a Bruker VERTEX 70 series FTIR spectrometer (Bruker Optics, Germany) with a horizontal ATR sampling accessory (MIRacle, Pike Technology, Inc.). The ATR–FTIR spectra were recorded in the wavenumber region of 4000−650 cm^{-1} with

a resolution of 4 cm^{-1} at RT using OPUS 5.5 software. Prior to each measurement, all the NPs were left at RT to dry for 48 h.

The impact of the human plasma on the stability of the polymeric functionazilationed NPs was also evaluated **(IV–V)**. For this purpose, 300 µg of the bare and polymer-conjugated PSi NPs were dispersed in 200 µL of PBS (pH 7.4). The NPs were then mixed with 1500 µL of human plasma and kept at 37°C for 2 h under stirring at 1140 rcf. Sampling (200µL) was performed at different pre-determined time intervals (15, 30, 60, 90 and 120 min) to measure the particle size and PdI using a Zetasizer Nano ZS instrument. Anonymous human plasma samples were obtained from the Finnish Red Cross Blood Service.

4.1.6 Drug loading and release (III and IV)

Drug loading was performed by an immersion method using concentrated solutions of drugs. For example, sorafenib (SFN)-loaded UnTHCPSi NPs were prepared by immersing 100 µg of the NPs in 2 mL of the drug solution (0.5 mg/mL) dissolved in acetone, and then stirring for 2h at RT **(III)**. Next, the excess amount of the drug was removed by centrifugation at 21382 rcf for 5 min (L-70 Ultracentrifuge, Beckman, USA), followed by three washes with MilliQ-water.

In vitro drug release profiles of the SFN-loaded UnTHCPSi NPs **(III)** were determined by dispersing 200 µg of the loaded NPs in different media, including human plasma, PBS (pH 7.4), and PBS containing 10% fetal bovine serum (FBS, pH 7.4) at 37°C. For this purpose, 200 µL of the release medium solution was withdrawn at predetermined time-points, and replaced with equal volumes of the corresponding fresh pre-warmed medium to retain a constant volume of the release medium. After sampling, the aliquots were centrifuged for 3 min at 21382 rcf and the amount of SFN in the supernatant was analyzed by high-performance liquid chromatography (HPLC) as described above. For drug release assessment in the plasma, the supernatant of the centrifuged samples was mixed with acetone at 1:1 ratio, and centrifuged to precipitate and separate the plasma proteins. All measurements were repeated at least three times.

Loading of the model anticancer drug, methotrexate (MTX), into the bare UnTHCPSi, Un-P and Un-P-P NPs was performed by immersing the NPs in the PBS solution of the drug (pH 8; 10 mg/mL) at a weight ratio of 20:1 w/w (drug:NPs) and stirring (570 rcf) at RT for 90 min **(IV)**. MTX-loaded NPs were separated from the free drug by centrifugation at 21382 rcf for 7 min. To remove the drug molecules loosely adsorbed on the surface of the NPs, the NPs were gently washed twice with MilliQ-water.
For drug release of MTX **(IV)** from bare UnTHCPSi, Un-P and Un-P-P NPs, 250 µg of the MTX-loaded NPs were redispersed in 20 mL of PBS (pH 7.4) at 37°C, and then, the same protocol used for SFN release study was also followed here, as described above.

The quantification of the model drugs for the loading degree **(III and IV)** and drug release experiments were performed by HPLC. Detailed description of the procedures for loading measurements and the HPLC experimental setups can be found in the respective original publications **(III and IV)**.

4.2 Cellular toxicity experiments

4.2.1 Cell lines and culture (I–V)

The human B cell lymphoma (Raji; **I**), human T cell lymphoma (Jurkat; **I**), human monocyte cells (U937; **I**), murine leukemic machrophage cells (RAW 264.7), and human breast adenocarcinoma cell (MDA-MB-231 and MCF-7, **III–V**) were selected for the *in vitro* studies (all from Amrican Type Culture Collection, USA) and monocyte-derived dendritic cells (MDDCs) for the *ex vivo* immunstimulation studies. The Raji, Jurkat, U937, MDA-MB-231 and MDDCs cells were grown in standard Rosewell Park Memorial Institute 1640 (RPMI 1640) medium supplemented by 10% (v/v) fetal bovine serum, 1% non-essential amino acids, 1% L-glutamine, penicillin (100 IU/ml), and streptomycin (100 mg/ml) (all from EuroClone S.p.A., Italy). RAW 264.7 and MCF-7 cells were cultured in Dulbecco's modified Eagle's medium (DMEM) supplemented using the same compounds mentioned for RPMI 1640 medium. The cell cultures were maintained in a standard incubator (BB 16 gas incubator, Heraeus Instruments GmbH, Germany) at 37°C with an atmosphere of 5% CO_2 and 95% humidity. For all the studied cell lines, the growth media were changed every other day until the time of the experiments. The subculturing was also performed when the cells were at 80% of confluency. For passaging and prior to each test, the adherent cells (RAW 264.7, MDA-MB-231 and MCF-7) were harvested with trypsin–PBS–ethylenediaminetetraacetic acid (EDTA) (0.25%, v/v).

4.2.2 Reactive oxygen species (ROS) assay (I)

For this assay, the Raji, Jurkat, U937, and RAW 264.7 immune cells were separately prepared in 10 μM 2′,7′-dichlorodihydrofluorescein diacetate (DCF-DA) solution with a concentration of 2×10^5 cells/mL and incubated for 1 h at 37°C. The solution was subsequently centrifuged in 1425 rcf for 5 min before washing and resuspending in HBSS at a final concentration of 2×10^5 cells/mL. Then, 100 μL of the cell suspension were added to each well (20000 cells/well). In the final step, 100 μL of the PSi NPs (TOPSi, TCPSi, APSTCPSi, THCPSi and UnTHCPSi) with the concentrations of 50, 100 and 200 μg/mL added to achieve the final PSi concentrations of 25, 50 and 100 μg/mL. After treatment for 6 and 24 h, dose and time-dependent measurements of the ROS generation were conducted by measuring the DCF fluorescence with Varioskan Flash. DCF-DA is nonfluorescent until the acetate groups are removed by the intracellular esterases (dichlorofluorescein formation) and the oxidation occurs within the cell (fluorophore DCF formation). Excitation and emission wavelengths were 498 and 522 nm, respectively, with hydrogen peroxide (0.09%) and HBSS treated cells as positive and negative controls, respectively. Data were obtained from at least three independent triplicates.

In addition to ROS assay, other toxicological parameters including reactive nitric oxide species (RNOS) and tumor necrosis factor alpha (TNF-α) were measured according to the deatailed procedures described in the respective original publication **(I)**.

4.2.3 ATP activity (I and III–V)

To assess the biocompatibility of the NPs, their toxicity towards the Raji **(I)**, Jurkat **(I)**, U937 **(I)**, RAW 264.7 **(I)**, MDA-MB-231 and MCF-7 **(III–V**) cells was evaluated by measuring the ATP activity as described elsewhere [5]. Typically, 100 µL of the cell suspensions with the concentration of 2×10^5 cells/mL in the cell media were seeded in 96-well plates and allowed to attach overnight. Thereafter, the cell media was removed and the wells were washed twice with 1× HBSS (pH 7.4) prior to the addition of 100 µL of the PSi NPs with different surface chemistries at the concentrations of 25, 50, and 100 µg/mL. After 6 and 24 h incubation at 37°C, 100 µL of the reagent assay (CellTiter-Glo® Luminescent Cell Viability Assay, Promega, USA) was added to each well and the luminescence was measured using a Varioskan Flash. Negative (HBSS buffer solution) and positive (1% Triton X-100) control wells were also used and treated similarly as described above. The viability of the negative control was taken as 100%. All assays were conducted at least in triplicate.

4.2.4 Genotoxicity analysis (I)

The detection of the genetoxicity induced by the PSi NPs was evaluated using the 5-bromo-20-deoxyuridine (BrdU) enzyme-linked immunosorbent assay (ELISA) based kit assay (Millipore, Corporation, MA, USA). For this assay, 100 µL of the cells were seeded and cultured at a concentration of 2×10^5 cells/mL in 96-well plates. After washing, 100 µL of the PSi NPs (50 and 200 µg/mL) prepared in HBSS (pH 7.4) were added to each well to achieve the final PSi concentrations of 25 and 100 µg/mL. According to the manufacturer's protocol, the cells were further supplemented with 20 µL of the BrdU reagent and incubated for 6 and 24 h at 37°C. Cells were then fixed with a fixative solution and the DNA was denatured in one-step by adding 200 µL/well of the fixative solution and incubated at RT for 30 min. After three-times of washings, 100 µL/well of anti-BrdU monoclonal Ab was added to bind to the BrdU in the newly synthesized cellular DNA. Then, peroxidase labeled goat anti-Mouse IgG was added to make immune complexes detectable after 30 min incubation with the 100 µL/well of TMB peroxidase substrate at RT in the dark. Finally, the reaction product was quantified by the addition of 2.5 N sulfuric acid stop solution and measuring the absorbance using a microplate reader (Varioskan Flash) at a wavelength of 450 nm. HBSS and 1% Triton X-100 treated cells were used as negative and positive controls, respectively. All experiments were carried out in triplicate for each type of PSi NP and concentration, and also for each cell type tested.

4.2.5 Hemocompatibility studies (I)

Heparin-stabilized fresh human blood was obtained from anonymous donors from the Finnish Red Cross Blood Service and used within 2 h. A 5-mL sample of the whole blood was mixed gently with 10 mL of Dulbecco's phosphate-buffered saline (D-PBS) before isolating the red blood cells (RBCs) from serum by centrifugation at 3000 rpm for 6 min.

The RBCs were then washed further for five times with sterile D-PBS solution. After washings, 2 mL of the RBCs were diluted to 40 mL by adding D-PBS (5% hematocrit) [265]. Next, 0.1 mL of the diluted RBC suspension was added to 0.4 mL of the PSi NP suspensions in D-PBS to a final concentration of 25, 50, 100, and 200 µg/mL. The suspension obtained was gently vortexed before incubating at static condition at RT for 1, 4, 8, 24, and 48 h. Afterwards, the samples were gently vortexed again and centrifuged at 18,531 rcf for 3 min. 100 µL of the supernatant was transferred to a new 96-well plate to measure the absorbance values of hemoglobin at 577 nm with a reference wavelength of 655 nm using a microplate reader. D-PBS and water (0.4 mL) were used as negative and positive controls, respectively.

To evaluate the morphological changes and also the PSi NP–RBC interactions, the diluted RBC suspension (5% hematocrit, 0.1 mL) was mixed with PSi NPs in PBS (0.4 mL) at the final concentration of 100 µg/mL and incubated at RT for 4 h. The samples were then fixed with 2.5% glutaraldehyde and further incubated at 37°C for 1 h, followed by post-fixation using 0.5% osmiumtetroxide in PBS for 1.5 h. The cells were then dehydrated in increasing concentrations of 50, 70, 96, and 100% of ethanol for 5, 10, 20 and 15 min, respectively. Finally, the cell suspensions were dropped onto plastic coverslips, dried, and sputter coated with platinum before being observed under scanning electron mycroscopy (SEM; Zeiss DSM 962).

4.2.6 *In vivo* biochemical and histopathological experiments (I)

For these experiments, 18-adult male Sprague–Dawley rats weighting between 250 and 275 g were used. All animals were kept at ventilated temperature-controlled animal room (20 ± 2 °C), with relative humidity of 60 ± 10%, and a 12-h light/dark daily cycle from 5 days before starting the study. During this period, the animals were housed in standard polycarbonate stainless steel wire-topped cages with free access to rat chow and water *ad libitum*. The rats were randomly divided to 6 groups of 3 animals: control group (treated with normal 0.9% sodium saline) and five experimental groups to receive a single injection of TOPSi, TCPSi, APSTCPSi, THCPSi and UnTHCPSi NPs (700 µg/kg) via tail vein. After 24 h, the rats were anesthetized and the plasma samples were collected by cardiac puncture and analysed for measuring lactate dehydrogenase (LDH), aspartate transaminase (AST) and sodium (Na) amount.

For the histological analyses, the tissue specimens from the liver, kidney and spleen of the rats were fixed in 10% solution of formalin in PBS and then processed routinely by embedding in paraffin. Afterwards, 5 mm sliced tissues were stained with hematoxylin and eosin (H&E) and examined under a light microscope (Olympus BH-2, Tokyo, Japan).

4.3 Immunostimulation experiments

4.3.1 Dendritic cells (DCs) maturation (II)

Since the PSi NPs with different surface chemistries did not show any sign of immunotoxicity on different immune cells at 25 μg/mL, this concentration was selected for further evaluation of possible surface chemistry dependent immunostimulatory responses. The first step was the generation of MDDCs. For this purposes, fresh peripheral blood mononuclear cells (PBMCs), obtained from 40 mL of the blood of individuals, were used for monocytes purification by means of anti-CD14 microbeads following the manufacturer's protocol (Miltenyi Biotec, Germany).

The $CD14^-$ fraction was placed in 10% dimethyl sulfoxide and frozen for a later lymphocyte proliferation test. To generate MDDCs, $CD14^+$ monocyte cells were incubated in RPMI 164 medium (Life Technologies, Invitrogen, USA) supplemented with 10% fetal calf serum (FCS; Life Technologies, Invitrogen, USA), penicillin (100 IU/mL), streptomycin (100 μg/mL), as well as recombinant human rhGM-CSF (200 ng/mL) and rhIL-4 (100 ng/mL) (both from R&D Systems Inc., USA) for 5 days at 37°C. The produced immature DC (imDCs) were then recovered and used in the experiments. The impact of PSi NPs on DC maturation was evaluated by measuring the CD80, CD83, CD86, and human leukocyte antigens-DR (HLA-DR) expression on the surface of the cells. The imDCs were co-incubated with the PSi NPs at a concentration of 25 μg/mL in 96-well plates (Nunc, Roskilde, Denmark) for 48 h at 37°C. The reason for 48 h exposure of the cells with the NPs was the preliminary studies that showed the maximum effect for cell stimulation at this time point. After treatment with different PSi NPs, the cells were labeled with CD80, CD83, CD86, and HLA-DR monoclonal antibodies (BD Pharmigen, CA). Then, the cells were analyzed using a FACSCanto II flow cytometer (BD Biosciences, USA), and all the data was processed with FLOWJO software (Tree Star, Inc, USA). The results were expressed as the percentage of cells expressing the aforementioned markers. Culture supernatants were collected and stored at –20°C for subsequent analysis of the secreted cytokines.

4.3.2 T cell proliferation and differentiation (II)

The CD14 negative cells containing peripheral blood lymphocytes (PBL) were first labeled with 2 μM CellTrace carboxyfluorescein succinimidyl ester (CFSE) proliferation kit (Life Technologies, Invitrogen, USA) by incubating at RT and darkness for 10 min. After washing, the labeled PBL (1.5×10^5) were co-cultured with 1.5×10^4 of autologous MDDCs (Nunc, Roskilde, Denmark) with different PSi NPs at a concentration of 25 μg/mL anf final volume of 250 μL or left untreated for 6 days at 37°C. Afterwards, the percentage of cells expressing $CD3^+CFSE^{low}$ was assessed by flow cytometry. The results were considered positive when the proliferation index (PI), calculated as:

$$PI = \frac{[\%CD3 + CFSE^{low} \text{ stimulated (lymphocytes + DCs)}] - [\%CD3 + CFSE^{low} \text{ unstimulated (lymphocytes + DCs)}]}{\%CD3 + CFSE^{low} \text{ (lymphocytes)}}$$

was >3 [266]. The percentage of CD4 and CD8 positive T cell subpopulations was also calculated after performing the same protocol and staining the cells with specific monoclonal Ab (BD Pharmigen, CA). Culture supernatants were collected and stored at –20°C for subsequent analysis of the secreted cytokines.

4.3.3 Cytokine secretion (II and III)

The production of IL-1β, IL-4, IL-6, IL-10, IL-12, IFN-γ, and TNF-α was measured after incubating imDC and imDC-PBL co-culture with the PSi NPs using FlowCytomix kit (Bender MedSystems, Austria) and following the manufacturer's protocol **(II)**. The results were expressed in pg/mL and were normalized after subtracting the respective production of the cytokine with the control groups. The cytokine secretion measurement was performed after 48 h for the imDC and after 6 days for the imDC-PBL co-cultures exposed to the PSi NPs.

To assess the immunostimulatory response of the anti-CD326 Ab-conjugated UnTHCPSi NPs in the cancer cells **(III)**, IL-2 secretion present in the supernatant of the samples prepared for antibody-dependent cell-mediated cytotoxicity (ADCC) was measured using a commercially available Human IL-2 ELISA kit (BD Biosciences, USA), as explained in the next section. The protocol performed for this ELISA assay was followed according to the manufacturer's instructions and is described in the Supporting Information of the respective publication **(III)**.

4.3.4 ADCC-mediated immunotherapeutic effect (III)

The ADCC test was performed to investigate if the effector immune cells were able to lyse the target cancer cells after attaching to the Fc portion of the Ab bound to the target cancer cells via their Fab section. Briefly, 100 µL of the MDA-MB-231 and MCF-7 cell suspensions at the concentration of 1.25×10^4 cells/mL were seeded in 96-well plates and allowed to attach overnight. Thereafter, 95 µL of the cell media was removed and replaced with 25 µL of the pre-warmed ADCC assay buffer. Then, 25 µL of the pure and Ab functionalized UnTHCPSi (Un-Ab) NPs at the concentrations of 10, 25, 50, 75, and 100 µg/mL were added to each well, followed by the addition of 1×10^5 of the effector immune cells dispersed in 25 µL of the ADCC assay buffer. The same amount of free Ab was also tested during the study. After 8 h of incubation at 37°C, 75 µL of the Bio-Glo™ Luciferase Assay Reagent was added to all the wells (ADCC Reporter Bioassay, Core Kit, USA) and incubated at RT for 30 min. The luminescence of the wells was then measured using a Varioskan Flash. Cell samples only treated with ADCC assay buffer were considered as control. Wells only containing ADCC assay buffer and the Bio-Glo™ Luciferase Assay Reagent were considered as background. The experiments were performed at least in triplicate for each sample.

4.4 Cellular association and intracellular distribution

4.4.1 Confocal microscopy and flow cytometry experiments (III–V)

The cellular interactions of the NPs with MDA-MB-231 and MCF-7 breast cancer cells were screened using an inverted confocal fluorescence microscopy (Leica SP5 II HCS A, Germany) **(III–V)**. For this purpose, Lab-Tek® 8-Chamber Slides (Thermo Fisher Scientific, USA) were used to seed the cells at a density of 5×10^4 cells/well. After overnight incubation at 37ºC, the cell medium was removed and 250 µL of the fluorescently labeled PSi NPs (50 µg/mL) was added to each chamber. The cells were then incubated for 3 h **(III)** and 6 h **(IV and V)** with the NPs before three-times washing with HBSS–HEPES (pH 7.4). Next, the plasma membrane of the cells was stained by a 3-min exposure of the cells to 200 µL of the CellMask® (3 µg/mL; Invitrogen, USA) at 37°C. Washing was then performed twice with HBSS–HEPES buffer before cell fixation by 2.5% glutaraldehyde for 20 min. To check the endosomal escape of the polymer modified UnTHCPSi NPs **(IV)**, the staining of the acidic organelles of the cells was done prior to cell membrane staining by adding 200 µL of the LysoTracker® Blue DND-22 (50 nM; Invitrogen, USA) to the cells and incubating for 30 min at 37°C. Washing was then performed twice with HBSS–HEPES (pH 7.4) to remove any free tracking agent. Finally, the intracellular localization was observed by confocal microscope.

To quantitatively measure the percentage of cells associated with the NPs, flow cytometry studies were performed. For these experiments, cells were seeded in 6-well plates at a density of 7×10^5 cells/well. After incubation at 37°C overnight, the cells were washed with HBSS–HEPES (pH 7.4) and treated with fluorescently labeled Un-Ab NPs (50 µg/mL) for 3 h **(III)** and the polymer-modified PSi NPs (50 µg/mL) for 6 h **(IV)**. Free NPs were then removed by washing three times with HBSS–HEPES. Afterwards, the cells were detached by incubating with 300 µL of trypsin-PBS-EDTA mixture for 2 min. Thereafter, the fixation of the cells was performed with 2.5% glutaraldehyde in PBS for 30 min and the samples were re-suspended in 700 µL of HBSS–HEPES (pH 7.4) prior to the measurements using LSR II flow cytometer (BD Biosciences, USA) with a laser excitation wavelength of 488 nm. For competition experiments, 1 µg of the free Ab was added to the cells 30 min before exposing to Un-Ab for 3 h. Data were analyzed and plotted using Kaluza® Flow Cytometry Analysis Software. To quench the fluorescence of the polymer-modified PSi NPs associted to the surface of the cell membrane **(IV)**, trypan blue (TB, 0.005% v/v) was used before cell fixation, followed by three-times washing. 10,000 events were exactly obtained for each sample. The data was analyzed and plotted using Weasel software. For the Un-Ab **(III)** and the polymer-modified PSi NPs **(IV and V)**, Alexa Fluor-488 and FITC were used as fluorescence labling agents, respectively.

4.4.2 TEM imaging (III–V)

To evaluate the intracellular localization of the NPs, TEM imaging of MDA-MB-231 and MCF-7 breast cancer cells was performed after treatment with bare, Ab-functionalized

(III) and polymer-modified **(IV and V)** UnTHCPSi NPs. For this purpose, 13 mm round shape coverslips were placed at the bottom of 24-well plates (Corning Inc. Life Sciences, USA). Next, 10^5 cells were seeded in DMEM and RPMI 1640 media for MCF-7 and MDA-MB-231 cells, respectively, and allowed to attach overnight. The cell culture media was then removed, and 500 µL of the NPs suspensions (50 µg/mL) were added to each well and the samples were incubated at 37°C for 3 h **(III)** and 6 h **(IV and V)**. Afterwards, the particle suspension was removed and the coverslips were washed twice with HBSS–HEPES before fixing the cells with 2.5% glutaraldehyde in 0.1 M PBS solution (pH 7.4) for 1 h at RT. After fixation, the coverslips were rinsed twice with HBSS–HEPES (pH 7.4) and sodium cacodylate buffer (NaCac) for 3 min prior post-fixation with 1% osmium tetroxide in 0.1 m NaCac buffer (pH 7.4). The cells were finally embedded in epoxy resin after dehydration of the cells with 30–100% ethanol for 10 min each. Ultrathin sections (60 nm) were cut parallel to the coverslip, post-stained with uranyl acetate and lead citrate, and observed by TEM.

4.4.3 *In vitro* anti-cell proliferative experiments (III–IV)

The *in vitro* anticancer effect of the SFN-loaded anti-CD326 Ab-functionalized UnTHCPSi NPs was evaluated by measuring the anti-proliferation effect on the MCF-7 and MDA-MB-231 breast cancer cells. Typically, 100 µL of both cell suspensions at the concentration of 1.5×10^5 cells/mL were seeded in 96-well plates and allowed to attach overnight. Thereafter, the cell media was replaced with 100 µL of the SFN-loaded UnTHCPSi NPs and SFN-loaded anti-CD326 Ab-functionalized UNTHCPSi NPs with different concentrations **(III)**. The pure SFN was also examined at the concentrations similar to the drug-loaded NPs in the same conditions. After 8 and 24 h incubation at 37°C, 100 µL of the CellTiter-Glo® reagent assay (Promega, USA) was added to each well and the luminescence of the wells was measured using a Varioskan Flash. Negative (HBSS buffer solution) and positive (1% Triton X-100) control wells were also used and treated similarly, as described above. All data sets were compared with a negative control of HBSS (pH 7.4), considered as 100% proliferation.

The antiproliferative effect of the MTX, MTX-loaded UnTHCPSi and MTX-loaded polymer-modified UnTHCPSi NPs was also evaluated after 6 h of incubation **(IV)**, using the same protocol as described above. All the experiments were performed at least in triplicate.

5 Results and discussion

5.1 Effect of the surface chemistry on the biocompatibility of the PSi NPs (I)

In order to establish a safe nano-based therapy, it is of utmost importance to demonstrate the non-toxic nature of the nanomaterial in question. Thus, the toxicological manifestations of the immune cells exposed to the PSi NPs were evaluated with the aim to demonstrate the effect of the surface chemistry of five different types of PSi NPs, namely TOPSi, TCPSi, APSTCPSi, THCPSi and UnTHCPSi with similar size, surface area and pore volume on the mechanism(s) of immuno-genotoxicity in different types of immune cells.

5.1.1 Analysis of the immunotoxicity mechanism of the PSi NPs

Since the monitoring of the cytotoxicity mechanism by performing only one toxicity assay alone cannot be reliable and cannot clarify the real and the most important pathways involved in the toxic effect of the NPs (leading to false-negative or false-positive results due to the different mechanisms involved in the toxicity reactions), the effects of the PSi NPs on the different toxicological mechanisms, such as loss of the cell membrane integrity, ROS production, RNOS release and TNF-α production in the immune cells, were evaluated. All these cytotoxicity-indicating parameters are mutually well-known independent biological mechanisms capable of affecting the mitochondrial metabolic activity (ATP content) in conjunction with each other or separately, and subsequently leading to indirect DNA damage [5, 267, 268]. In fact, the loss of membrane integrity, oxidative stress and pro-inflammatory responses, all act via decreasing of the ATP content that finally results in indirect DNA damage [269]. On the other hand, direct DNA damage may also occur when NPs initiate an apoptotic stage in the cells in the absence of a significant change in ROS, RNOS, TNF-α or ATP content [270].

Hereupon, all the cytotoxicity results of the PSi NPs tested are summarized in Table 4 to unveil the toxicity mechanism(s) as a function of the surface chemistry of the PSi NPs. As indicated in the Table 4, direct genotoxicity can be observed when significant DNA proliferation inhibition occurs despite negligible oxidative stress and proinflammatory responses, and the absence of change in the proper functionality of the cell membrane and mitochondria [271]. On the other hand, indirect DNA damage takes place when promoted ROS, RNOS, and TNF-α secretion lead to ATP depletion and DNA damage. In this case, there is no significant difference between ATP and DNA proliferation values of the affected cells [272]. The third possibility is when moderate changes in ROS, RNOS, TNF-α and ATP content is followed by a high degree of reduced DNA proliferation, i.e., both direct and indirect mechanisms are involved, simultaneously. Table 4 also shows that depending on the cell type, surface chemistry and concentration, the PSi NPs can initiate direct, indirect or both of these genotoxicity mechanisms in immune cells.

The data gathered demonstrated that the positively charged APSTCPSi NPs present the lowest biocompatibility because of inducing various cytotoxicity mechanisms. This result is in line with the significant increase of the cytotoxicity observed in RAW 264.7 macrophage cells after exposure to amine-modified porous SiO_2 NPs [265]. The higher cytotoxicity of APSTCPSi NPs can be explained by their strong interactions with the negatively charged cell membranes. Generally, amine-modified positively charged particles can depolarize the membrane potential and increase the intracellular Ca^{2+} concentration by triggering the plasma membrane Ca^{2+} influx pathway as well as by enhancing the Ca^{2+} release from the endoplasmic reticulum [273]. This effect eventually perturbs the cell membrane by the phase transition of the lipid bilayer [273]. The plausible explanation for the high biocompatibility of the TOPSi and TCPSi NPs in comparison to the other studied PSi NPs is attributed to their hydrophilicity. In this case, instead of strong and direct interactions with the cell membranes, these NPs make weak interactions with the cell surface proteins via the aqueous layer surrounding the NP's surface [5]. The higher cytotoxicity observed for the THCPSi NPs compared to the TOPSi and TCPSi NPs can be attributed to the lower hydrophilicity and facilitated interactions with the cell membrane [5]. Moreover, the higher toxicity of UnTHCPSi NPs in comparison to THCPSi NPs seems to be resulted from the surface hydroxyl groups and hydrocarbon chains that facilitate more interactions with the ion-exchange pathways and the lipids and esters of the phospholipids in the cell membrane [274]. Overall, in this study, the cytotoxicity rank order of the PSi NPs was as follows: APSTCPSi > UnTHCPSi > THCPSi > TCPSi ≈ TOPSi. In general, Table 4 demonstrates that the different PSi NPs can induce various cytotoxicity mechanisms in different cells. For instance, ROS and TNF-α production seemed to be the main mechanisms of cytotoxicity in RAW264.7 macrophage cells, whereas the cytotoxicity in Jurkat cells was likely due to the RNOS production **(I)**. This observation suggests that cells behave differently in the presence of the PSi NPs, and also that the PSi NPs' toxicity is induced via different mechanisms depending on the cell line characteristics, such as doubling time, metabolic activity, growth pattern (i.e., whether being adherent or suspended cells), and the type of nanomaterial in contact with them [275, 276]. The results of the cytotoxicity analysis performed for U937 and RAW 264.7 cells can be found in the respective original publication **(I)**.

The main reason for selecting various immune cells for the cytotoxicity analyses was the fact that less attention to this issue has been paid in the literature, and that the NPs applied for immunostimulatory purposes can show different behaviors in different types of immune cells. In addition, the NPs can also differently affect the behavior of the immune cells by slight modification of their physicochemical properties, concentration and exposure time. Herein, the idea was to clarify that while one specific type of NP can show high safety on one type of immune cells, it can probably, in turn, induce cytotoxic effects in other type of immune cells. Accordingly, for nano-based immunotherapeutic purposes, it is crucial to investigate the effect of the NPs on different types of immune cells as the proper function of the immune system is highly dependent on the activity of all the components. Therefore, any cytotoxicity observed on even one type of immune cells may induce different unwanted physiological alterations and lead to reduced therapeutic effects.

Table 4. *Overview of the cytotoxicity mechanism analyses of the immune cells exposed to different PSi NPs as a function of the NPs' surface chemistry and concentration. The results of the cytotoxicity analysis performed for U937 and RAW 264.7 cells can be found in the respective original publication* ***(I)***.

PSi NP	Concentration (μg/mL)	ROS	RNOS	TNF-α	ATP content	DNA damage	Cytotoxicity mechanisms
		Raji cells					
TOPSi	25	1	1	1	1	1	**a**
	100	2	1	2	1	3	**b**
TCPSi	25	1	1	1	1	1	**a**
	100	1	2	2	1	3	**b**
APSTCPSi	25	3	2	1	2	2	**c**
	100	3	2	4	2	3	**d**
THCPSi	25	1	1	2	1	1	**a**
	100	2	2	4	2	2	**c**
UnTHCPSi	25	1	1	1	1	1	**a**
	100	1	1	1	1	3	**b**
		Jurkat cells					
TOPSi	25	1	3	1	1	1	**a**
	100	1	4	1	4	4	**c**
TCPSi	25	1	2	1	1	1	**a**
	100	1	4	1	4	3	**c**
APSTCPSi	25	1	4	1	4	3	**c**
	100	3	4	2	4	4	**c**
THCPSi	25	1	3	1	1	1	**a**
	100	1	4	1	4	3	**c**
UnTHCPSi	25	1	4	2	1	1	**a**
	100	2	4	4	4	4	**c**

1: ROS production <15 % of the positive control; <1.2-fold increase of RNOS and TNF-α compared to the control; ATP-content and DNA proliferation >80%.

2: ROS production of 15–25% of the positive control; 1.2–1.4-fold increase of RNOS and TNF-α compared to the control; ATP-content and DNA proliferation of 60–80%.

3: ROS production of 25–35% of the positive control; 1.4–1.6-fold increase of RNOS and TNF-α compared to the control; ATP-content and DNA proliferation of 40–60%.

4: ROS production >35 % of the positive control; >1.6-fold increase of RNOS and TNF-α compared to the control; ATP-content and DNA proliferation of <40%.

a Very low toxicity. In this case, despite small production of ROS, RNOS and TNF-α, there was no change in the ATP-content or DNA proliferation.

b Direct DNA damage. In this case, ROS, RNOS or TNF-α production could not reduce the ATP-content and the ATP-content value was considerably higher than the DNA proliferation values.

c Indirect DNA damage. In this category, despite a decrease in the ATP-content due to ROS, RNOS or TNF-α production, there was no significant difference between the ATP and DNA proliferation values or even the ATP-content was less than the DNA proliferation results.

d Simultaneously direct and indirect DNA damage. In this case, ROS, RNOS and TNF-α production caused a decrease in the ATP-content; however, the DNA proliferation results were considerably less than the the ATP-content, indicating that both mechanisms are involved in the cytotoxicity.

5.1.2 Hemocompatibility

In order to evaluate the impact of the PSi NPs' surface chemistry on the RBCs, the amount of lysed hemoglobin was determined after exposure to the PSi NPs. Shorter incubation times (1, 4 and 8 h) caused very small RBC destruction in comparison to the long exposure time (24 h), for all the PSi NPs tested (Figure 8A–C), highlighting the time dependency of the hemolysis process. In addition, while 25 µg/mL of all the PSi NPs did not induce more than 6% hemolysis after 24 h, 200 µg/mL of the PSi NPs significantly increased the extent of hemolysis, indicating a clear concentration dependency in the hemolysis by the NPs. Overall, this data pointed towards a synchronous relationship of the PSi NPs concentration and the exposure time with the RBC hemolysis. Generally, the hemolytic activity of APSTCPSi and UnTHCPSi NPs was higher than that of observed for TOPSi, TCPSi and THCPSi NPs. The plausible explanation for this behavior is the hydrophilicity of TOPSi and TCPSi that hinders their interaction with the cell membrane and more predominant effect of the negative charge of the THCPSi NPs compared to their hydrophobicity, which probably causes less interactions of the NPs with the surface negative charges of the RBCs. Contrarily, despite the hydrophilic nature, more predominant impact of the positive surface charge of APSTCPSi NPs facilitated the interactions with the negatively charged RBCs' surface membranes, which, in turn, led to the highest rate of hemolysis compared to the other PSi NPs. Interestingly, the comparison between UnTHCPSi and THCPSi NPs also showed that the former caused a greater hemolysis rate, demonstrating a relatively stronger interaction of the hydroxyl groups on the surface of the UnTHCPSi NPs with the cell surface. Overall, the hemolytic activity results suggested that the negatively charged hydrophilic PSi NPs (TOPSi and TCPSi) are more hemocompatible than the positively charged hydrophilic APSTCPSi. This is in line with previous reports comparing positively charged amine-modified mesoporous SiO_2 materials with their bare counterparts [265].

Since the lack of hemolysis does not guarantee the hemocompatibility of the PSi NPs, the surface interactions between RBCs and PSi NPs was also investigated by SEM imaging. As shown in Figure 8D, very small amounts of TOPSi and THCPSi NPs were adsorbed onto the surface of erythrocytes. In contrast, a large amount of UnTHCPSi NPs were attached onto the cell membranes of RBCs after 4 h, inducing strong shrinkage and morphological changes because of the membrane wrapping around the PSi NPs, which can ultimately lead to hemolysis. All these findings demonstrated the hemocompatibility capacity of the PSi NPs in the following order: TOPSi ≈ THCPSi > TCPSi > UnTHCPSi ≈ APSTCPSi.

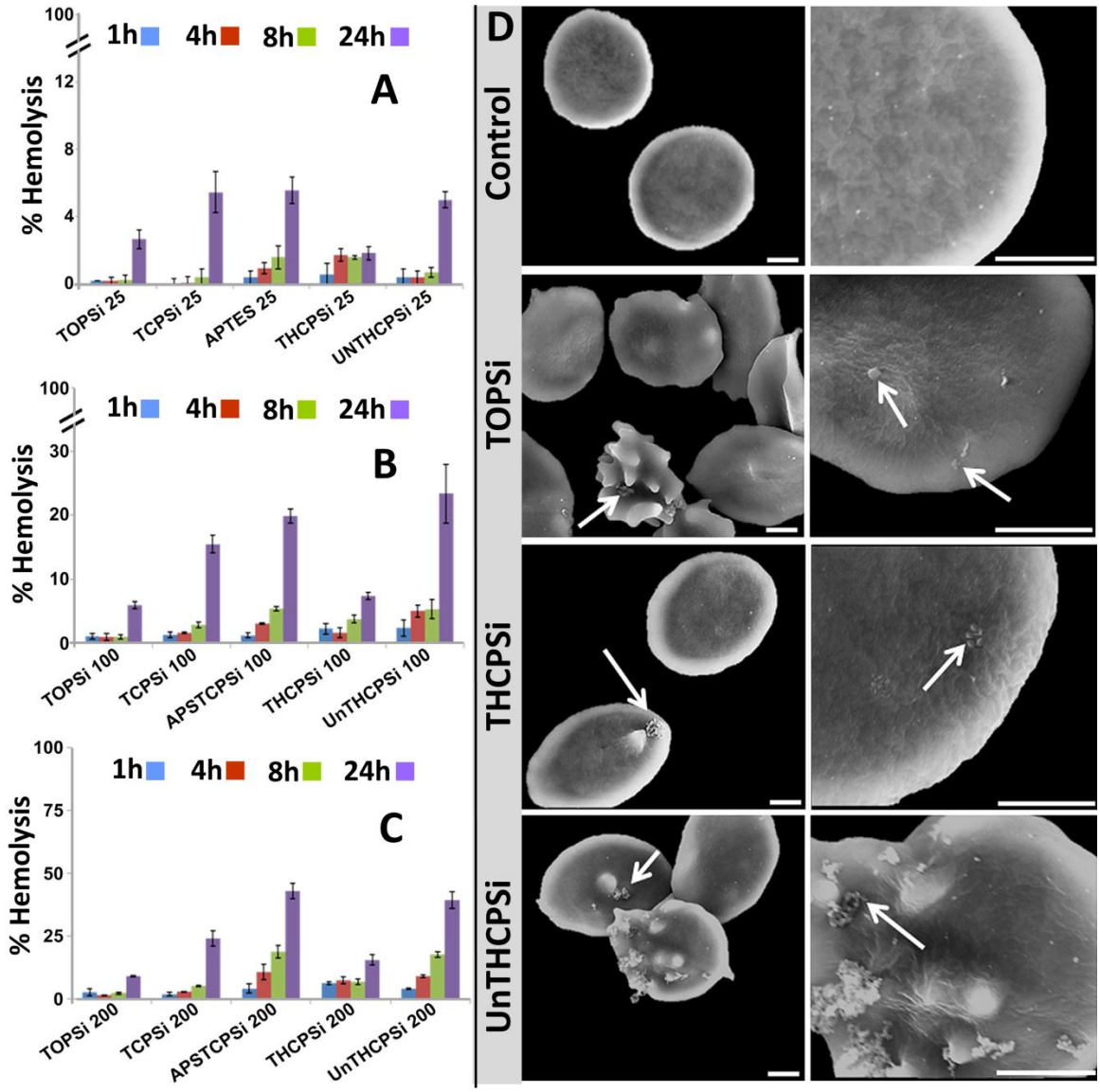

Figure 8 *Hemotoxicity of the PSi NPs. Hemolytic activities were monitored within 24 h of incubation of the human erythrocytes at 37°C with incremental concentrations of 25 (A), 100 (B), and 200 (C) µg/mL of different PSi NPs. The presence of the lysed hemoglobin in the supernatant was measured by a spectrophotometric method at 577 nm. Effect of the PSi NPs on the morphology of the RBCs (D). SEM pictures of RBCs incubated at RT for 4 h with 100 µg/mL of different PSi NPs. Morphological changes of the surface of RBCs are indicated by the white arrows. The higher the PSi NP attachment to the surface, the higher the spiculation was observed on the cell's surface. The SEM images increase in magnification from left to right. Scale bars are 2 µm. Copyright © (2013) Elsevier B. V., reprinted with permission from [277].*

5.1.3 in vivo histopathological and biochemical biocompatibility

In order to investigate the *in vitro-in vivo* correlation of the PSi NPs cytotoxicity, the kidney, liver and spleen of the rats injected with the PSi NPs were subjected to histopathological analysis. As it can be seen in Figure 9, no evidence of severe histopathological changes like necrosis was detectable among the experimental groups.

However, mild to moderate adverse histological changes were observed in some cases. For example, the animals injected with TOPSi and THCPSi NPs showed slight structural changes, including mild inflammatory cell infiltration with TOPSi and mild reduction of the glomerular Bowman's space with THCPSi NPs in the kidney. In addition to the glomerular degeneration and inflammatory cell infiltration in the animals treated with UnTHCPSi, these NPs could also cause loss of integrity in the kidney. The hepatic central vein intima dilation and disruption was also observed in the liver after injection of the UnTHCPSi NPs. In the spleen, red pulp expansion and relative white pulp shrinkage were observed in the UnTHCPSi treated group, indicating a decrease in the number of lymphocytes in the spleen.

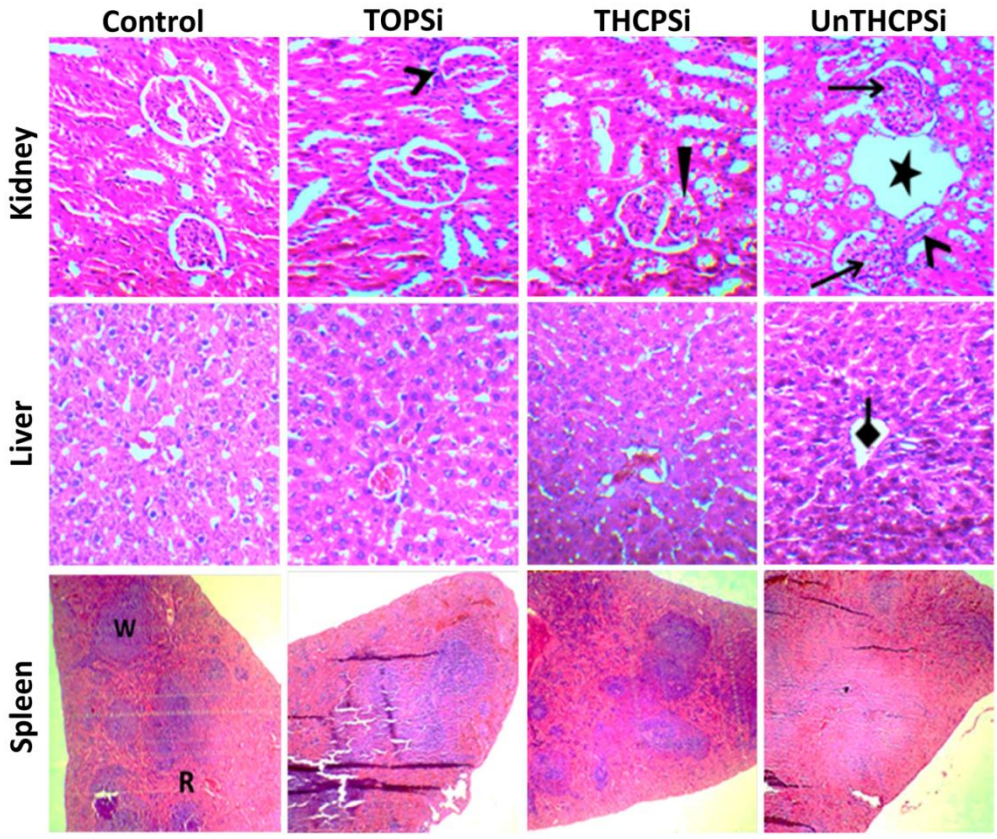

Figure 9 *Representative histological results following intravenous injection of the different PSi NPs in rats. The H&E staining of the kidney revealed less toxicity of TOPSi, TCPSi and THCPSi than APTCPSi and UnTHCPSi NPs* ***(I)****. The histological changes included mild (TOPSi, TCPSi and APTCPSi) and moderate (UnTHCPSi) inflammatory cell infiltration (>), mild reduction of the glomerular Bowman's space (▬), glomerular degeneration (→), and loss of integrity (★). Examination of the livers showed hepatic central vein intima dilation and disruption (⟞) in UnTHCPSi treated rats and normal structure for TOPSi and THCPSi NPs. In the spleen, depletion of white pulp (W) compared to the red pulp (R) was observed in the UnTHCPSi treated rats. Normal structures of the tissues of the rats treated with saline only are also shown for comparison. The histological changes induced by APSTCPSi and TCPSi NPs in the examined tissues can be found in the respective original publications* ***(I)****. Copyright © (2013) Elsevier B. V., reprinted with permission from [277].*

To investigate whether the mild histological changes may cause changes in the normal functionality of the tested organs, LDH, AST and Na contents were measured in the blood samples of the rats treated with the PSi NPs **(I)**. The results showed significantly altered values after intravenous administration of APSTCPSi and UnTHCPSi in rats, confirming the mild toxic effects of the aforementioned PSi NPs in the liver. Nevertheless, no change in the other biochemical and hematological parameters were observed, particularly not in the serum creatinine level and blood urea nitrogen that are markers of the kidney function. This shows that the histological changes did not lead to significant abnormalities in the tested organs. In addition, the hematological factors also did not show any significant variation compared to the control for all the tested NPs. Altogether, the *in vivo* results can be regarded as an indicative proof of remarkable biosafety for all the PSi NPs tested despite the higher cytotoxicity reactions observed for APSTCPSi and UnTHCPSi PSi NPs.

5.2 Effect of surface chemistry of the PSi NPs on the immunostimulatory responses (II)

Since the previous studies showed acceptable safety of all the tested PSi NPs at 25 µg/mL, this concentration was selected for further investigations in terms of immunostimulatory responses. It was hypothesized that the failures or efficient responses of the nano-based immunotherapeutic formulations may, at least partially, arise from the impact of the NPs' surface chemistry on the induction of antagonistic–agonistic effects through interacting with various immunological pathways.

5.2.1 Inducing DC maturation and stimulation by PSi NPs

One of the fundamental steps for eliciting an effective immune response is the maturation of DCs. Accordingly, the PSi NPs were characterized for their potential to induce MDDC maturation *ex vivo* by determining the expression of CD83, a well-known maturation marker, co-stimulatory molecules CD80 and CD86, and antigen presenting marker MHC-II (Figure 10). Untreated MDDCs were used as imDC controls characterized by low or negligible expression of DC maturation markers. The results showed that the NPs can induce different levels of MDDC maturation compared to imDC. For example, the UnTHCPSi, TCPSi and APSTCPSi NPs slightly stimulated the expression of CD86 and HLA-DR. In contrast, the other PSi NPs promoted the upregulation of all the markers to different extents, depending on their surface chemistry. For example, the percentage of all the measured markers was significantly increased after exposure to the TOPSi and THCPSi NPs. In addition, while Un-P induced significant expression of the CD83, CD86 and HLA-DR markers, the APM NPs overexpressed CD86 co-stimulatory molecule and HLA-DR. These results suggest obvious surface chemistry dependent effects on the co-stimulatory and maturation markers' expression. Overall, TOPSi and THCPSi induced the highest rates of MDDC maturation, while TCPSi and APSTCPSi NPs induced very low maturation in MDDC.

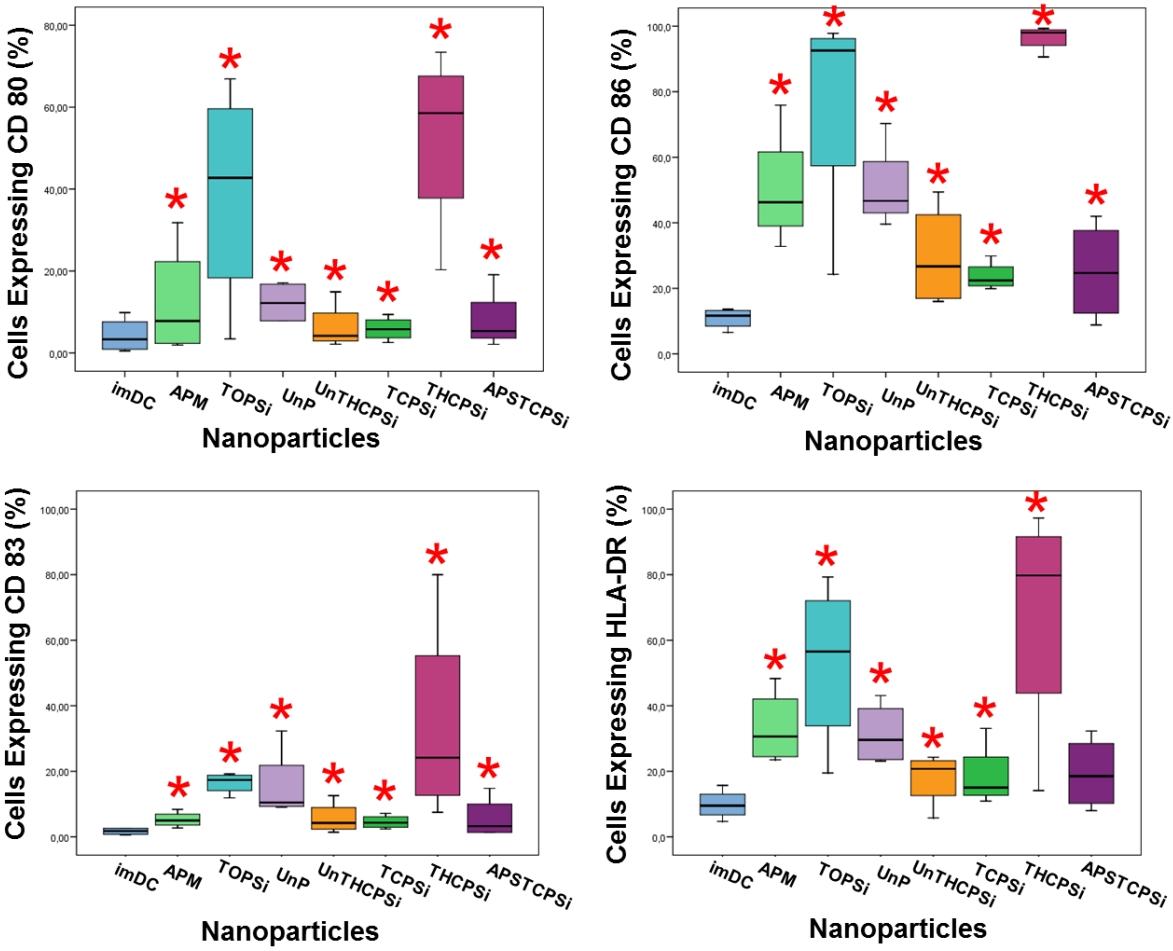

Figure 10 *Percentage of the cells expressing CD80, CD83, CD86 and HLA-DR on DCs. DCs were derived from healthy human monocytes and the expression of markers was measured after 48 h of incubation with the PSi NPs at the concentration of 25 µg/mL. Cells were stained using specific antibodies against each marker and analyzed by flow cytometry. The effect of each NP was compared with imDC by using the Wilcoxon test and the level of significance was set at the probability of *p < 0.05. Copyright © (2013) Elsevier B. V., reprinted with permission from [278].*

DCs are the primary target of many immunostimulative agents due to their ability to initiate both cellular and humoral immune responses [279], by providing MHCII–TCR and CD80/86–CD28 signals, which are not only crucial for T cell activation, but also for T cell proliferation and differentiation [280, 281]. If the first signal activates concurrent with the absence of the second signal, the immune-tolerance will occur due to the T cell anergy [282], leading to immune system suppression. Thus, by exploiting the properties of the NPs to synergistically improve the effect of the immunotherapeutic molecules by affecting the aforementioned markers, the NPs can be useful for immunotherapeutic applications. The increased expression of co-stimulatory molecules (Figure 10) can improve the functionality of DCs in capturing the fragments of pathogens and physically presenting peptides of foreign antigen to T cells in the cleft of surface receptors known as the MHC molecules [283]. Our results suggest the high potential of TOPSi (SiO_x-layer) and THCPSi (SiC_xH_y-layer) NPs for inducing DC maturation, which is very important in facilitating the

activation of immune responses and inducing T cell differentiation [284]. This finding can open up a possibility for using the PSi NPs in immunotherapy against different diseases.

5.2.2 Cytokine secretion and T cell responses

The secretion of cytokines during the DC maturation studies was investigated in parallel to the expression of surface markers using flow cytometry and after 48 h exposure of the DCs to the NPs. The TOPSi and THCPSi NPs were the only NPs with the ability of enhancing the secretion of all the examined cytokines, except for IL-4 that is the indicative of Th2 cells (Figure 11A). This result is in agreement with the expression of the maturation markers on the surface of the DCs, where TOPSi and THCPSi NPs induced the highest level of maturation. The other NPs were only able to downregulate the secretion of IL-4 and showed no effect on the other tested cytokines. These results show the potential of these two PSi NPs for immunostimulative purposes owing to the different pathways that can be activated by each one of the increased cytokines. For example, IFN-γ and IL-12 drive naive T cells to differentiate into Th1 cells and induce cellular immunity against intracellular pathogens, while IL-6, IL-1β and TNF-α contribute in the positive regulation of immunostimulative responses [39-42, 50, 51, 285].

This demonstrates the potential of NPs with higher C–H structures on the outermost surface layer to highly stimulate the immune responses. All the NPs tested containing nitrogen or oxygen on the outermost backbone layer of Si had lower immunoactivation responses than the THCPSi and TOPSi. This is in good agreement with the study of Moyano *et al.* [7], who demonstrated a low immune response for NPs with less hydrophobicity and with oxygen or nitrogen on their surfaces. The high immunostimulatory response of TOPSi, despite the presence of oxygen on its surface and hydrophilicity, was related to its significantly higher dissolution rate in aqueous solution [286] compared to the TCPSi and THCPSi, leading to silicic acid formation, a safe compound with immunostimulating properties [287].

In contrast to the potential of TOPSi and THCPSi NPs on the immunostimulation, the cells exposed to the TCPSi and APSTCPSi NPs showed lower co-stimulatory molecule expression and no cytokine release in the DCs. These results, together with no detectable levels of immune cell proliferation, suggested that these NPs did not induce immunostimulatory response, showing their potential use for the delivery of immunosuppressive compounds as a result of no significant immunostimulative properties [288].

Since it is generally accepted that the co-stimulatory signal activation and cytokine secretion are the most effective inducers of T cell differentiation, the impact of the PSi NPs on T lymphocyte proliferation was investigated by co-culturing CFSE loaded autologous PBL with MDDCs co-cultured with different PSi NPs. The results showed that TCPSi and APSTCPSi NPs did not induce T lymphocyte proliferation (Figure 11B). In contrast, positive T cell proliferation index (PI > 3) [266] was observed at different rates when the cells were treated with APM, TOPSi, Un-P, UnTHCPSi and THCPSi NPs, suggesting that the surface chemistry of the PSi NPs can affect the rate of lymphocyte proliferation.

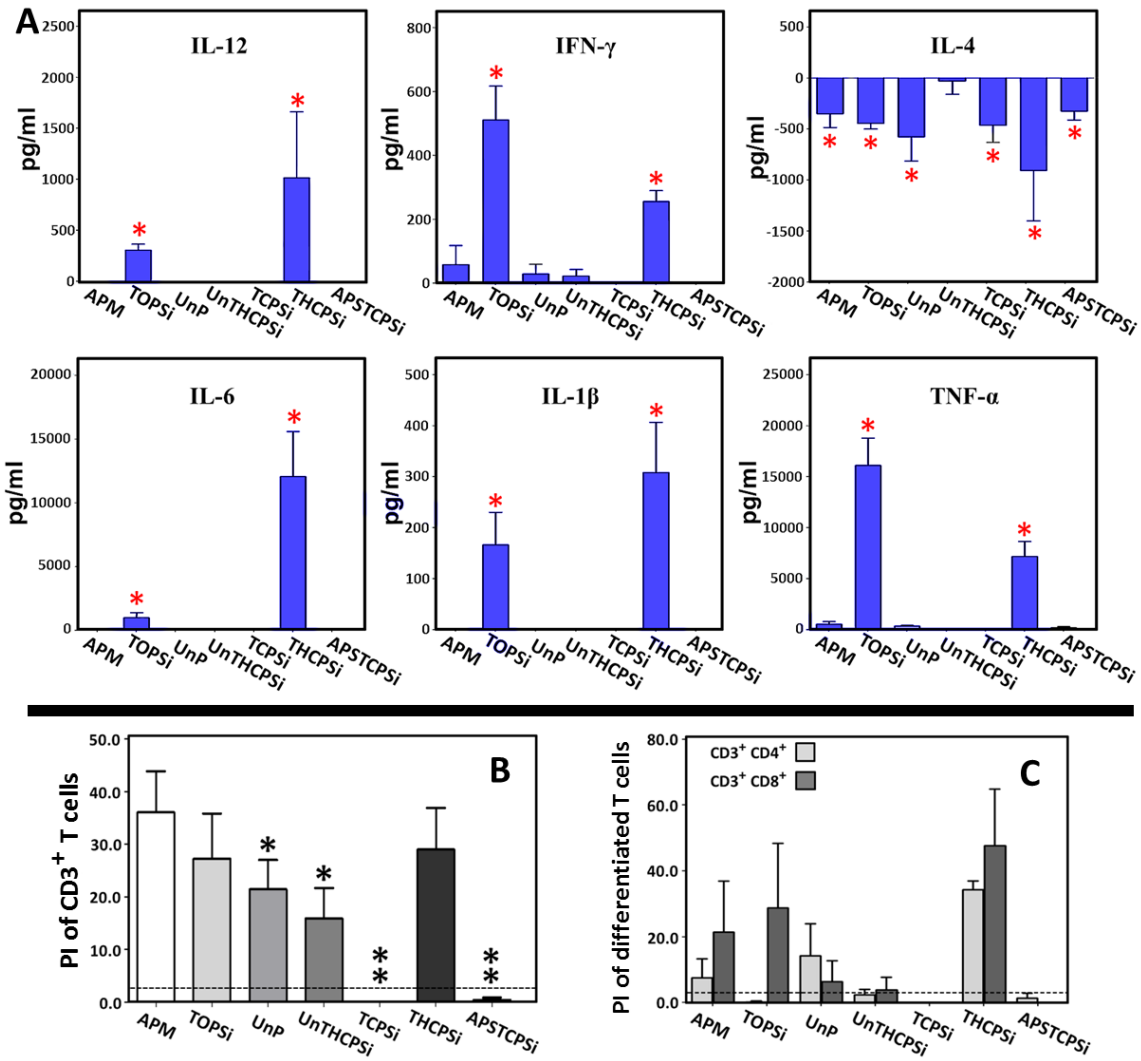

Figure 11 *Cytokine secretion from matured DCs cultured with different PSi NPs at 25 µg/mL for 48 h (A). The analyzed cytokines included IFN-γ, IL-12, IL-1 β, IL-4, IL-6, and TNF-α. The data was normalized after subtracting the respective cytokine production with imDC and presented as average values. Wilcoxon test was used for the statistical analysis and the level of significance was set at the probability of *p < 0.05. Lymphocyte proliferative responses are presented after the treatment of the cells with different PSi NPs (25 µg/mL) for 6 days at 37°C. The direct impact of different PSi NPs on inducing $CD3^+$ (A) as well as $CD4^+$ and $CD8^+$ (B) T cells proliferative responses were investigated. TCPSi and APSTCPSi NPs were the only ones without the capability of inducing $CD3^+$ T cell proliferation. The level of significance was set at the probabilities of *p < 0.05 and **p < 0.01, measured for all the particles against APM NPs. Copyright © (2013) Elsevier B. V., reprinted with permission from [278].*

In addition, the proliferative responses of $CD4^+$ and $CD8^+$ T lymphocytes were determined (Figure 11C). The results showed that Un-P, THCPSi and APM NPs induced a positive proliferation for both the $CD4^+$ and $CD8^+$ T cells. TOPSi NPs were the only type of PSi NPs that were able to induce proliferation only in the $CD8^+$ T cells. TCPSi and APSTCPSi NPs did not produce a positive proliferative response for any of the T cell subpopulations. With the exception of Un-P, other stimulative NPs slightly induced more proliferation of $CD8^+$ T cell subpopulation than $CD4^+$ T cell subpopulation.

5.3 Antibody functionalized PSi NPs for targeted cancer chemo-immunotherapy (III)

To further investigate the importance of the surface properties of the NPs and their biological interactions, Ab-functionalized PSi NPs were prepared and tested for the potential of combined targeting, chemotherapy and immunotherapy to synergistically increase the efficacy of cancer treatment. The Abs on the surface of the NPs have the ability to render targeting as wells as immunostimulatory properties to the NPs (mainly via ADCC activation).

5.3.1 Ab-mediated cell–NP interactions

To evaluate the impact of the surface modification of PSi NPs with Ab on both the cellular inteactions and the immune responses, anti-CD326 Ab-functionalized UnTHCPSi (Un-Ab) NPs were prepared. To confirm the specificity of CD326-mediated targeting of the NPs, the cell uptake was studied by confocal microscopy using CD326 overexpressing MCF-7 cells and MDA-MB-231 control cells, which have negligible expression of the receptor on their surface (Figure 12A and B). Results showed that when Alexa Fluor 488-labelled Un-Ab NPs were tested in MCF-7 cells, many of the NPs interacted with the cell membrane and resulted in a substantial increase in the cellular association, as seen by the green color in the confocal image. In contrast, for MDA-MB-231 cells exposed to the Un-Ab NPs, no targeting to the CD326 negative cells was observed. Similarly, after incubation of the cells with the Alexa Fluor 488-labeled UnTHCPSi NPs **(III)**, very weak green fluorescent signal was detectable in both the cell lines, showing weak cell–NP interactions. These results indicate that many of the NPs were able to interact with the CD326 positive cells after surface modification with the Ab. To further support these results, TEM imaging of both the cancer cells exposed to the free and Ab-functionalized NPs was performed. The results showed that after 3 h incubation with the UnTHCPSi NPs, there was no observable cellular association with either of the cancer cells (Figure 12C and E). In contrast, in MCF-7 cells, high localization of the Un-Ab was observed in the proximity of the cell membrane and inside the cells (Figure 12D), attributed to the NPs targeting towards the CD326 receptors of the cells. Very few Un-Ab NPs were also taken-up by the MDA-MB-231 cells (Figure 12F), possibly via nonspecific endocytosis and owing to the surface charge of the NPs (zeta-potential of 11.6 ± 1.1 mV). In addition, since a few of MDA-MB-231 cells express CD326 receptor on their surface, the observed cellular association can also be related to the interaction of Un-Ab NPs with the positive CD326 in the MDA-MB-231cells.

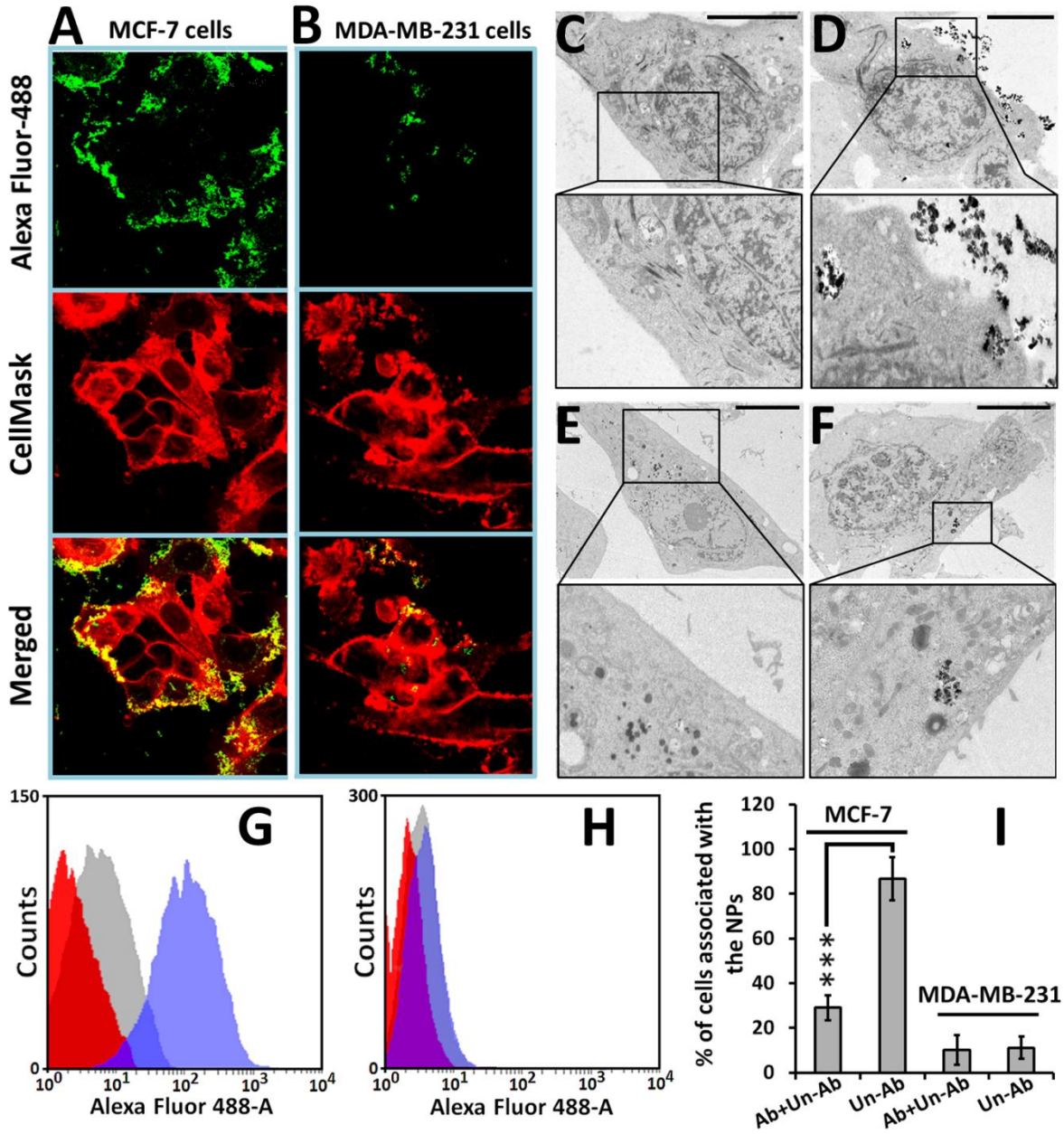

Figure 12 *Confocal fluorescence microscopy analysis of the MCF-7 (A) and MDA-MB-231 (B) cells incubated with 50 µg/mL of the Un-Ab NPs at 37°C for 3 h. CellMask® and Alexa Fluor-488® were used for staining of the cell membranes and the NPs in red and green color, respectively. TEM images of MCF-7 (C and D) and MDA-MB-231 (E and F) cells treated with 50 µg/mL of the bare and Un-Ab NPs for 3 h. Competitive inhibition cellular uptake for Un-Ab NPs in MCF-7 (G) and MDA-MB-231 (H) cells after pre-incubation with free anti-CD326 Ab for 30 min and followed 3 h exposure time with the NPs. The red, blue, and grey histograms are representative of the cells incubated with HBSS (control), the cells exposed to the Un-Ab with no pre-incubation step, and competitive cellular uptake of the Un-Ab NPs after pre-incubating with free Ab, respectively. Quantitative determination for the cell–NP interactions (I). About 10,000 events were evaluated for each measurement. Error bars represent s.d. ($n \geq 3$). The level of the significant differences of the non-competitive and competitive samples was set at a probability of ***$p < 0.005$. Copyright © (2014) Springer, reprinted with permission from [289].*

To validate the significant role of the Ab on the high cellular interactions of the Un-Ab NPs with MCF-7 cells, a competitive inhibition assay was also performed. The flow cytometry histograms (Figure 12G and H) showed significant decrease of the fluorescence intensity of the tested MCF-7 cells exposed to both the free Ab and Un-Ab NPs when compared to the cells exposed to the Un-Ab NPs alone. These results demonstrated that by using free Ab as a competitive inhibitor, the cellular interactions of the Un-Ab NPs were reduced due to the lower availability of the CD326 receptor on the cell surface for the NPs. Moreover, and in turn, this also suggested a specific targeting of the surface expressing CD326 cells via the developed Un-Ab nanovectors. As expected, the results for MDA-MB-231 cells were in contrast to the MCF-7 cells and showed no difference between the Un-Ab and Un-Ab pre-exposed to the free Ab. The quantitative analysis of the flow cytometry results are shown in Figure 12I.

5.3.2 Immunotherapeutic potential of Ab-functionalized UnTHCPSi NPs

To investigate the immunotherapeutic potential of the Un-Ab NPs and to check whether the Ab function could be affected after the conjugation onto the NPs' surface, the ADCC induction was performed as the main immunocytotoxic mechanism of the monoclonal Ab [290] for the free Ab, Ab-conjugated NPs, and pure NPs. Figure 13A shows that while the Un-Ab and free Ab could significantly induce the concentration dependent ADCC activity in MCF-7 cells in a similar manner, no considerably increased ADCC activity was detectable in MDA-MB-231 cells. In addition, in both the cancer cells, no increase of the ADCC activity was observed after treatment with the bare UnTHCPSi NPs and controls (data not shown). Since the ADCC activation is an immunotherapeutic mechanism in which an effector immune cell lyses a target cell, whose surface antigens are occupied by an Ab where its Fc portion is attached to the FcγRIII surface domains of the immune cells [291], the main reason for the absence of ADCC activation in MDA-MB-231 cells is the lack of CD326 antigen on the cell's surface.

In addition to the direct effect of the ADCC activation on lysing the targeted cancer cells, this mechanism can also indirectly improve the immunotherapeutic effect by enhancing cytokine production from the activated effector immune cells interacting with the target cells via the Ab [292]. Therefore, the IL-2 release was screened to evaluate whether the binding of the immune cells to the membrane surface antigens via FcγRIII could activate the cytokine secretion. As shown in Figure 13B, and in concordance with the ADCC results, the data showed no significant increase in the values for both the concentrations of the UnTHCPSi, Un-Ab, and free Ab in MDA-MB-231 cells, because of the low expression of CD326 on the surface of these cells. In MCF-7 cells (Figure 13C), while there was no increase in the IL-2 amount for UnTHCPSi NPs compared to the control (mixture of cancer and immune cells treated with medium), the IL-2 release was significantly increased after the treatment of the MCF-7 cells with Un-Ab, as well as with an equal amount of free Ab-conjugated to 25 and 100 μg/mL of the NPs. Since IL-2 induces immune responses via stimulating the proliferation of T cells against the specific recognized antigen [293], it can be used as an immunotherapeutic cancer suppressor in the developed nanovectors. Taken altogether, these results confirmed the crucial role of

immune–cancer cell interactions for the cell-mediated immune defenses via ADCC activation and subsequent enhancement of the levels of the corresponding cytokines at the site of interaction.

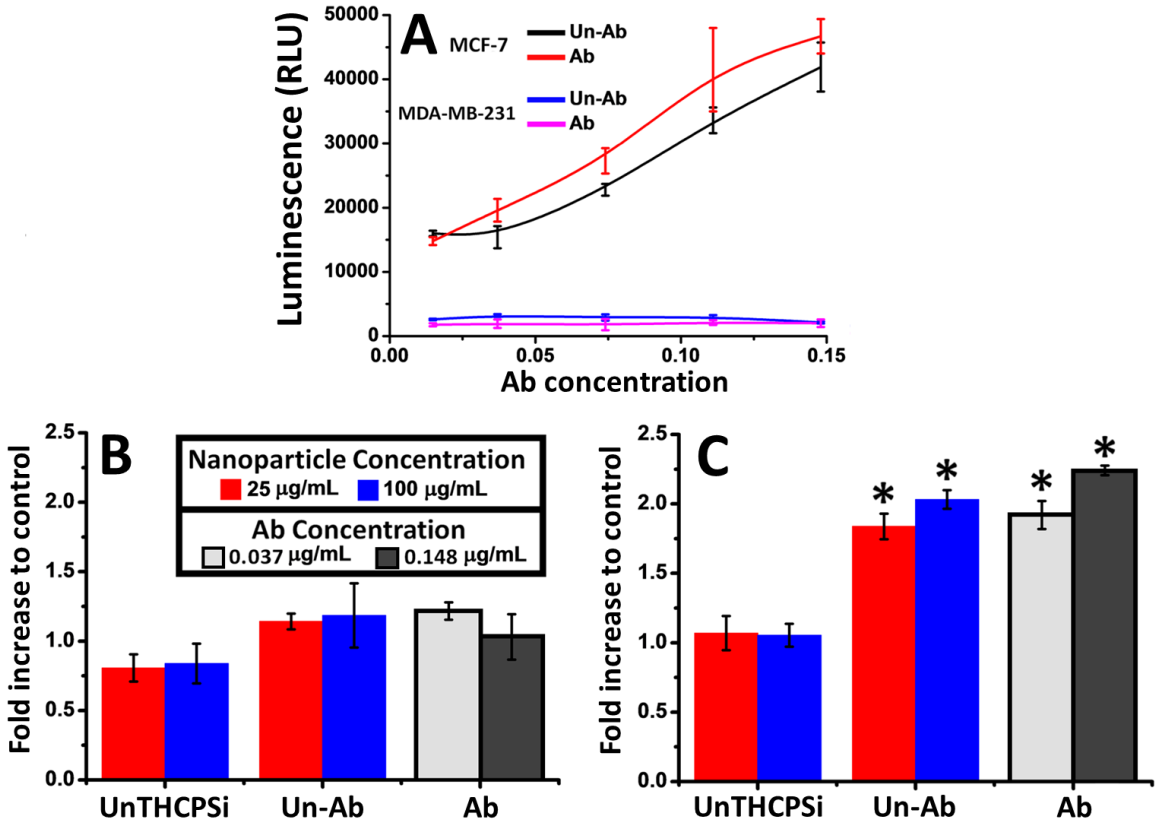

Figure 13 *Immunological effects of the developed Un-Ab NPs on the breast cancer cells. The ADCC activity (A) was determined after the incubation of the target cells with the effector cells (effector immune cell to the target cell ratio of 8:1), along with various concentrations of free anti-CD326 monoclonal Ab, as well as Un-Ab with an equal amount of the free tested Ab for 8 h. IL-2 production assessment in MDA-MB-231 (B) and MCF-7 (C) cells after 24 h incubation with UnTHCPSi and Un-Ab at the concentrations of 25 and 100 µg/mL, as well as of free Ab at concentrations of 0.037 and 0.0148 µg/mL (equivalent to the amount of Ab-conjugated to the low and high concentrations of the tested Un-Ab NPs). All the data sets were compared with the samples containing cancer and immune cells treated with the medium alone. The data shows the mean ± s.d (n = 4). The level of the significant differences was set at a probability of *p < 0.05, compared to the samples treated with medium. Copyright © (2014) Springer, reprinted with permission from [289].*

As it has been shown that the inhibitory effect of Ab-mediated immunotherapeutic mechanisms occur at the highest rate in earlier stages of the disease or when the tumor burden is small [294], it is illusive to expect efficient antitumor activity with just single Ab therapy in advanced cancer, where immune function is impaired as a consequence the nature of the disease [295]. Hence, our approach for the development of drug-loaded Un-Ab nanovectors points to the applicability of such nanovectors in getting synergistic anticancer response by increasing drug delivery to the target site, as well as ADCC activation and cytokine release. Nevertheless, we are currently at an early stage of

understanding about the therapeutic potential of Ab in targeted nanosystems and more studies are needed to develop efficient chemo-immunotherapeutic formulations by the Ab-conjugated drug loaded nanocarriers.

5.3.3 Drug release and anticancer effect

Although it is often assumed that the drugs loaded inside targeted NPs are released after reaching the target site, there is a high possibility for rapid unfavorable drug release after the intravenous administration [296]. Therefore, nanosystems with minimum drug release in the blood circulation are desirable for successful drug targeting. In this context, and as shown in Figure 14A, only ca. 15% of the pure drug was dissolved in human plasma over a 6 h period, ascribed to the very low solubility of SFN [297]. The use of PSi NPs led to a significant increase in the solubility of the anticancer drug to ca. 40% in 4 h. In contrast, for the Un-Ab, the accumulative drug release was less than 30% over the same time period. It can be deduced that the electrostatic interaction between the drug and the Ab may take place and slow down the drug release. Besides, as Ab conjugation was performed after the drug loading, pores can be partially blocked by the Ab and delay the drug release. The drug release amount remained constant until 24 h in all the tested samples (data not shown). Accordingly, it can be concluded that, although the developed nanovectors could improve the solubility of SFN in human plasma, the major part of drug (approximately 70%) was not immediately released and remained inside the pores of the NPs, suggesting the possibility of efficient delivery to the cancer cells via the CD326 receptor targeting.

After confirming the ability of the SFN-loaded Un-Ab NPs in sustaining the drug release and targeting, the assessment of the anti-proliferation effect of the NPs was also evaluated. An ATP-based luminescence assay was performed in both the cancer cells after 24 h exposure to the pure SFN, SFN-UnTHCPSi and SFN-Un-Ab NPs (Figures 14B and C). The anti-proliferative action on the MDA-MB-231 cells with negligible surface expression of the CD326 antigen showed no significant differences in the inhibitory effect of the SFN-UnTHCPSi NPs after Ab conjugation due to the very low cellular interaction with the cells, as shown in the confocal microscopy studies (Figure 12A and B). In MDA-MB-231 cells, the higher effect of the pure drug can be ascribed to its higher availability for the cells compared to the loaded ones, where majority of the drug is inside the NPs' pores and very low cellular interactions occur between the NPs and cells. These results demonstrated the absence of specific anticancer effect of the SFN-Un-Ab in MDA-MB-231 cells, and also suggested that the proliferation inhibition effect in MDA-MB-231 cells is mostly originated from the amount of drug released from the NPs rather than from the cellular uptake of the drug-loaded NPs.

In MCF-7 cells (Figure 14C), the cell proliferation inhibition effect of the targeted SFN-Un-Ab NPs and pure drug was higher than that of the SFN-UnTHCPSi NPs at the studied time-points. This is attributed to the superior interaction of the SFN-Un-Ab NPs with the cells and better accessibility of the pure drug to the cells compared to the SFN-UnTHCPSi NPs. Although the SFN-Un-Ab NPs showed less inhibitory effect than the pure drug at 8 h **(III)**, owing to their low drug release and the time needed for the uptake of the NPs, a similar trend was observed for both the samples after 24 h (Figure 14C). This

can be explained by the high CD326-mediated endocytosis of the SFN-Un-Ab over time, which probably resulted in the accumulation of the drug inside the cells and subsequent anticancer effect. Generally, very slow drug release in the bloodstream and increased cellular uptake by employing a functional surface moiety like Ab can be considered as a good combination for specific drug targeting to the cancer cells by means of NPs [298]. Moreover, the specific anticancer effect can be synergized *in vivo* by applying a suitable Ab with the ability of inducing ADCC activation and cytokine secretion from the effector immune cells, as explained in the previous sections. This approach can be applied to decrease the dosage required for efficient cancer treatment and also to minimize the side effects of the conventional anticancer drugs via desirable drug delivery kinetics to the right site in the body.

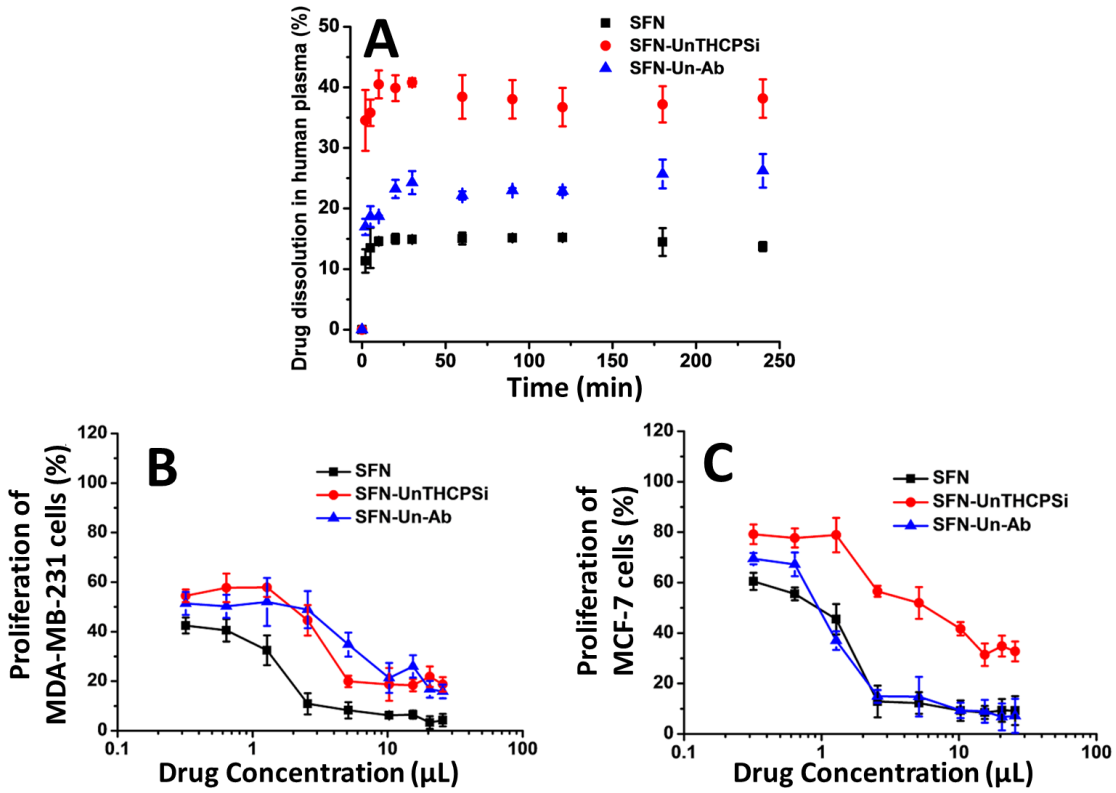

Figure 14 *Dissolution profiles of pure SFN, SFN-UnTHCPSi and SFN-Un-Ab in human plasma at 37°C (A). Growth inhibition effect of the pure SFN, SFN-UnTHCPSi and SFN-Un-Ab NPs are presented in MDA-MB-231 (B) and MCF-7 (C) cells. The NPs were suspended in the PBS containing 10% of FBS (pH 7.4). The cells were exposed to the samples for 24 h at 37ºC. The highest concentration of the pure SFN was prepared in 0.7% v/v of acetone in PBS containing 10% FBS solution (pH 7.4). The rest of the drug concentrations were prepared by a serial dilution of the highest drug concentration using PBS containing 10% FBS. The cell viability in 0.7% acetone solution was 96 ± 3%. The data represent the mean ± s.d. (n = 3). All measurements were performed in triplicate. Copyright © (2014) Springer, reprinted with permission from [289].*

5.4 Surface polymeric engineering of the PSi NPs for the cellular interaction enhancement (IV and V)

In addition to the surface functionalization with the Ab to enhance specific interactions with the cells, numerous attempts have been made to find new approaches to improve unfavorably low cellular interactions of the NPs by other methods [299, 300]. For example, cell penetrating peptides have been widely used for cellular uptake enhancement despite several disadvantages, such as low metabolic stability, possible immunogenicity, and dependency of their membrane translocation ability on the amino acids arrangement and site of conjugation with the NPs [301, 302]. Surface polymeric functionalization is one of the desirable alternatives that can be applied not only to affect the NP's properties by manipulation of the intrinsic smoothness, size, shape, charge, hydrophilicity, homogenicity, and stability, but also to act as a driving force for improving cellular internalization, endosomal escape, and drug release profiles with the final aim to achieve a subtle therapeutic effect [303].

5.4.1 Stability, cellular association and endosomal escape

Ideally, nanocarriers injected into the bloodstream should show minimal interactions with the plasma proteins in order to avoid agglomeration and rapid clearance by the macrophages [304]. To circumvent this problem, NPs can be modified, for example, with different kinds of polymers that resist the protein adsorption [305]. Figure 15A1 shows that the polymer-conjugated UnTHCPSi NPs exhibited a significantly lower variation in size and PdI compared to the bare NPs, indicating less interactions with human plasma proteins. Although it is known that the surface functionalization of the NPs with PEI can increase the stability of the NPs by reducing nonspecific protein adsorption [306], these results showed that PMVE-MA may also lead to a similar effect and decrease the NP interactions with plasma proteins.

One of the unavoidable problems associated with the PSi NPs is their intrinsic instability in aqueous solutions due to their tendency to aggregate, leading to significant decreases in their interfacial area, dispersibility, and cellular associations [195]. Accordingly, the stability assessment in aqueous medium was evaluated and showed that while the hydrodynamic diameter of the UnTHCPSi NPs was increased to over 1 μm in less than 90 min as a result of the NP aggregation, the polymer-functionalized particles showed no substantial change in the particle size (Figure 15A2). Further stability assessment of the NPs for 2 days revealed no change in the size of the polymer-conjugated NPs from 2 h to 48 h (data not shown). The appearance of the NPs after storing at RT for 4 h is shown in Figure 15A3. It was observed that the native UnTHCPSi NPs were aggregated and precipitated over time due to the hydrophobic properties, whereas the polymer functionalized NPs were quite stable and very well dispersed because of the improved hydrophilicity and repulsion forces between the NPs [307, 308].

The cellular trafficking and endosomal escape was also evaluated in MCF-7 and MDA-MB-231 breast cancer cell lines by confocal fluorescence microscopy and simultaneous imaging of the PSi NPs, cell membrane, and the acidic compartments of the

cells. Since the drug loaded NPs entrapped in endosomes and lysosomes can be easily degraded by specific enzymes, the endosomal escape of the NPs is a critical prerequisite for effective therapeutic response [256]. While our results showed negligible cell uptake of the UnTHCPSi NPs in both the cell lines, an increase in the cellular internalization of Un-P and Un-P-P NPs was confirmed by observing the turquoise color in the merged picture as a result of the colocalization of the green fluorescence of the PSi NPs and the blue color of the MDA-MB-231 and MCF-7 cells (Figure 15B). In addition, for both the cell lines, only few NPs were located inside the acidic endosomal compartments, as shown by the overlapped yellow color (green NPs and red acidic compartments) in the merged picture. Some of the particles also remained on the surface of the cell membrane, presented as a green color. These observations indicate that the polymer-modified NPs were able to interact with the cells, escape from the acidic compartments and localize in the cytosol more efficiently. The plausible explanation for the above observation is that the free available amine groups in the PEI layer of the Un-P-P NPs can induce endosomal escape via "proton-sponge" or "endosome buffering" effects [309]. In addition, the endosomal escape could be probably due to the fact that, although the maleic acid amide (MAA) constructed by the conjugation of the carboxyl groups of maleic acid to the amine groups of PEI in Un-P-P is stable at extracellular neutral pH, it is capable to be rapidly hydrolyzed at the endosomal acidic pH [310, 311], leading to a high impact on the proton sponge effect because of the presence of both available free hidden amine groups of the PEI and those that become free after PMVE-MA dissociation. Another explanation for this observation could be the ability of PMVE-MA layer to fuse into the lipid bilayer of the acidic compartments of the endosomes and disrupt them, similarly to previous reports for other specific anionic polymers [312, 313].

The confocal results showed that the Un-P NPs can cross the cell membranes of the MDA-MB-231 cells after 6 h of incubation, confirming that the PEI conjugation successfully endow the UnTHCPSi NPs with a cellular association function. In contrast, the observed lower cellular uptake by the MCF-7 cells can be ascribed to the higher resistance of the MCF-7 cells compared to the MDA-MB-231 cells, as well as its tendency to make condensed clusters, minimizing its interactions with the NPs.

To confirm the confocal imaging results, the flow cytometry experiments were conducted in the presence and absence of TB (which acts as a fluorescence quenching agent). In the samples that were not treated with the TB, while there was no change in the fluorescence peak of the bare UnTHCPSi NPs in both the cell lines compared to the control (Figure 15C1 and C3), the fluorescence intensity of the cells incubated with Un-P and Un-P-P NPs was considerably shifted to the right, a clear evidence for the high cellular association of the polymer-conjugated NPs and the cells. For the TB treated samples (Figure 15C2 and C4), the quenching agent was not able to completely remove all the fluorescence of the cells treated with the polymer-conjugated NPs, revealing the cellular internalization of the NPs in 6 h.

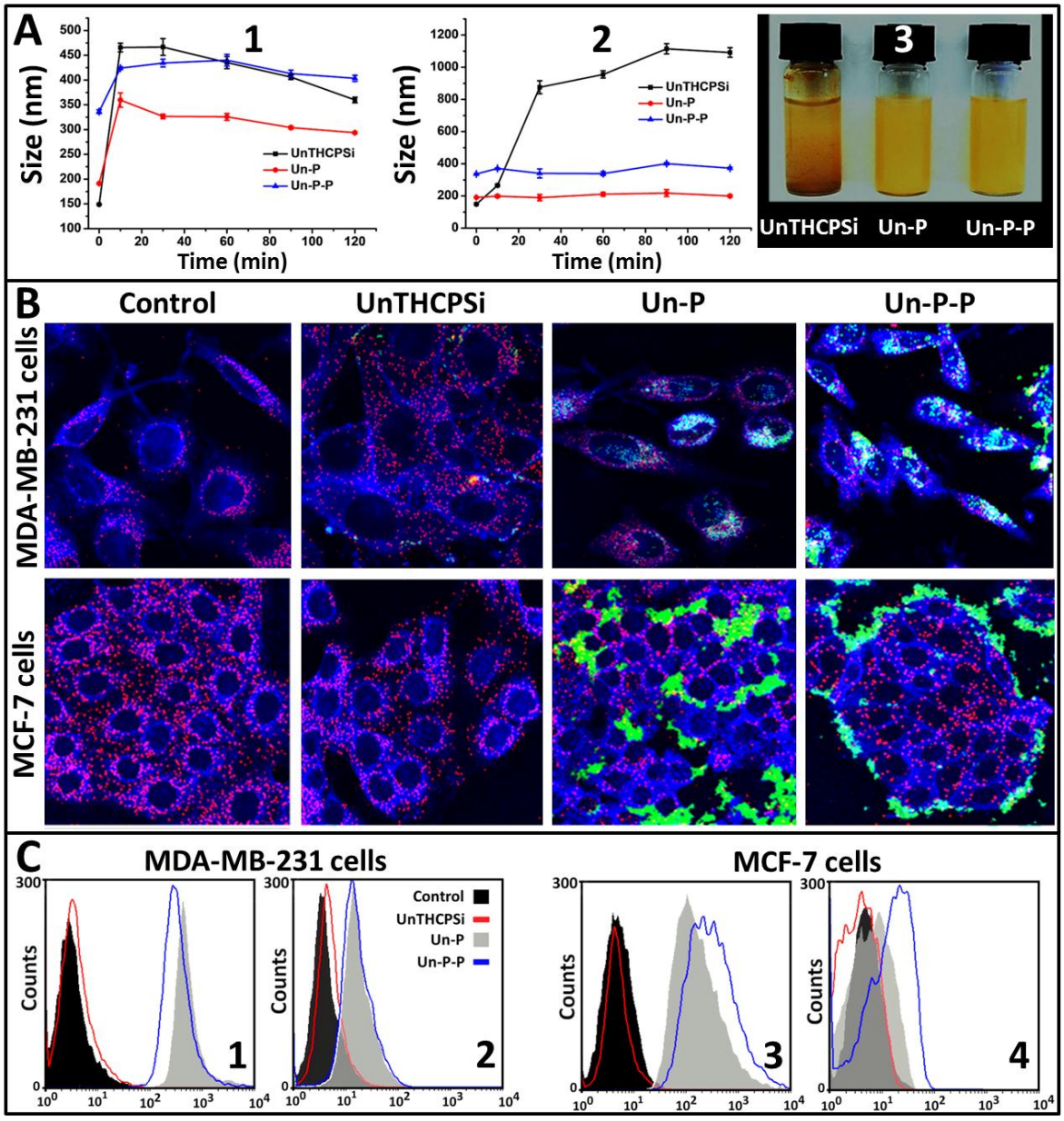

Figure 15 *The stability of the bare and surface modified PSi NPs in human plasma (A1) and aqueous solution (A2) over 2h at 37°C. Colloidal stability (A3) was measured after 4 h of incubation in static conditions. Values denote the mean ± s.d. (n = 3). Merged panel of the confocal fluorescence microscopy analysis of the cells incubated with HBSS buffer (pH 7.4) as control, as well as 50 µg/mL of UnTHCPSi, Un-P, and Un-P-P at 37°C for 6 h (B). Lysotracker and CellMask for staining the lysosomes and the cell membranes are shown in red and blue pseudo-colors, respectively. The image shows the internalized NPs outside of the acidic endosomal compartments in turquoise color and those co-localized in early endosomes and lysosomes in yellow color. The NPs that are located on the surface of the cell membrane are shown in green color. Flow cytometry analyses of MDA-MB-231 and MCF-7 cells before (C1 and C3) and after (C2 and C4) extracellular fluorescence quenching by TB to evaluate both cellular uptake and extracellular binding of the NPs with the cell membrane. The cells were incubated with UnTHCPSi, Un-P, and Un-P-P NPs for 6 h at 37°C. The results are representative of three independent experiments. Copyright © (2013) Elsevier B. V., reprinted with permission from [314].*

Although many reports in the literature have demonstrated the ability of some specific types of positively charged polymers, such as PEI, for successful improvement of the cellular internalization and endosomal escape [315], these materials have shown drawbacks in terms of making overt pores in the lipid bilayers, which can eventually lead to cellular toxicity by disturbing the concentration balance of ions and proteins that are essential to maintain the normal function of the cells [316, 317]. Thus, the application of specific polymer-conjugated nanostructures, which are capable to avoid cellular toxicity while increasing the cellular trafficking and releasing their payloads in the cytoplasm, is essential for designing superior nanomedicines.

To show the important role of the outer polymer layer (PMVE-MA) of the developed nanosystems in the enhanced cellular interaction, PMVE-MA-conjugated APSTCPSi NPs were prepared without the PEI layer. The hydrodynamic size, zeta-potential, and PdI of the particles were investigated before and after functionalization (Figure 16A–C). The size of the NPs increased from 168 ± 2.2 to 201 ± 1.8 nm, and a significant change of the zeta-potential from positive (33 ± 2.4 mV) to negative (−31 + 2.8 mV) was observed, indicating successful polymeric conjugation to the PSi NPs' surface. The PdI of all NPs was less than 0.2.

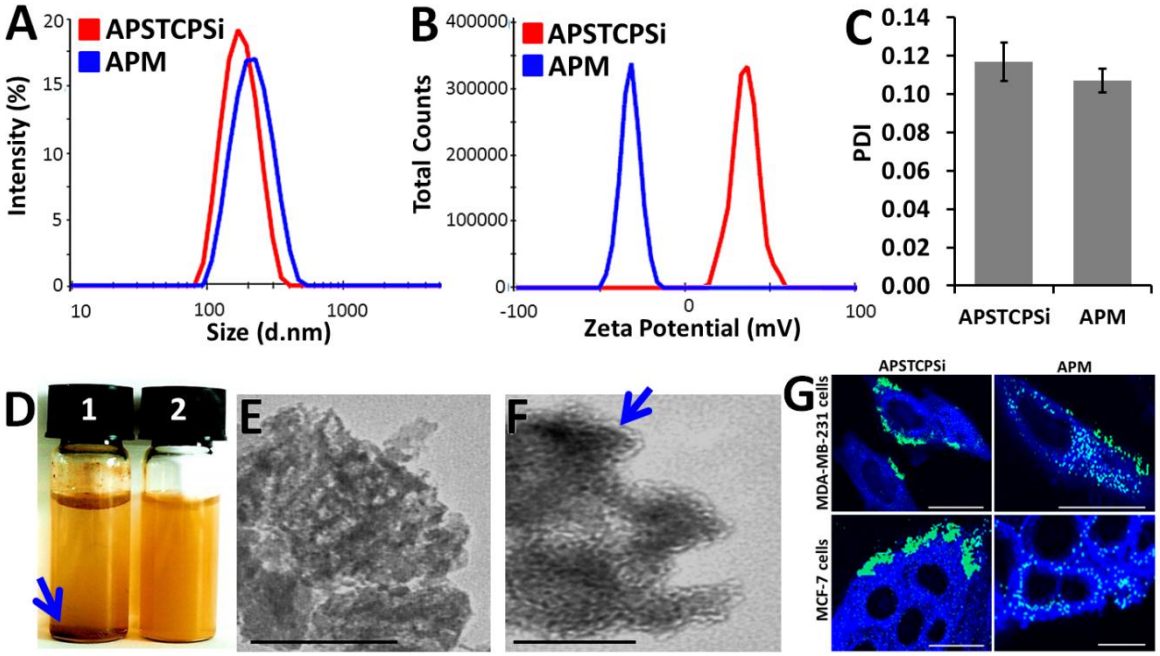

Figure 16 *Size (A), zeta-potential (B), and PdI (C) of the PSi NPs after preparation, colloidal stability after 2 h incubation of APSTCPSi (D1) and APM (D2) NPs at RT. TEM images of APSTCPSi (E) and APM (F) with the scale bars of 100 nm, and confocal fluorescence microscopy analysis of the MDAMB-231 and MCF-7 cells incubated with 50 μg/mL of APSTCPSi and APM NPs at 37°C for 6 h. The arrows in section D and F indicate APSTCPSi NPs precipitation in aqueous solution and the polymer layer on the surface of APM NPs, respectively. CellMask for staining of the cell membranes is shown in blue pseudo-color. The picture shows the APSTCPSi NPs on the surface membrane in green color and internalized APM NPs in turquoise color. The scale bars in the lower right panels for MDA-MB231 and MCF-7 cells correspond to 20 μm. Copyright © (2013) John Wiley & Sons, Inc., reprinted with permission from [318].*

The colloidal stability evaluation of the samples after 2 h storage at RT in static conditions showed that while the APSTCPSi NPs agglomerated very fast, the APM NPs were highly stable owing to the enhanced surface hydrophilicity of the NPs (Figure 16D). TEM images (Figure 16E and F) showed a surface coverage on top of the pores for APM NPs, which is not observed in the APSTCPSi NPs.

In order to demonstrate the relevant bioadhesive potential of PMVE-MA, the cellular interaction of the NPs was further explored by confocal microscopy using simultaneous imaging of the PSi NPs and the cell membrane of the cells (Figure 16G). The results showed the localization of the APSTCPSi NPs on the outer cellular membranes of the MDA-MB-231 and MCF-7 cells, and a further increase in the cellular penetration of the APM NPs, as it could be seen by the change of PSi NPs' green fluorescence on the surface of the cell membrane to turquoise for the NPs located inside the cells in the merged picture. The high cellular uptake of the APM NPs can be hypothetically attributed to the presence of PMVE-MA, which is probably able to fuse into the lipid bilayer of the membrane, similarly to what has also been observed for other specific surface anionic NPs [319, 320]. In this nanosystem, the cellular internalization can be attributed to the nonspecific binding of the particles to the existing cationic sites on the cell membrane, high dispersibility of the NPs, as well as the bioadhesive properties of the PMVE-MA polymer [144]. The pronounced difference in the cellular uptake of the bare and APM NPs supports the fact that the surface chemical modification is among the most efficient strategies for the modulation of biological functions of the NPs. However, the cellular uptake of the NPs could also be dependent on many other factors such as size, shape, surface charge, aggregation/agglomeration states, purity of the NPs, and NP–cell incubation conditions, making the actual uptake assessment of a given type of NPs rather complex [5].

5.4.2 Drug loading, release study and antiproliferation effect

Next, the drug-loading of the NPs by comparing the drug loading degree before and after polymeric conjugation was investigated. MTX was chosen as a model anticancer drug due to its potency in breast cancer treatment [321], and the presence of both carboxyl and amine groups in its structure. The latter unique property of this drug can enhance the probability of its interactions with the amine and carboxyl groups of the polymers conjugated to the NPs, and consequently, increase its loading degree in the PSi NPs. The loading degree of MTX in the UnTHCPSi NPs was 6.4 ± 1.2%, whereas the PEI and PMVE-MA conjugation improved the MTX loading degrees to 12.6 ± 0.1 and 14.0 ± 0.5%, respectively. The low MTX loading in the bare UnTHCPSi can be attributed to the low affinity of the drug to the pores of the bare NPs, because of the intrinsic hydrophobic nature of the pores. Contrarily, polymer-conjugated NPs are prone to inter-particle hydrogen and electrostatic bonding with the drug, leading to the improved drug loading. This suggests that the polymer conjugation could increase the loading of the drug due to the more interactions of the drug's functional groups with the free amine and carboxyl groups of the polymer-conjugated PSi NPs. The drug release profiles of MTX-loaded PSi NPs were also evaluated. Figure 17A shows the sustained drug release profiles after polymeric conjugation. The UnTHCPSi NPs released all the MTX in less than 5 min in

PBS (pH 7.4) due to the rapid diffusion of the drug from the pores. Contrarily, the release rate from PEI- and PEI-PMVEMA-conjugated PSi NPs were significantly slower than that of observed for the bare PSi NPs, showing a constant drug release up to about 95 and 70% within the first 3 h, respectively. Afterwards, no significant change was observed in the cumulative drug release until 12 h. This suggests that the polymer layers provide an easy means to tune the drug release profile by capping on top of the PSi NPs and the hydrogen and electrostatic binding with the drug molecules [322]. A plausible explanation for the slower drug release rate from the Un-P-P NPs compared to the Un-P NPs is the presence of both carboxyl and amine groups in the MTX structure, which increases the possibility of interaction with the amine groups of PEI and the carboxyl groups of PMVE-MA in Un-P-P NPs.

In order to demonstrate that the Un-P-P NPs can efficiently deliver the anticancer drug inside the cells, the cell proliferation was analyzed in breast cancer cells exposed to the MTX-loaded PSi NPs using an ATP-based activity assay (Figure 17B and C). The results showed that the free drug and the MTX-loaded UnTHCPSi NPs had the same proliferation inhibition pattern, reducing the cell viability from 90% to less than 35% for the MDA-MB-231 cells and from 95% to around 50% for the MCF-7 cells. In contrast, the MTX-loaded Un-P-P NPs exhibited more efficient therapeutic efficiency than the free and MTX-loaded UnTHCPSi NPs in both the cell lines. In the MDA-MB-231 and MCF-7 cells, the proliferation rate was decreased from 64% to less than 10% and from 77% to around 27%, respectively, after the exposure to the Un-P-P NPs. All the data sets were compared with the negative control HBSS (pH 7.4), considered as 100% proliferation. These results clearly revealed the potent cytotoxic effect of the developed nanosystem in the breast cancer cells. The lower effect of the MTX-loaded UnTHCPSi NPs can be attributed to the low cellular uptake of the particles. In addition, the higher proliferation inhibition of the MTX-Un-P-P in the MDA-MB-231 cells compared to the MCF-7 cells is attributed to the higher cellular internalization of the NPs in the former one. Since the anticancer effect of the MTX is related to its potency to penetrate inside the cells and inhibit folic acid reductase and DNA synthesis during cellular replication [323, 324], the higher therapeutic efficiency of the Un-P-P NPs can be probably explained by the ability of the nanocarriers to deliver higher amounts of the MTX inside the cells, resulting in a higher cytotoxicity effect.

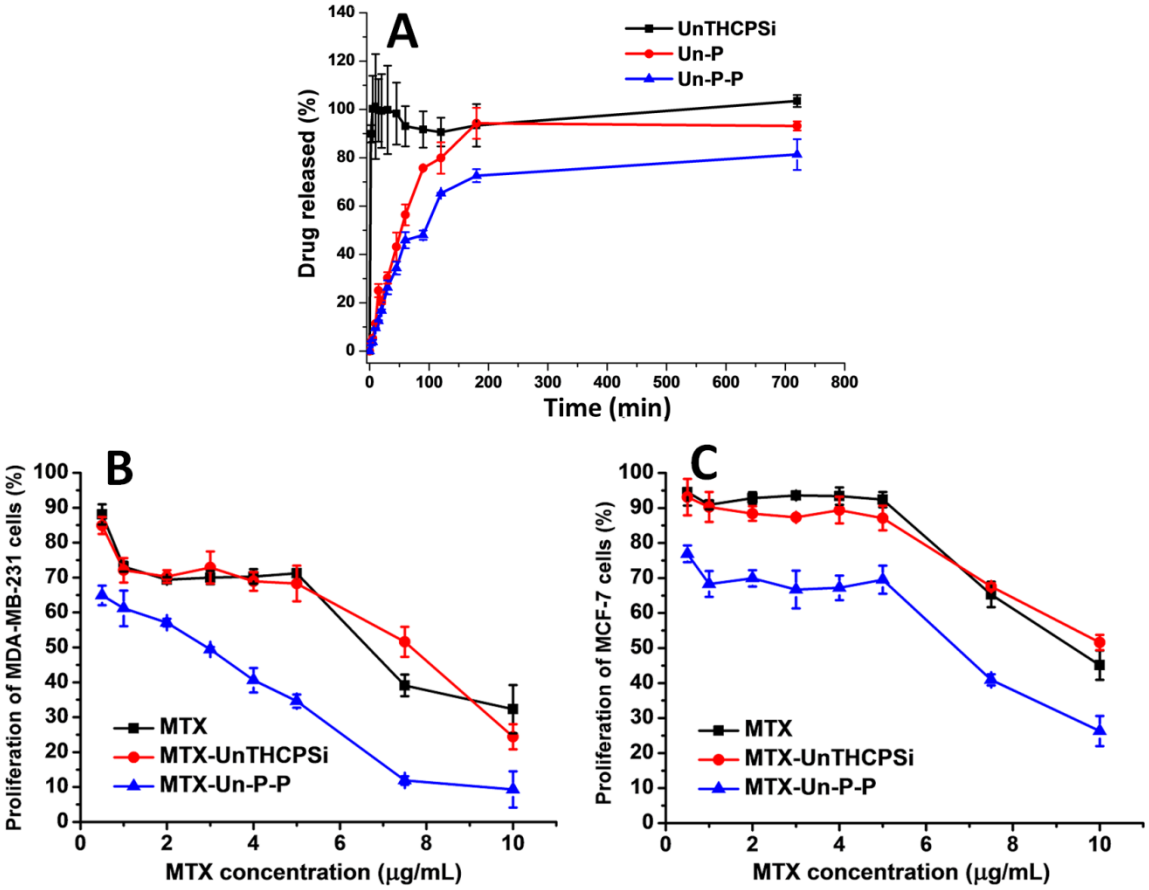

Figure 17 *Drug release profiles of MTX-loaded UnTHCPSi and polymer-conjugated PSi NPs in PBS (pH 7.4) at 37°C (A). Proliferation of MDA-MB-231 (B) and MCF-7 (C) cells after exposure to free MTX, MTX-UnTHCPSi and MTX-Un-P-P for 6 h at 37°C. In MDA-MB-231 cells, free MTX and MTX-UnTHCPSi showed a mild concentration-independent cell proliferation reduction and MTX-Un-P-P revealed potent concentration-dependent cell proliferation decrease. In MCF-7 cells, while free drug and MTX-UnTHCPSi showed very high cell proliferation, MTX-Un-P-P induced a moderate cell proliferation reduction effect independent of the concentration tested. Data are expressed as the mean of three independent experiments ± s.d. (n = 3). Copyright © (2013) Elsevier B. V., reprinted with permission from [314].*

6 Conclusions

In this dissertation, the impact of the surface modification of the PSi NPs on the biological responses was investigated at the cellular level by evaluating the cytotoxicity, immune responses, and cellular interactions. Such studies can clarify how various functional groups, biomolecules, or polymers on the surface of the PSi NPs can render new properties to the NPs for specific applications like immunotherapy, cancer therapy, or targeting to the right site of interest.

First, the mechanisms involved in the genotoxicity of immune cells were investigated after exposure to different PSi NPs. The toxicity of the PSi NPs was found to be predominantly surface chemistry- and charge-dependent. The cytotoxicity of the PSi NPs was more affected by the surface charge of the NPs than their hydrophilic/hydrophobic surface properties. However, for similar surface charges, the NPs with hydrophobic surfaces, i.e., THCPSi and UnTHCPSi NPs, were more cytotoxic than the hydrophilic ones (i.e., TOPSi and TCPSi NPs). More importantly, it was demonstrated that no single methodology is likely to meet all the requirements to comprehensively study the biosafety profiles of the PSi NPs, as there are different mechanisms for toxicity induction.

Next, it was demonstrated that, at the non-toxic concentrations, the surface chemistry of the PSi NPs has a significant effect on the immune responses by modulating the expression of co-stimulatory signals and cytokine release by DCs. TOPSi (SiO_x-layer) and THCPSi (SiC_xH_y-layer) were more effective inducers of immunoactivation responses by enhancing the expression of CD80, CD83, CD86 and MHC-II, as well as increasing the secretion of cytokines mediating T cell differentiation. In contrast, TCPSi and APSTCPSi (both SiC_x-layer based) NPs did not show any signs of immunostimulation, suggesting their potential for the delivery of immunosuppressive compounds due to the negligible effects on the DCs and T cells.

Then, Ab-functionalized drug loaded PSi nanovectors were developed to mediate chemo-immunotherapy approaches. It was shown that with proper attachment of the Ab on the surface of the particles, this biomolecule can be served as a targeting moiety, immunotherapeutic biomolecule, as well as a cap for blocking drug molecules within the pores and minimizing their premature release.

Finally, it was shown that the polymeric functionalization of the PSi NPs can be also a proper strategy to improve safety, stability, cellular interaction, and endosomal escape of the NPs, all important attributes for therapeutic applications. Functionalized PSi NPs were prepared by covalent conjugation of PEI and PMVE-MA polymers onto the surface of UnTHCPSi NPs with high potential for sustained drug release and intracellular delivery in breast cancer cells. These particles showed more potent antiproliferative properties on cancer cells compared to the pure tested anticancer drug (MTX).

Overall, the work in this thesis demonstrates how the surface modification of the PSi NPs can render new biological properties to the particles, opening new insights for the applications of the PSi NPs for biomedical applications and holding promises for further progresses in cancer therapy.

References

[1] Aillon KL, Xie Y, El-Gendy N, Berkland CJ, Forrest ML. Effects of nanomaterial physicochemical properties on in vivo toxicity. Adv Drug Deliv Rev 2009;61:457-66.

[2] Fischer HC, Chan WC. Nanotoxicity: the growing need for in vivo study. Curr Opin Biotechnol 2007;18:565-71.

[3] Morishige T, Yoshioka Y, Inakura H, Tanabe A, Yao X, Tsunoda S, Tsutsumi Y, Mukai Y, Okada N, Nakagawa S. Cytotoxicity of amorphous silica particles against macrophage-like THP-1 cells depends on particle-size and surface properties. Pharmazie 2010;65:596-9.

[4] Santos HA, Bimbo LM, Lehto VP, Airaksinen AJ, Salonen J, Hirvonen J. Multifunctional porous silicon for therapeutic drug delivery and imaging. Curr Drug Discov Technol 2011;8:228-49.

[5] Santos HA, Riikonen J, Salonen J, Mäkilä E, Heikkila T, Laaksonen T, Peltonen L, Lehto VP, Hirvonen J. In vitro cytotoxicity of porous silicon microparticles: effect of the particle concentration, surface chemistry and size. Acta Biomater 2010;6:2721-31.

[6] Stano A, Nembrini C, Swartz MA, Hubbell JA, Simeoni E. Nanoparticle size influences the magnitude and quality of mucosal immune responses after intranasal immunization. Vaccine 2012;30:7541-6.

[7] Moyano DF, Goldsmith M, Solfiell DJ, Landesman-Milo D, Miranda OR, Peer D, Rotello VM. Nanoparticle hydrophobicity dictates immune response. J Am Chem Soc 2012;134:3965-7.

[8] Fifis T, Gamvrellis A, Crimeen-Irwin B, Pietersz GA, Li J, Mottram PL, McKenzie IF, Plebanski M. Size-dependent immunogenicity: therapeutic and protective properties of nano-vaccines against tumors. J Immunol 2004;173:3148-54.

[9] Kalkanidis M, Pietersz GA, Xiang SD, Mottram PL, Crimeen-Irwin B, Ardipradja K, Plebanski M. Methods for nano-particle based vaccine formulation and evaluation of their immunogenicity. Methods 2006;40:20-9.

[10] Mallapragada SK, Narasimhan B. Immunomodulatory biomaterials. Int J Pharm 2008;364:265-71.

[11] Nandakumar KS, Shakya AK. Polymers as immunological adjuvants: An update on recent developments. J BioSci Biotech 2012;1:199-210.

[12] Oyewumi MO, Kumar A, Cui Z. Nano-microparticles as immune adjuvants: correlating particle sizes and the resultant immune responses. Expert Rev Vaccines 2010;9:1095-107.

[13] Klippstein R, Pozo D. Nanotechnology-based manipulation of dendritic cells for enhanced immunotherapy strategies. Nanomedicine 2010;6:523-9.

[14] Corrigall VM, Solau-Gervais E, Panayi GS. Lack of CD80 expression by fibroblast-like synoviocytes leading to anergy in T lymphocytes. Arthritis Rheum 2000;43:1606-15.

[15] Hirai T, Yoshikawa T, Nabeshi H, Yoshida T, Tochigi S, Uji M, Ichihashi K, Akase T, Yamashita T, Yamashita K, Nagano K, Abe Y, Kamada H, Tsunoda S, Yoshioka Y, Itoh N, Tsutsumi Y. Size-dependent immune-modulating effect of amorphous nanosilica particles. Pharmazie 2011;66:727-8.

[16] Secret E, Smith K, Dubljevic V, Moore E, Macardle P, Delalat B, Rogers ML, Johns TG, Durand JO, Cunin F, Voelcker NH. Antibody-Functionalized Porous Silicon Nanoparticles for Vectorization of Hydrophobic Drugs. Advanced Healthcare Materials 2013;2:718-27.

[17] Byrne JD, Betancourt T, Brannon-Peppas L. Active targeting schemes for nanoparticle systems in cancer therapeutics. Adv Drug Deliv Rev 2008;60:1615-26.

[18] Chattopadhyay N, Fonge H, Cai Z, Scollard D, Lechtman E, Done SJ, Pignol JP, Reilly RM. Role of antibody-mediated tumor targeting and route of administration in nanoparticle tumor accumulation in vivo. Mol Pharm 2012;9:2168-79.

[19] Weiner LM, Surana R, Wang S. Monoclonal antibodies: versatile platforms for cancer immunotherapy. Nat Rev Immunol 2010;10:317-27.

[20] Berlin JM, Pham TT, Sano D, Mohamedali KA, Marcano DC, Myers JN, Tour JM. Noncovalent functionalization of carbon nanovectors with an antibody enables targeted drug delivery. ACS Nano 2011;5:6643-50.

[21] Gu L, Ruff LE, Qin Z, Corr M, Hedrick SM, Sailor MJ. Multivalent porous silicon nanoparticles enhance the immune activation potency of agonistic CD40 antibody. Adv Mater 2012;24:3981-7.

[22] Illum L, Jones PD, Baldwin RW, Davis SS. Tissue distribution of poly(hexyl 2-cyanoacrylate) nanoparticles coated with monoclonal antibodies in mice bearing human tumor xenografts. J Pharmacol Exp Ther 1984;230:733-6.

[23] Scott D, Nitecki DE, Kindler H, Goodman JW. Immunogenicity of biotinylated hapten-avidin complexes. Mol Immunol 1984;21:1055-60.

[24] Tian H, Guo Z, Chen J, Lin L, Xia J, Dong X, Chen X. PEI conjugated gold nanoparticles: efficient gene carriers with visible fluorescence. Adv Healthc Mater 2012;1:337-41.

[25] Sudeep PK, Page Z, Emrick T. PEGylated silicon nanoparticles: synthesis and characterization. Chem Commun (Camb) 2008:6126-7.

[26] Shahbazi MA, Herranz B, Santos HA. Nanostructured porous Si-based nanoparticles for targeted drug delivery. Biomatter 2012;2:296-312.

[27] Gajewski TF, Woo SR, Zha Y, Spaapen R, Zheng Y, Corrales L, Spranger S. Cancer immunotherapy strategies based on overcoming barriers within the tumor microenvironment. Curr Opin Immunol 2013;25:268-76.

[28] Monjazeb AM, Hsiao HH, Sckisel GD, Murphy WJ. The role of antigen-specific and non-specific immunotherapy in the treatment of cancer. J Immunotoxicol 2012;9:248-58.

[29] Gedeon PC, Riccione KA, Fecci PE, Sampson JH. Antibody-based immunotherapy for malignant glioma. Semin Oncol 2014;41:496-510.

[30] Chandramohan V, Mitchell DA, Johnson LA, Sampson JH, Bigner DD. Antibody, T-cell and dendritic cell immunotherapy for malignant brain tumors. Future Oncol 2013;9:977-90.

[31] Nembrini C, Stano A, Dane KY, Ballester M, van der Vlies AJ, Marsland BJ, Swartz MA, Hubbell JA. Nanoparticle conjugation of antigen enhances cytotoxic T-cell responses in pulmonary vaccination. Proc Natl Acad Sci U S A 2011;108:E989-97.

[32] Biron CA, Hutt-Fletcher LM, Wertz GT, Pagano JS. Interferon production and activation of non-specific effector cells by stimulation with lymphoblastoid cell lines in vitro. Int J Cancer 1981;27:185-90.

[33] Ferris RL, Jaffee EM, Ferrone S. Tumor antigen-targeted, monoclonal antibody-based immunotherapy: clinical response, cellular immunity, and immunoescape. J Clin Oncol 2010;28:4390-9.

[34] Ma M, Zhang Y, Gong H, Li F, Gu N. Silica-coated magnetite nanoparticles labeled by nimotuzumab, a humanised monoclonal antibody to epidermal growth factor receptor: preparations, specific targeting and bioimaging. J Nanosci Nanotechnol 2013;13:6541-5.

[35] Tao L, Zhang K, Sun Y, Jin B, Zhang Z, Yang K. Anti-epithelial cell adhesion molecule monoclonal antibody conjugated fluorescent nanoparticle biosensor for sensitive detection of colon cancer cells. Biosens Bioelectron 2012;35:186-92.

[36] Jacene HA, Filice R, Kasecamp W, Wahl RL. Comparison of 90Y-ibritumomab tiuxetan and 131I-tositumomab in clinical practice. J Nucl Med 2007;48:1767-76.

[37] Monjanel H, Deville L, Ram-Wolff C, Venon MD, Franchi P, Benet C, de Kerviler E, Malphettes M, Thieblemont C, Brice P. Brentuximab vedotin in heavily treated Hodgkin

and anaplastic large-cell lymphoma, a single centre study on 45 patients. Br J Haematol 2014;166:306-8.

[38] Signori E, Iurescia S, Massi E, Fioretti D, Chiarella P, De Robertis M, Rinaldi M, Tonon G, Fazio VM. DNA vaccination strategies for anti-tumour effective gene therapy protocols. Cancer Immunol Immunother 2010;59:1583-91.

[39] Lee S, Margolin K. Cytokines in cancer immunotherapy. Cancers (Basel) 2011;3:3856-93.

[40] Pawelec G. The role of cytokines in tumor immunotherapy. Report on the 2nd Frankfurt International Cytokine Symposium 25-27 June 1992, Frankfurter Hof, Frankfurt, Germany. Mol Biother 1992;4:201-3.

[41] Pezzutto A. [Immunotherapy: cytokines and tumor cell vaccines]. Internist (Berl) 1998;39:1131-8.

[42] Van Kampen KR. Immunotherapy and cytokines. Semin Vet Med Surg (Small Anim) 1997;12:186-92.

[43] Olioso P, Giancola R, Di Riti M, Contento A, Accorsi P, Iacone A. Immunotherapy with cytokine induced killer cells in solid and hematopoietic tumours: a pilot clinical trial. Hematol Oncol 2009;27:130-9.

[44] Jia L, Jin H, Zhou J, Chen L, Lu Y, Ming Y, Yu Y. A potential anti-tumor herbal medicine, Corilagin, inhibits ovarian cancer cell growth through blocking the TGF-beta signaling pathways. BMC Complement Altern Med 2013;13:33.

[45] Luo Y. Blocking IL-10 enhances bacillus Calmette-Guerin induced T helper Type 1 immune responses and anti-bladder cancer immunity. Oncoimmunology 2012;1:1183-5.

[46] Berretta F, St-Pierre J, Piccirillo CA, Stevenson MM. IL-2 contributes to maintaining a balance between CD4+Foxp3+ regulatory T cells and effector CD4+ T cells required for immune control of blood-stage malaria infection. J Immunol 2011;186:4862-71.

[47] Chen CY, Huang D, Yao S, Halliday L, Zeng G, Wang RC, Chen ZW. IL-2 simultaneously expands Foxp3+ T regulatory and T effector cells and confers resistance to severe tuberculosis (TB): implicative Treg-T effector cooperation in immunity to TB. J Immunol 2012;188:4278-88.

[48] Hofer T, Krichevsky O, Altan-Bonnet G. Competition for IL-2 between Regulatory and Effector T Cells to Chisel Immune Responses. Front Immunol 2012;3:268.

[49] Humrich JY, Morbach H, Undeutsch R, Enghard P, Rosenberger S, Weigert O, Kloke L, Heimann J, Gaber T, Brandenburg S, Scheffold A, Huehn J, Radbruch A, Burmester GR, Riemekasten G. Homeostatic imbalance of regulatory and effector T cells due to IL-2 deprivation amplifies murine lupus. Proc Natl Acad Sci U S A 2010;107:204-9.

[50] Pawelec G, Rees RC, Kiessling R, Madrigal A, Dodi A, Baxevanis C, Gambacorti-Passerini C, Masucci G, Zeuthen J. Cells and cytokines in immunotherapy and gene therapy of cancer. Crit Rev Oncog 1999;10:83-127.

[51] Verbik D, Joshi S. Immune cells and cytokines - their role in cancer-immunotherapy (review). Int J Oncol 1995;7:205-23.

[52] Lesterhuis WJ, de Vries IJ, Adema GJ, Punt CJ. Dendritic cell-based vaccines in cancer immunotherapy: an update on clinical and immunological results. Ann Oncol 2004;15 Suppl 4:iv145-51.

[53] Kapsenberg ML. Dendritic-cell control of pathogen-driven T-cell polarization. Nat Rev Immunol 2003;3:984-93.

[54] Coosemans A, Tuyaerts S, Vanderstraeten A, Vergote I, Amant F, Van Gool SW. Dendritic cell immunotherapy in uterine cancer. Hum Vaccin Immunother 2014;10.

[55] D HY, Appel S. Current status and future perspectives of dendritic cell-based cancer immunotherapy. Scand J Immunol 2013;78:167-71.

[56] Hanke N, Alizadeh D, Katsanis E, Larmonier N. Dendritic cell tumor killing activity and its potential applications in cancer immunotherapy. Crit Rev Immunol 2013;33:1-21.

[57] Subbotin VM. Dendritic cell-based cancer immunotherapy: the stagnant approach and a theoretical solution. Drug Discov Today 2014;19:834-7.

[58] De Vries IJ, Krooshoop DJ, Scharenborg NM, Lesterhuis WJ, Diepstra JH, Van Muijen GN, Strijk SP, Ruers TJ, Boerman OC, Oyen WJ, Adema GJ, Punt CJ, Figdor CG. Effective migration of antigen-pulsed dendritic cells to lymph nodes in melanoma patients is determined by their maturation state. Cancer Res 2003;63:12-7.

[59] Offringa R. Antigen choice in adoptive T-cell therapy of cancer. Curr Opin Immunol 2009;21:190-9.

[60] King J, Waxman J, Stauss H. Advances in tumour immunotherapy. QJM 2008;101:675-83.

[61] Rivoltini L, Canese P, Huber V, Iero M, Pilla L, Valenti R, Fais S, Lozupone F, Casati C, Castelli C, Parmiani G. Escape strategies and reasons for failure in the interaction between tumour cells and the immune system: how can we tilt the balance towards immune-mediated cancer control? Expert Opin Biol Ther 2005;5:463-76.

[62] Homma S, Komita H, Sagawa Y, Ohno T, Toda G. Antitumour activity mediated by CD4+ cytotoxic T lymphocytes against MHC class II-negative mouse hepatocellular carcinoma induced by dendritic cell vaccine and interleukin-12. Immunology 2005;115:451-61.

[63] Martin SJ, Amarante-Mendes GP, Shi L, Chuang TH, Casiano CA, O'Brien GA, Fitzgerald P, Tan EM, Bokoch GM, Greenberg AH, Green DR. The cytotoxic cell protease granzyme B initiates apoptosis in a cell-free system by proteolytic processing and activation of the ICE/CED-3 family protease, CPP32, via a novel two-step mechanism. EMBO J 1996;15:2407-16.

[64] Lowin B, Peitsch MC, Tschopp J. Perforin and granzymes: crucial effector molecules in cytolytic T lymphocyte and natural killer cell-mediated cytotoxicity. Curr Top Microbiol Immunol 1995;198:1-24.

[65] Peters PJ, Borst J, Oorschot V, Fukuda M, Krahenbuhl O, Tschopp J, Slot JW, Geuze HJ. Cytotoxic T lymphocyte granules are secretory lysosomes, containing both perforin and granzymes. J Exp Med 1991;173:1099-109.

[66] Arroyo A, Modriansky M, Serinkan FB, Bello RI, Matsura T, Jiang J, Tyurin VA, Tyurina YY, Fadeel B, Kagan VE. NADPH oxidase-dependent oxidation and externalization of phosphatidylserine during apoptosis in Me2SO-differentiated HL-60 cells. Role in phagocytic clearance. J Biol Chem 2002;277:49965-75.

[67] Liu C, Noorchashm H, Sutter JA, Naji M, Prak EL, Boyer J, Green T, Rickels MR, Tomaszewski JE, Koeberlein B, Wang Z, Paessler ME, Velidedeoglu E, Rostami SY, Yu M, Barker CF, Naji A. B lymphocyte-directed immunotherapy promotes long-term islet allograft survival in nonhuman primates. Nat Med 2007;13:1295-8.

[68] Callard RE, Basten A, Waters LK. Immune function in aged mice. II. B-cell function. Cell Immunol 1977;31:26-36.

[69] James SL, Labine M, Sher A. Mechanisms of protective immunity against Schistosoma mansoni infection in mice vaccinated with irradiated cercariae. I. Analysis of antibody and T-lymphocyte responses in mouse strains developing differing levels of immunity. Cell Immunol 1981;65:75-83.

[70] Valdez RA, McGuire TC, Brown WC, Davis WC, Knowles DP. An in vivo model to investigate lymphocyte-mediated immunity during acute hemoparasitic infections. Use of a monoclonal antibody to selectively deplete CD4+ T lymphocytes from thymectomized calves. Ann N Y Acad Sci 2000;916:233-6.

[71] Ndungu FM, Olotu A, Mwacharo J, Nyonda M, Apfeld J, Mramba LK, Fegan GW, Bejon P, Marsh K. Memory B cells are a more reliable archive for historical antimalarial responses than plasma antibodies in no-longer exposed children. Proc Natl Acad Sci U S A 2012;109:8247-52.

[72] Rizzi M, Knoth R, Hampe CS, Lorenz P, Gougeon ML, Lemercier B, Venhoff N, Ferrera F, Salzer U, Thiesen HJ, Peter HH, Walker UA, Eibel H. Long-lived plasma cells

and memory B cells produce pathogenic anti-GAD65 autoantibodies in Stiff Person Syndrome. PLoS One 2010;5:e10838.

[73] Yoshida T, Mei H, Dorner T, Hiepe F, Radbruch A, Fillatreau S, Hoyer BF. Memory B and memory plasma cells. Immunol Rev 2010;237:117-39.

[74] Lindorfer MA, Wiestner A, Zent CS, Taylor RP. Monoclonal antibody (mAb)-based cancer therapy: Is it time to reevaluate dosing strategies? Oncoimmunology 2012;1:959-61.

[75] Scott AM, Wolchok JD, Old LJ. Antibody therapy of cancer. Nat Rev Cancer 2012;12:278-87.

[76] Meyer S, Leusen JH, Boross P. Regulation of complement and modulation of its activity in monoclonal antibody therapy of cancer. MAbs 2014;6.

[77] Taniguchi H, Imai K. [An overview of antibody therapy against cancer]. Nihon Rinsho 2012;70:2087-92.

[78] Vivek R, Thangam R, NipunBabu V, Rejeeth C, Sivasubramanian S, Gunasekaran P, Muthuchelian K, Kannan S. Multifunctional HER2-antibody conjugated polymeric nanocarrier-based drug delivery system for multi-drug-resistant breast cancer therapy. ACS Appl Mater Interfaces 2014;6:6469-80.

[79] Wang SY, Weiner G. Complement and cellular cytotoxicity in antibody therapy of cancer. Expert Opin Biol Ther 2008;8:759-68.

[80] Bonsignori M, Pollara J, Moody MA, Alpert MD, Chen X, Hwang KK, Gilbert PB, Huang Y, Gurley TC, Kozink DM, Marshall DJ, Whitesides JF, Tsao CY, Kaewkungwal J, Nitayaphan S, Pitisuttithum P, Rerks-Ngarm S, Kim JH, Michael NL, Tomaras GD, Montefiori DC, Lewis GK, DeVico A, Evans DT, Ferrari G, Liao HX, Haynes BF. Antibody-dependent cellular cytotoxicity-mediating antibodies from an HIV-1 vaccine efficacy trial target multiple epitopes and preferentially use the VH1 gene family. J Virol 2012;86:11521-32.

[81] Jegaskanda S, Weinfurter JT, Friedrich TC, Kent SJ. Antibody-dependent cellular cytotoxicity is associated with control of pandemic H1N1 influenza virus infection of macaques. J Virol 2013;87:5512-22.

[82] Le Garff-Tavernier M, Herbi L, de Romeuf C, Nguyen-Khac F, Davi F, Grelier A, Boudjoghra M, Maloum K, Choquet S, Urbain R, Vieillard V, Merle-Beral H. Antibody-dependent cellular cytotoxicity of the optimized anti-CD20 monoclonal antibody ublituximab on chronic lymphocytic leukemia cells with the 17p deletion. Leukemia 2014;28:230-3.

[83] Prang N, Preithner S, Brischwein K, Goster P, Woppel A, Muller J, Steiger C, Peters M, Baeuerle PA, da Silva AJ. Cellular and complement-dependent cytotoxicity of Ep-CAM-specific monoclonal antibody MT201 against breast cancer cell lines. Br J Cancer 2005;92:342-9.

[84] Song JX, Cao WL, Li FQ, Shi LN, Jia X. Anti-Sp17 monoclonal antibody with antibody-dependent cell-mediated cytotoxicity and complement-dependent cytotoxicity activities against human ovarian cancer cells. Med Oncol 2012;29:2923-31.

[85] Xiang SD, Wilson K, Day S, Fuchsberger M, Plebanski M. Methods of effective conjugation of antigens to nanoparticles as non-inflammatory vaccine carriers. Methods 2013;60:232-41.

[86] Correia-Pinto JF, Csaba N, Alonso MJ. Vaccine delivery carriers: insights and future perspectives. Int J Pharm 2013;440:27-38.

[87] Marrack P, McKee AS, Munks MW. Towards an understanding of the adjuvant action of aluminium. Nat Rev Immunol 2009;9:287-93.

[88] Sun HX, Xie Y, Ye YP. Advances in saponin-based adjuvants. Vaccine 2009;27:1787-96.

[89] Park YM, Lee SJ, Kim YS, Lee MH, Cha GS, Jung ID, Kang TH, Han HD. Nanoparticle-based vaccine delivery for cancer immunotherapy. Immune Netw 2013;13:177-83.

[90] Rappuoli R, Aderem A. A 2020 vision for vaccines against HIV, tuberculosis and malaria. Nature 2011;473:463-9.

[91] Wu KY, Wu M, Fu ML, Li H, Yang Y, Zhang H, Cheng C, Wang ZZ, Wang XY, Lu XB, Liu DG, Gao R. A novel chitosan CpG nanoparticle regulates cellular and humoral immunity of mice. Biomed Environ Sci 2006;19:87-95.

[92] Hamdy S, Haddadi A, Hung RW, Lavasanifar A. Targeting dendritic cells with nano-particulate PLGA cancer vaccine formulations. Adv Drug Deliv Rev 2011;63:943-55.

[93] Reischl D, Zimmer A. Drug delivery of siRNA therapeutics: potentials and limits of nanosystems. Nanomedicine 2009;5:8-20.

[94] Sheng KC, Kalkanidis M, Pouniotis DS, Esparon S, Tang CK, Apostolopoulos V, Pietersz GA. Delivery of antigen using a novel mannosylated dendrimer potentiates immunogenicity in vitro and in vivo. Eur J Immunol 2008;38:424-36.

[95] Gjetting T, Jolck RI, Andresen TL. Effective nanoparticle-based gene delivery by a protease triggered charge switch. Adv Healthc Mater 2014;3:1107-18.

[96] Dobrovolskaia MA, Patri AK, Simak J, Hall JB, Semberova J, De Paoli Lacerda SH, McNeil SE. Nanoparticle size and surface charge determine effects of PAMAM dendrimers on human platelets in vitro. Mol Pharm 2012;9:382-93.

[97] Trombetta ES, Mellman I. Cell biology of antigen processing in vitro and in vivo. Annu Rev Immunol 2005;23:975-1028.

[98] Davis ID, Chen W, Jackson H, Parente P, Shackleton M, Hopkins W, Chen Q, Dimopoulos N, Luke T, Murphy R, Scott AM, Maraskovsky E, McArthur G, MacGregor D, Sturrock S, Tai TY, Green S, Cuthbertson A, Maher D, Miloradovic L, Mitchell SV, Ritter G, Jungbluth AA, Chen YT, Gnjatic S, Hoffman EW, Old LJ, Cebon JS. Recombinant NY-ESO-1 protein with ISCOMATRIX adjuvant induces broad integrated antibody and CD4(+) and CD8(+) T cell responses in humans. Proc Natl Acad Sci U S A 2004;101:10697-702.

[99] Bachmann MF, Jennings GT. Vaccine delivery: a matter of size, geometry, kinetics and molecular patterns. Nat Rev Immunol 2010;10:787-96.

[100] Foged C, Brodin B, Frokjaer S, Sundblad A. Particle size and surface charge affect particle uptake by human dendritic cells in an in vitro model. Int J Pharm 2005;298:315-22.

[101] Xiang SD, Scholzen A, Minigo G, David C, Apostolopoulos V, Mottram PL, Plebanski M. Pathogen recognition and development of particulate vaccines: does size matter? Methods 2006;40:1-9.

[102] Reichert S, Welker P, Calderon M, Khandare J, Mangoldt D, Licha K, Kainthan RK, Brooks DE, Haag R. Size-dependant cellular uptake of dendritic polyglycerol. Small 2011;7:820-9.

[103] Tomic S, Ethokic J, Vasilijic S, Ogrinc N, Rudolf R, Pelicon P, Vucevic D, Milosavljevic P, Jankovic S, Anzel I, Rajkovic J, Rupnik MS, Friedrich B, Colic M. Size-dependent effects of gold nanoparticles uptake on maturation and antitumor functions of human dendritic cells in vitro. PLoS One 2014;9:e96584.

[104] Shima F, Uto T, Akagi T, Baba M, Akashi M. Size effect of amphiphilic poly(gamma-glutamic acid) nanoparticles on cellular uptake and maturation of dendritic cells in vivo. Acta Biomater 2013;9:8894-901.

[105] Kasturi SP, Skountzou I, Albrecht RA, Koutsonanos D, Hua T, Nakaya HI, Ravindran R, Stewart S, Alam M, Kwissa M, Villinger F, Murthy N, Steel J, Jacob J, Hogan RJ, Garcia-Sastre A, Compans R, Pulendran B. Programming the magnitude and persistence of antibody responses with innate immunity. Nature 2011;470:543-7.

[106] Yotsumoto S, Aramaki Y, Kakiuchi T, Tsuchiya S. Induction of antigen-dependent interleukin-12 production by negatively charged liposomes encapsulating antigens. Vaccine 2004;22:3503-9.

[107] van den Berg JH, Oosterhuis K, Hennink WE, Storm G, van der Aa LJ, Engbersen JF, Haanen JB, Beijnen JH, Schumacher TN, Nuijen B. Shielding the cationic charge of nanoparticle-formulated dermal DNA vaccines is essential for antigen expression and immunogenicity. J Control Release 2010;141:234-40.

[108] Hillaireau H, Couvreur P. Nanocarriers' entry into the cell: relevance to drug delivery. Cell Mol Life Sci 2009;66:2873-96.

[109] Reddy ST, van der Vlies AJ, Simeoni E, Angeli V, Randolph GJ, O'Neil CP, Lee LK, Swartz MA, Hubbell JA. Exploiting lymphatic transport and complement activation in nanoparticle vaccines. Nat Biotechnol 2007;25:1159-64.

[110] Cruz LJ, Rosalia RA, Kleinovink JW, Rueda F, Lowik CW, Ossendorp F. Targeting nanoparticles to CD40, DEC-205 or CD11c molecules on dendritic cells for efficient CD8 T cell response: A comparative study. J Control Release 2014;192C:209-18.

[111] Chenevier P, Grandjean C, Loing E, Malingue F, Angyalosi G, Gras-Masse H, Roux D, Melnyk O, Bourel-Bonnet L. Grafting of synthetic mannose receptor-ligands onto onion vectors for human dendritic cells targeting. Chem Commun (Camb) 2002:2446-7.

[112] Ramakrishna V, Treml JF, Vitale L, Connolly JE, O'Neill T, Smith PA, Jones CL, He LZ, Goldstein J, Wallace PK, Keler T, Endres MJ. Mannose receptor targeting of tumor antigen pmel17 to human dendritic cells directs anti-melanoma T cell responses via multiple HLA molecules. J Immunol 2004;172:2845-52.

[113] Cruz LJ, Tacken PJ, Fokkink R, Joosten B, Stuart MC, Albericio F, Torensma R, Figdor CG. Targeted PLGA nano- but not microparticles specifically deliver antigen to human dendritic cells via DC-SIGN in vitro. J Control Release 2010;144:118-26.

[114] Varga N, Sutkeviciute I, Guzzi C, McGeagh J, Petit-Haertlein I, Gugliotta S, Weiser J, Angulo J, Fieschi F, Bernardi A. Selective targeting of dendritic cell-specific intercellular adhesion molecule-3-grabbing nonintegrin (DC-SIGN) with mannose-based glycomimetics: synthesis and interaction studies of bis(benzylamide) derivatives of a pseudomannobioside. Chemistry 2013;19:4786-97.

[115] Flacher V, Tripp CH, Stoitzner P, Haid B, Ebner S, Del Frari B, Koch F, Park CG, Steinman RM, Idoyaga J, Romani N. Epidermal Langerhans cells rapidly capture and present antigens from C-type lectin-targeting antibodies deposited in the dermis. J Invest Dermatol 2010;130:755-62.

[116] Caminschi I, Proietto AI, Ahmet F, Kitsoulis S, Shin Teh J, Lo JC, Rizzitelli A, Wu L, Vremec D, van Dommelen SL, Campbell IK, Maraskovsky E, Braley H, Davey GM, Mottram P, van de Velde N, Jensen K, Lew AM, Wright MD, Heath WR, Shortman K, Lahoud MH. The dendritic cell subtype-restricted C-type lectin Clec9A is a target for vaccine enhancement. Blood 2008;112:3264-73.

[117] Dudziak D, Kamphorst AO, Heidkamp GF, Buchholz VR, Trumpfheller C, Yamazaki S, Cheong C, Liu K, Lee HW, Park CG, Steinman RM, Nussenzweig MC. Differential antigen processing by dendritic cell subsets in vivo. Science 2007;315:107-11.

[118] Foged C, Sundblad A, Hovgaard L. Targeting vaccines to dendritic cells. Pharm Res 2002;19:229-38.

[119] Kempf M, Mandal B, Jilek S, Thiele L, Voros J, Textor M, Merkle HP, Walter E. Improved stimulation of human dendritic cells by receptor engagement with surface-modified microparticles. J Drug Target 2003;11:11-8.

[120] Kipper MJ, Shen E, Determan A, Narasimhan B. Design of an injectable system based on bioerodible polyanhydride microspheres for sustained drug delivery. Biomaterials 2002;23:4405-12.

[121] Kersten G, Hirschberg H. Antigen delivery systems. Expert Rev Vaccines 2004;3:453-62.

[122] Katare YK, Panda AK, Lalwani K, Haque IU, Ali MM. Potentiation of immune response from polymer-entrapped antigen: toward development of single dose tetanus toxoid vaccine. Drug Deliv 2003;10:231-8.

[123] Foster S, Duvall CL, Crownover EF, Hoffman AS, Stayton PS. Intracellular delivery of a protein antigen with an endosomal-releasing polymer enhances CD8 T-cell production and prophylactic vaccine efficacy. Bioconjug Chem 2010;21:2205-12.

[124] Kazzaz J, Neidleman J, Singh M, Ott G, O'Hagan DT. Novel anionic microparticles are a potent adjuvant for the induction of cytotoxic T lymphocytes against recombinant p55 gag from HIV-1. J Control Release 2000;67:347-56.

[125] Jung T, Kamm W, Breitenbach A, Hungerer KD, Hundt E, Kissel T. Tetanus toxoid loaded nanoparticles from sulfobutylated poly(vinyl alcohol)-graft-poly(lactide-co-glycolide): evaluation of antibody response after oral and nasal application in mice. Pharm Res 2001;18:352-60.

[126] Sloat BR, Sandoval MA, Hau AM, He Y, Cui Z. Strong antibody responses induced by protein antigens conjugated onto the surface of lecithin-based nanoparticles. J Control Release 2010;141:93-100.

[127] Kendall M. Engineering of needle-free physical methods to target epidermal cells for DNA vaccination. Vaccine 2006;24:4651-6.

[128] Heikenwalder M, Polymenidou M, Junt T, Sigurdson C, Wagner H, Akira S, Zinkernagel R, Aguzzi A. Lymphoid follicle destruction and immunosuppression after repeated CpG oligodeoxynucleotide administration. Nat Med 2004;10:187-92.

[129] Diwan M, Elamanchili P, Cao M, Samuel J. Dose sparing of CpG oligodeoxynucleotide vaccine adjuvants by nanoparticle delivery. Curr Drug Deliv 2004;1:405-12.

[130] Sharma S, Mukkur TK, Benson HA, Chen Y. Pharmaceutical aspects of intranasal delivery of vaccines using particulate systems. J Pharm Sci 2009;98:812-43.

[131] Nandedkar TD. Nanovaccines: recent developments in vaccination. J Biosci 2009;34:995-1003.

[132] Weber C, Drogoz A, David L, Domard A, Charles MH, Verrier B, Delair T. Polysaccharide-based vaccine delivery systems: Macromolecular assembly, interactions with antigen presenting cells, and in vivo immunomonitoring. J Biomed Mater Res A 2010;93:1322-34.

[133] Primard C, Rochereau N, Luciani E, Genin C, Delair T, Paul S, Verrier B. Traffic of poly(lactic acid) nanoparticulate vaccine vehicle from intestinal mucus to sub-epithelial immune competent cells. Biomaterials 2010;31:6060-8.

[134] Camacho AI, Da Costa Martins R, Tamayo I, de Souza J, Lasarte JJ, Mansilla C, Esparza I, Irache JM, Gamazo C. Poly(methyl vinyl ether-co-maleic anhydride) nanoparticles as innate immune system activators. Vaccine 2011;29:7130-5.

[135] Binjawadagi B, Dwivedi V, Manickam C, Ouyang K, Wu Y, Lee LJ, Torrelles JB, Renukaradhya GJ. Adjuvanted poly(lactic-co-glycolic) acid nanoparticle-entrapped inactivated porcine reproductive and respiratory syndrome virus vaccine elicits cross-protective immune response in pigs. Int J Nanomedicine 2014;9:679-94.

[136] Garlapati S, Garg R, Brownlie R, Latimer L, Simko E, Hancock RE, Babiuk LA, Gerdts V, Potter A, van Drunen Littel-van den Hurk S. Enhanced immune responses and protection by vaccination with respiratory syncytial virus fusion protein formulated with CpG oligodeoxynucleotide and innate defense regulator peptide in polyphosphazene microparticles. Vaccine 2012;30:5206-14.

[137] Silva JM, Videira M, Gaspar R, Preat V, Florindo HF. Immune system targeting by biodegradable nanoparticles for cancer vaccines. J Control Release 2013;168:179-99.

[138] Jiang W, Gupta RK, Deshpande MC, Schwendeman SP. Biodegradable poly(lactic-co-glycolic acid) microparticles for injectable delivery of vaccine antigens. Adv Drug Deliv Rev 2005;57:391-410.

[139] Jia F, Liu X, Li L, Mallapragada S, Narasimhan B, Wang Q. Multifunctional nanoparticles for targeted delivery of immune activating and cancer therapeutic agents. J Control Release 2013;172:1020-34.

[140] Cohen S, Alonso MJ, Langer R. Novel approaches to controlled-release antigen delivery. Int J Technol Assess Health Care 1994;10:121-30.

[141] Gomez S, Gamazo C, San Roman B, Vauthier C, Ferrer M, Irachel JM. Development of a novel vaccine delivery system based on Gantrez nanoparticles. J Nanosci Nanotechnol 2006;6:3283-9.

[142] Amidi M, Romeijn SG, Verhoef JC, Junginger HE, Bungener L, Huckriede A, Crommelin DJ, Jiskoot W. N-trimethyl chitosan (TMC) nanoparticles loaded with influenza subunit antigen for intranasal vaccination: biological properties and immunogenicity in a mouse model. Vaccine 2007;25:144-53.

[143] Sangha R, Butts C. L-BLP25: a peptide vaccine strategy in non small cell lung cancer. Clin Cancer Res 2007;13:s4652-4.

[144] Verma A, Stellacci F. Effect of surface properties on nanoparticle-cell interactions. Small 2010;6:12-21.

[145] Duan X, Li Y. Physicochemical characteristics of nanoparticles affect circulation, biodistribution, cellular internalization, and trafficking. Small 2013;9:1521-32.

[146] Champion JA, Walker A, Mitragotri S. Role of particle size in phagocytosis of polymeric microspheres. Pharm Res 2008;25:1815-21.

[147] Shang L, Nienhaus K, Nienhaus GU. Engineered nanoparticles interacting with cells: size matters. J Nanobiotechnology 2014;12:5.

[148] Canton I, Battaglia G. Endocytosis at the nanoscale. Chem Soc Rev 2012;41:2718-39.

[149] Rejman J, Oberle V, Zuhorn IS, Hoekstra D. Size-dependent internalization of particles via the pathways of clathrin- and caveolae-mediated endocytosis. Biochem J 2004;377:159-69.

[150] Huang J, Bu L, Xie J, Chen K, Cheng Z, Li X, Chen X. Effects of nanoparticle size on cellular uptake and liver MRI with polyvinylpyrrolidone-coated iron oxide nanoparticles. ACS Nano 2010;4:7151-60.

[151] Lu F, Wu SH, Hung Y, Mou CY. Size effect on cell uptake in well-suspended, uniform mesoporous silica nanoparticles. Small 2009;5:1408-13.

[152] Wang SH, Lee CW, Chiou A, Wei PK. Size-dependent endocytosis of gold nanoparticles studied by three-dimensional mapping of plasmonic scattering images. J Nanobiotechnology 2010;8:33.

[153] Jiang W, Kim BY, Rutka JT, Chan WC. Nanoparticle-mediated cellular response is size-dependent. Nat Nanotechnol 2008;3:145-50.

[154] Andersson PO, Lejon C, Ekstrand-Hammarstrom B, Akfur C, Ahlinder L, Bucht A, Osterlund L. Polymorph- and size-dependent uptake and toxicity of TiO(2) nanoparticles in living lung epithelial cells. Small 2011;7:514-23.

[155] Schübbe. S, Schumann. C, Cavelius. C, Koch. M, Müller. T, Kraegeloh. A. Size dependent localization and quantitative evaluation of the intracellular migration of silica nanoparticles in caco-2 cells. Chem Mater 2012;24:914-23.

[156] Xu A, Yao M, Xu G, Ying J, Ma W, Li B, Jin Y. A physical model for the size-dependent cellular uptake of nanoparticles modified with cationic surfactants. Int J Nanomedicine 2012;7:3547-54.

[157] He C, Hu Y, Yin L, Tang C, Yin C. Effects of particle size and surface charge on cellular uptake and biodistribution of polymeric nanoparticles. Biomaterials 2010;31:3657-66.

[158] Slowing, II, Wu CW, Vivero-Escoto JL, Lin VS. Mesoporous silica nanoparticles for reducing hemolytic activity towards mammalian red blood cells. Small 2009;5:57-62.

[159] Zhao Y, Sun X, Zhang G, Trewyn BG, Slowing, II, Lin VS. Interaction of mesoporous silica nanoparticles with human red blood cell membranes: size and surface effects. ACS Nano 2011;5:1366-75.

[160] Lorenz MR, Holzapfel V, Musyanovych A, Nothelfer K, Walther P, Frank H, Landfester K, Schrezenmeier H, Mailander V. Uptake of functionalized, fluorescent-labeled polymeric particles in different cell lines and stem cells. Biomaterials 2006;27:2820-8.

[161] Calatayud MP, Sanz B, Raffa V, Riggio C, Ibarra MR, Goya GF. The effect of surface charge of functionalized Fe3O4 nanoparticles on protein adsorption and cell uptake. Biomaterials 2014;35:6389-99.

[162] Wang M, Miller AD, Thanou M. Effect of surface charge and ligand organization on the specific cell-uptake of uPAR-targeted nanoparticles. J Drug Target 2013;21:684-92.

[163] Nan A, Bai X, Son SJ, Lee SB, Ghandehari H. Cellular uptake and cytotoxicity of silica nanotubes. Nano Lett 2008;8:2150-4.

[164] Kelf TA, Sreenivasan VK, Sun J, Kim EJ, Goldys EM, Zvyagin AV. Non-specific cellular uptake of surface-functionalized quantum dots. Nanotechnology 2010;21:285105.

[165] Kenzaoui BH, Vila MR, Miquel JM, Cengelli F, Juillerat-Jeanneret L. Evaluation of uptake and transport of cationic and anionic ultrasmall iron oxide nanoparticles by human colon cells. Int J Nanomedicine 2012;7:1275-86.

[166] Chen L, McCrate JM, Lee JC, Li H. The role of surface charge on the uptake and biocompatibility of hydroxyapatite nanoparticles with osteoblast cells. Nanotechnology 2011;22:105708.

[167] Yue ZG, Wei W, Lv PP, Yue H, Wang LY, Su ZG, Ma GH. Surface charge affects cellular uptake and intracellular trafficking of chitosan-based nanoparticles. Biomacromolecules 2011;12:2440-6.

[168] Patil S, Sandberg A, Heckert E, Self W, Seal S. Protein adsorption and cellular uptake of cerium oxide nanoparticles as a function of zeta potential. Biomaterials 2007;28:4600-7.

[169] Wilhelm C, Billotey C, Roger J, Pons JN, Bacri JC, Gazeau F. Intracellular uptake of anionic superparamagnetic nanoparticles as a function of their surface coating. Biomaterials 2003;24:1001-11.

[170] Musyanovych A, Dausend J, Dass M, Walther P, Mailander V, Landfester K. Criteria impacting the cellular uptake of nanoparticles: a study emphasizing polymer type and surfactant effects. Acta Biomater 2011;7:4160-8.

[171] Ehrenberg MS, Friedman AE, Finkelstein JN, Oberdorster G, McGrath JL. The influence of protein adsorption on nanoparticle association with cultured endothelial cells. Biomaterials 2009;30:603-10.

[172] Liang Z, Liu Y, Li X, Wu Q, Yu J, Luo S, Lai L, Liu S. Surface-modified gold nanoshells for enhanced cellular uptake. J Biomed Mater Res A 2011;98:479-87.

[173] Win KY, Feng SS. Effects of particle size and surface coating on cellular uptake of polymeric nanoparticles for oral delivery of anticancer drugs. Biomaterials 2005;26:2713-22.

[174] Hao Y, Yang X, Song S, Huang M, He C, Cui M, Chen J. Exploring the cell uptake mechanism of phospholipid and polyethylene glycol coated gold nanoparticles. Nanotechnology 2012;23:045103.

[175] Almeida PV, Shahbazi MA, Mäkilä E, Kaasalainen M, Salonen J, Hirvonen J, Santos HA. Amine-modified hyaluronic acid-functionalized porous silicon nanoparticles for targeting breast cancer tumors. Nanoscale 2014;6:10377-87.

[176] Heikkila T, Santos HA, Kumar N, Murzin DY, Salonen J, Laaksonen T, Peltonen L, Hirvonen J, Lehto VP. Cytotoxicity study of ordered mesoporous silica MCM-41 and SBA-15 microparticles on Caco-2 cells. Eur J Pharm Biopharm 2010;74:483-94.

[177] Powers KW, Brown SC, Krishna VB, Wasdo SC, Moudgil BM, Roberts SM. Research strategies for safety evaluation of nanomaterials. Part VI. Characterization of nanoscale particles for toxicological evaluation. Toxicol Sci 2006;90:296-303.

[178] Frohlich E. The role of surface charge in cellular uptake and cytotoxicity of medical nanoparticles. Int J Nanomedicine 2012;7:5577-91.

[179] Yin H, Too HP, Chow GM. The effects of particle size and surface coating on the cytotoxicity of nickel ferrite. Biomaterials 2005;26:5818-26.

[180] Garnett MC, Kallinteri P. Nanomedicines and nanotoxicology: some physiological principles. Occup Med (Lond) 2006;56:307-11.

[181] Adam N, Schmitt C, Galceran J, Companys E, Vakurov A, Wallace R, Knapen D, Blust R. The chronic toxicity of ZnO nanoparticles and ZnCl2 to Daphnia magna and the use of different methods to assess nanoparticle aggregation and dissolution. Nanotoxicology 2014;8:709-17.

[182] Lanone S, Boczkowski J. Biomedical applications and potential health risks of nanomaterials: molecular mechanisms. Curr Mol Med 2006;6:651-63.

[183] Rahman I. Regulation of nuclear factor-kappa B, activator protein-1, and glutathione levels by tumor necrosis factor-alpha and dexamethasone in alveolar epithelial cells. Biochem Pharmacol 2000;60:1041-9.

[184] Unfried K, Albrecht C, Klotz LO, Von Mikecz A, Grether-Beck S, Schins RPF. Cellular response to nanoparticles: target structures and mechanisms. Nanotoxicology 2007;1 52-71.

[185] Kinnari P, Mäkilä E, Heikkila T, Salonen J, Hirvonen J, Santos HA. Comparison of mesoporous silicon and non-ordered mesoporous silica materials as drug carriers for itraconazole. Int J Pharm 2011;414:148-56.

[186] Bimbo LM, Mäkilä E, Laaksonen T, Lehto VP, Salonen J, Hirvonen J, Santos HA. Drug permeation across intestinal epithelial cells using porous silicon nanoparticles. Biomaterials 2011;32:2625-33.

[187] Salonen J, Kaukonen AM, Hirvonen J, Lehto VP. Mesoporous silicon in drug delivery applications. J Pharm Sci 2008;97:632-53.

[188] Mäkilä E, Ferreira MP, Kivela H, Niemi SM, Correia A, Shahbazi MA, Kauppila J, Hirvonen J, Santos HA, Salonen J. Confinement effects on drugs in thermally hydrocarbonized porous silicon. Langmuir 2014;30:2196-205.

[189] Santos HA, Bimbo LM, Herranz B, Shahbazi MA, Hirvonen J, Salonen J. Nanostructured Porous Silicon in Preclinical Imaging: Moving From Bench to Bed Side. J Mater Res 2013;28:152-64.

[190] Godin B, Tasciotti E, Liu X, Serda RE, Ferrari M. Multistage nanovectors: from concept to novel imaging contrast agents and therapeutics. Acc Chem Res 2011;44:979-89.

[191] Yokoi K, Godin B, Oborn CJ, Alexander JF, Liu X, Fidler IJ, Ferrari M. Porous silicon nanocarriers for dual targeting tumor associated endothelial cells and macrophages in stroma of orthotopic human pancreatic cancers. Cancer Lett 2013;334:319-27.

[192] Wan Y, Apostolou S, Dronov R, Kuss B, Voelcker NH. Cancer-targeting siRNA delivery from porous silicon nanoparticles. Nanomedicine (Lond) 2014.

[193] Mäkilä E, Bimbo LM, Kaasalainen M, Herranz B, Airaksinen AJ, Heinonen M, Kukk E, Hirvonen J, Santos HA, Salonen J. Amine modification of thermally carbonized porous silicon with silane coupling chemistry. Langmuir 2012;28:14045-54.

[194] Bimbo LM, Sarparanta M, Santos HA, Airaksinen AJ, Mäkilä E, Laaksonen T, Peltonen L, Lehto VP, Hirvonen J, Salonen J. Biocompatibility of thermally hydrocarbonized porous silicon nanoparticles and their biodistribution in rats. ACS Nano 2010;4:3023-32.

[195] Sarparanta M, Bimbo LM, Rytkonen J, Mäkilä E, Laaksonen TJ, Laaksonen P, Nyman M, Salonen J, Linder MB, Hirvonen J, Santos HA, Airaksinen AJ. Intravenous

delivery of hydrophobin-functionalized porous silicon nanoparticles: stability, plasma protein adsorption and biodistribution. Mol Pharm 2012;9:654-63.

[196] Santos HA, Mäkilä E, Airaksinen AJ, Bimbo LM, Hirvonen J. Porous silicon nanoparticles for nanomedicine: preparation and biomedical applications. Nanomedicine (Lond) 2014;9:535-54.

[197] Sarparanta M, Mäkilä E, Heikkila T, Salonen J, Kukk E, Lehto VP, Santos HA, Hirvonen J, Airaksinen AJ. (1)(8)F-labeled modified porous silicon particles for investigation of drug delivery carrier distribution in vivo with positron emission tomography. Mol Pharm 2011;8:1799-806.

[198] Martinez JO, Boada C, Yazdi IK, Evangelopoulos M, Brown BS, Liu X, Ferrari M, Tasciotti E. Short and long term, in vitro and in vivo correlations of cellular and tissue responses to mesoporous silicon nanovectors. Small 2013;9:1722-33.

[199] Yazdi IK, Murphy MB, Loo C, Liu X, Ferrari M, Weiner BK, Tasciotti E. Cefazolin-loaded mesoporous silicon microparticles show sustained bactericidal effect against Staphylococcus aureus. J Tissue Eng 2014;5:2041731414536573.

[200] Anglin EJ, Cheng L, Freeman WR, Sailor MJ. Porous silicon in drug delivery devices and materials. Adv Drug Deliv Rev 2008;60:1266-77.

[201] Haidary SM, Emma PC, Nihad KA. Nanoporous Silicon as Drug Delivery Systems for Cancer Therapies. Journal of Nanomaterials 2012;2012.

[202] Hart BR, Letant SE, Kane SR, Hadi MZ, Shields SJ, Reynolds JG. New method for attachment of biomolecules to porous silicon. Chem Commun (Camb) 2003:322-3.

[203] Kleps I, Ignat T, Miu M, Craciunoiu F, Trif M, Simion M, Bragaru A, Dinescu A. Nanostructured silicon particles for medical applications. J Nanosci Nanotechnol 2010;10:2694-700.

[204] Salonen J, Laitinen L, Kaukonen AM, Tuura J, Bjorkqvist M, Heikkila T, Vaha-Heikkila K, Hirvonen J, Lehto VP. Mesoporous silicon microparticles for oral drug delivery: loading and release of five model drugs. J Control Release 2005;108:362-74.

[205] Tay L, Rowell NL, Poitras D, Fraser JW, Lockwood DJ, Boukherroub R. Bovine serum albumin adsorption on passivated porous silicon layers. Canadian Journal of Chemistry 2004;82:1545-53.

[206] Anglin EJ, Schwartz MP, Ng VP, Perelman LA, Sailor MJ. Engineering the chemistry and nanostructure of porous silicon Fabry-Perot films for loading and release of a steroid. Langmuir 2004;20:11264-9.

[207] Parkhutik V, Chirvony V, Matveyeva E. Optical properties of porphyrin molecules immobilized in nano-porous silicon. Biomol Eng 2007;24:71-3.

[208] Wang CF, Mäkilä EM, Kaasalainen MH, Liu D, Sarparanta MP, Airaksinen AJ, Salonen JJ, Hirvonen JT, Santos HA. Copper-free azide-alkyne cycloaddition of targeting peptides to porous silicon nanoparticles for intracellular drug uptake. Biomaterials 2014;35:1257-66.

[209] Gu L, Park JH, Duong KH, Ruoslahti E, Sailor MJ. Magnetic luminescent porous silicon microparticles for localized delivery of molecular drug payloads. Small 2010;6:2546-52.

[210] Barnes TJ, Jarvis KL, Prestidge CA. Recent advances in porous silicon technology for drug delivery. Ther Deliv 2013;4:811-23.

[211] Ozeki T, Tagami T. Functionally engineered nanosized particles in pharmaceutics: improved oral delivery of poorly water-soluble drugs. Curr Pharm Des 2013;19:6259-69.

[212] Jin S, Ye K. Nanoparticle-mediated drug delivery and gene therapy. Biotechnol Prog 2007;23:32-41.

[213] Bimbo LM, Denisova OV, Mäkilä E, Kaasalainen M, De Brabander JK, Hirvonen J, Salonen J, Kakkola L, Kainov D, Santos HA. Inhibition of influenza A virus infection in vitro by saliphenylhalamide-loaded porous silicon nanoparticles. ACS Nano 2013;7:6884-93.

[214] Wang F, Hui H, Barnes TJ, Barnett C, Prestidge CA. Oxidized mesoporous silicon microparticles for improved oral delivery of poorly soluble drugs. Mol Pharm 2010;7:227-36.

[215] Park JS, Kinsella JM, Jandial DD, Howell SB, Sailor MJ. Cisplatin-loaded porous Si microparticles capped by electroless deposition of platinum. Small 2011;7:2061-9.

[216] Wu EC, Andrew JS, Cheng L, Freeman WR, Pearson L, Sailor MJ. Real-time monitoring of sustained drug release using the optical properties of porous silicon photonic crystal particles. Biomaterials 2011;32:1957-66.

[217] Wu EC, Park JH, Park J, Segal E, Cunin F, Sailor MJ. Oxidation-triggered release of fluorescent molecules or drugs from mesoporous Si microparticles. ACS Nano 2008;2:2401-9.

[218] Chhablani J, Nieto A, Hou H, Wu EC, Freeman WR, Sailor MJ, Cheng L. Oxidized porous silicon particles covalently grafted with daunorubicin as a sustained intraocular drug delivery system. Invest Ophthalmol Vis Sci 2013;54:1268-79.

[219] Hou H, Nieto A, Ma F, Freeman WR, Sailor MJ, Cheng L. Tunable sustained intravitreal drug delivery system for daunorubicin using oxidized porous silicon. J Control Release 2014;178:46-54.

[220] Cheng L, Anglin E, Cunin F, Kim D, Sailor MJ, Falkenstein I, Tammewar A, Freeman WR. Intravitreal properties of porous silicon photonic crystals: a potential self-reporting intraocular drug-delivery vehicle. Br J Ophthalmol 2008;92:705-11.

[221] De Rosa E, Chiappini C, Fan D, Liu X, Ferrari M, Tasciotti E. Agarose surface coating influences intracellular accumulation and enhances payload stability of a nano-delivery system. Pharm Res 2011;28:1520-30.

[222] Shrestha N, Shahbazi MA, Araujo F, Zhang H, Mäkilä EM, Kauppila J, Sarmento B, Salonen JJ, Hirvonen JT, Santos HA. Chitosan-modified porous silicon microparticles for enhanced permeability of insulin across intestinal cell monolayers. Biomaterials 2014;35:7172-9.

[223] Araujo F, Shrestha N, Shahbazi MA, Fonte P, Mäkilä EM, Salonen JJ, Hirvonen JT, Granja PL, Santos HA, Sarmento B. The impact of nanoparticles on the mucosal translocation and transport of GLP-1 across the intestinal epithelium. Biomaterials 2014;35:9199-207.

[224] Kilpelainen M, Monkare J, Vlasova MA, Riikonen J, Lehto VP, Salonen J, Jarvinen K, Herzig KH. Nanostructured porous silicon microparticles enable sustained peptide (Melanotan II) delivery. Eur J Pharm Biopharm 2011;77:20-5.

[225] Kilpelainen M, Riikonen J, Vlasova MA, Huotari A, Lehto VP, Salonen J, Herzig KH, Jarvinen K. In vivo delivery of a peptide, ghrelin antagonist, with mesoporous silicon microparticles. J Control Release 2009;137:166-70.

[226] Kovalainen M, Monkare J, Kaasalainen M, Riikonen J, Lehto VP, Salonen J, Herzig KH, Jarvinen K. Development of porous silicon nanocarriers for parenteral peptide delivery. Mol Pharm 2013;10:353-9.

[227] Kovalainen M, Monkare J, Mäkilä E, Salonen J, Lehto VP, Herzig KH, Jarvinen K. Mesoporous silicon (PSi) for sustained peptide delivery: effect of psi microparticle surface chemistry on peptide YY3-36 release. Pharm Res 2012;29:837-46.

[228] De Stefano L, De Tommasi E, Rea I, Rotiroti L, Giangrande L, Oliviero G, Borbone N, Galeone A, Piccialli G. Oligonucleotides direct synthesis on porous silicon chip. Nucleic Acids Symp Ser (Oxf) 2008:721-2.

[229] McInnes SJ, Voelcker NH. Porous silicon-based nanostructured microparticles as degradable supports for solid-phase synthesis and release of oligonucleotides. Nanoscale Res Lett 2012;7:385.

[230] Rytkonen J, Arukuusk P, Xu W, Kurrikoff K, Langel U, Lehto VP, Narvanen A. Porous silicon-cell penetrating peptide hybrid nanocarrier for intracellular delivery of oligonucleotides. Mol Pharm 2014;11:382-90.

[231] Zhang M, Xu R, Xia X, Yang Y, Gu J, Qin G, Liu X, Ferrari M, Shen H. Polycation-functionalized nanoporous silicon particles for gene silencing on breast cancer cells. Biomaterials 2014;35:423-31.

[232] Bonanno LM, Segal E. Nanostructured porous silicon-polymer-based hybrids: from biosensing to drug delivery. Nanomedicine (Lond) 2011;6:1755-70.

[233] Hernandez-Montelongo J, Naveas N, Degoutin S, Tabary N, Chai F, Spampinato V, Ceccone G, Rossi F, Torres-Costa V, Manso-Silvan M, Martel B. Porous silicon-cyclodextrin based polymer composites for drug delivery applications. Carbohydr Polym 2014;110:238-52.

[234] Liu D, Zhang H, Herranz-Blanco B, Mäkilä E, Lehto VP, Salonen J, Hirvonen J, Santos HA. Microfluidic assembly of monodisperse multistage pH-responsive polymer/porous silicon composites for precisely controlled multi-drug delivery. Small 2014;10:2029-38.

[235] Zhang H, Liu D, Shahbazi MA, Mäkilä E, Herranz-Blanco B, Salonen J, Hirvonen J, Santos HA. Fabrication of a multifunctional nano-in-micro drug delivery platform by microfluidic templated encapsulation of porous silicon in polymer matrix. Adv Mater 2014;26:4497-503.

[236] Wu Z, Jiang Y, Kim T, Lee K. Effects of surface coating on the controlled release of vitamin B1 from mesoporous silica tablets. J Control Release 2007;119:215-21.

[237] Pastor E, Matveeva E, Valle-Gallego A, Goycoolea FM, Garcia-Fuentes M. Protein delivery based on uncoated and chitosan-coated mesoporous silicon microparticles. Colloids Surf B Biointerfaces 2011;88:601-9.

[238] Perelman LA, Pacholski C, Li YY, VanNieuwenhze MS, Sailor MJ. pH-triggered release of vancomycin from protein-capped porous silicon films. Nanomedicine (Lond) 2008;3:31-43.

[239] Vasani RB, McInnes SJ, Cole MA, Jani AM, Ellis AV, Voelcker NH. Stimulus-responsiveness and drug release from porous silicon films ATRP-grafted with poly(N-isopropylacrylamide). Langmuir 2011;27:7843-53.

[240] Liu DF, Mäkilä E, Zhang HB, Herranz B, Kaasalainen M, Kinnari P, Salonen J, Hirvonen J, Santos HA. Nanostructured Porous Silicon-Solid Lipid Nanocomposite: Towards Enhanced Cytocompatibility and Stability, Reduced Cellular Association, and Prolonged Drug Release. Advanced Functional Materials 2013;23:1893-902.

[241] Blanco E, Sangai T, Hsiao A, Ferrati S, Bai L, Liu X, Meric-Bernstam F, Ferrari M. Multistage delivery of chemotherapeutic nanoparticles for breast cancer treatment. Cancer Lett 2013;334:245-52.

[242] Kinsella JM, Ananda S, Andrew JS, Grondek JF, Chien MP, Scadeng M, Gianneschi NC, Ruoslahti E, Sailor MJ. Enhanced magnetic resonance contrast of Fe(3)O(4) nanoparticles trapped in a porous silicon nanoparticle host. Adv Mater 2011;23:H248-53.

[243] Munoz Noval A, Garcia R, Ruiz Casas D, Losada Bayo D, Sanchez Vaquero V, Torres Costa V, Martin Palma RJ, Garcia MA, Garcia Ruiz JP, Serrano Olmedo JJ, Munoz Negrete JF, del Pozo Guerrero F, Manso Silvan M. Design and characterization of biofunctional magnetic porous silicon flakes. Acta Biomater 2013;9:6169-76.

[244] Meraz IM, Melendez B, Gu J, Wong ST, Liu X, Andersson HA, Serda RE. Activation of the inflammasome and enhanced migration of microparticle-stimulated dendritic cells to the draining lymph node. Mol Pharm 2012;9:2049-62.

[245] Meraz IM, Hearnden CH, Liu X, Yang M, Williams L, Savage DJ, Gu J, Rhudy JR, Yokoi K, Lavelle EC, Serda RE. Multivalent presentation of MPL by porous silicon microparticles favors T helper 1 polarization enhancing the anti-tumor efficacy of doxorubicin nanoliposomes. PLoS One 2014;9:e94703.

[246] Chou LY, Ming K, Chan WC. Strategies for the intracellular delivery of nanoparticles. Chem Soc Rev 2011;40:233-45.

[247] Huang X, Teng X, Chen D, Tang F, He J. The effect of the shape of mesoporous silica nanoparticles on cellular uptake and cell function. Biomaterials 2010;31:438-48.

[248] Kafshgari MH, Harding FJ, Voelcker NH. Insights into Cellular Uptake of Nanoparticles. Curr Drug Deliv 2014.

[249] Kulkarni SA, Feng SS. Effects of particle size and surface modification on cellular uptake and biodistribution of polymeric nanoparticles for drug delivery. Pharm Res 2013;30:2512-22.

[250] Rosenholm JM, Meinander A, Peuhu E, Niemi R, Eriksson JE, Sahlgren C, Linden M. Targeting of porous hybrid silica nanoparticles to cancer cells. ACS Nano 2009;3:197-206.

[251] Chung TH, Wu SH, Yao M, Lu CW, Lin YS, Hung Y, Mou CY, Chen YC, Huang DM. The effect of surface charge on the uptake and biological function of mesoporous silica nanoparticles in 3T3-L1 cells and human mesenchymal stem cells. Biomaterials 2007;28:2959-66.

[252] Porta F, Lamers GE, Morrhayim J, Chatzopoulou A, Schaaf M, den Dulk H, Backendorf C, Zink JI, Kros A. Folic acid-modified mesoporous silica nanoparticles for cellular and nuclear targeted drug delivery. Adv Healthc Mater 2013;2:281-6.

[253] Wang Z, Xu B, Zhang L, Zhang J, Ma T, Zhang J, Fu X, Tian W. Folic acid-functionalized mesoporous silica nanospheres hybridized with AIE luminogens for targeted cancer cell imaging. Nanoscale 2013;5:2065-72.

[254] Maxfield FR, McGraw TE. Endocytic recycling. Nat Rev Mol Cell Biol 2004;5:121-32.

[255] Maeda Y, Pittella F, Nomoto T, Takemoto H, Nishiyama N, Miyata K, Kataoka K. Fine-tuning of charge-conversion polymer structure for efficient endosomal escape of siRNA-loaded calcium phosphate hybrid micelles. Macromol Rapid Commun 2014;35:1211-5.

[256] Pittella F, Zhang M, Lee Y, Kim HJ, Tockary T, Osada K, Ishii T, Miyata K, Nishiyama N, Kataoka K. Enhanced endosomal escape of siRNA-incorporating hybrid nanoparticles from calcium phosphate and PEG-block charge-conversional polymer for efficient gene knockdown with negligible cytotoxicity. Biomaterials 2011;32:3106-14.

[257] Chu D, Xu W, Pan R, Ding Y, Sui W, Chen P. Rational modification of oligoarginine for highly efficient siRNA delivery: structure-activity relationship and mechanism of intracellular trafficking of siRNA. Nanomedicine 2014.

[258] Suma T, Miyata K, Ishii T, Uchida S, Uchida H, Itaka K, Nishiyama N, Kataoka K. Enhanced stability and gene silencing ability of siRNA-loaded polyion complexes formulated from polyaspartamide derivatives with a repetitive array of amino groups in the side chain. Biomaterials 2012;33:2770-9.

[259] Huang S, Fan Y, Cheng Z, Kong D, Yang P, Quan Z, Zhang C, Lin J. Magnetic Mesoporous Silica Spheres for Drug Targeting and Controlled Release. J Phys Chem C 2009;113 1775-84.

[260] Rosenholm JM, Sahlgren C, Linden M. Towards multifunctional, targeted drug delivery systems using mesoporous silica nanoparticles--opportunities & challenges. Nanoscale 2010;2:1870-83.

[261] Kinnari PJ, Hyvonen ML, Mäkilä EM, Kaasalainen MH, Rivinoja A, Salonen JJ, Hirvonen JT, Laakkonen PM, Santos HA. Tumour homing peptide-functionalized porous silicon nanovectors for cancer therapy. Biomaterials 2013;34:9134-41.

[262] Padari K, Koppel K, Lorents A, Hallbrink M, Mano M, Pedroso de Lima MC, Pooga M. S4(13)-PV cell-penetrating peptide forms nanoparticle-like structures to gain entry into cells. Bioconjug Chem 2010;21:774-83.

[263] Mitsueda A, Shimatani Y, Ito M, Ohgita T, Yamada A, Hama S, Graslund A, Lindberg S, Langel U, Harashima H, Nakase I, Futaki S, Kogure K. Development of a novel nanoparticle by dual modification with the pluripotential cell-penetrating peptide

PepFect6 for cellular uptake, endosomal escape, and decondensation of an siRNA core complex. Biopolymers 2013;100:698-704.

[264] Parodi A, Quattrocchi N, van de Ven AL, Chiappini C, Evangelopoulos M, Martinez JO, Brown BS, Khaled SZ, Yazdi IK, Enzo MV, Isenhart L, Ferrari M, Tasciotti E. Synthetic nanoparticles functionalized with biomimetic leukocyte membranes possess cell-like functions. Nat Nanotechnol 2013;8:61-8.

[265] Yu T, Malugin A, Ghandehari H. Impact of silica nanoparticle design on cellular toxicity and hemolytic activity. ACS Nano 2011;5:5717-28.

[266] Sanchez-Quintero MJ, Torres MJ, Blazquez AB, Gomez E, Fernandez TD, Dona I, Ariza A, Andreu I, Melendez L, Blanca M, Mayorga C. Synergistic effect between amoxicillin and TLR ligands on dendritic cells from amoxicillin-delayed allergic patients. PLoS One 2013;8:e74198.

[267] AshaRani PV, Low Kah Mun G, Hande MP, Valiyaveettil S. Cytotoxicity and genotoxicity of silver nanoparticles in human cells. ACS Nano 2009;3:279-90.

[268] Xia T, Kovochich M, Brant J, Hotze M, Sempf J, Oberley T, Sioutas C, Yeh JI, Wiesner MR, Nel AE. Comparison of the abilities of ambient and manufactured nanoparticles to induce cellular toxicity according to an oxidative stress paradigm. Nano Lett 2006;6:1794-807.

[269] Lai DY. Toward toxicity testing of nanomaterials in the 21st century: a paradigm for moving forward. Wiley Interdiscip Rev Nanomed Nanobiotechnol 2012;4:1-15.

[270] Schins RP. Mechanisms of genotoxicity of particles and fibers. Inhal Toxicol 2002;14:57-78.

[271] Singh N, Manshian B, Jenkins GJ, Griffiths SM, Williams PM, Maffeis TG, Wright CJ, Doak SH. NanoGenotoxicology: the DNA damaging potential of engineered nanomaterials. Biomaterials 2009;30:3891-914.

[272] Ruizendaal L, Sourav Bhattacharjee S, Pournazari K, Rosso-Vasic M, de Haan LhJ, Alink GM, Marcelis ATM, Zuilhof H. Synthesis and cytotoxicity of silicon nanoparticles with covalently attached organic monolayers. Nanotoxicology 2009;3:339-47.

[273] Kim ST, Saha K, Kim C, Rotello VM. The role of surface functionality in determining nanoparticle cytotoxicity. Acc Chem Res 2013;46:681-91.

[274] Besic Gyenge E, Darphin X, Wirth A, Pieles U, Walt H, Bredell M, Maake C. Uptake and fate of surface modified silica nanoparticles in head and neck squamous cell carcinoma. J Nanobiotechnology 2011;9:32.

[275] Asefa T, Tao Z. Biocompatibility of mesoporous silica nanoparticles. Chem Res Toxicol 2012;25:2265-84.

[276] Tao Z, Toms BB, Goodisman J, Asefa T. Mesoporosity and functional group dependent endocytosis and cytotoxicity of silica nanomaterials. Chem Res Toxicol 2009;22:1869-80.

[277] Shahbazi MA, Hamidi M, Mäkilä EM, Zhang H, Almeida PV, Kaasalainen M, Salonen JJ, Hirvonen JT, Santos HA. The mechanisms of surface chemistry effects of mesoporous silicon nanoparticles on immunotoxicity and biocompatibility. Biomaterials 2013;34:7776-89.

[278] Shahbazi MA, Fernandez TD, Mäkilä EM, Le Guevel X, Mayorga C, Kaasalainen MH, Salonen JJ, Hirvonen JT, Santos HA. Surface chemistry dependent immunostimulative potential of porous silicon nanoplatforms. Biomaterials 2014;35:9224-35.

[279] Cho NH, Cheong TC, Min JH, Wu JH, Lee SJ, Kim D, Yang JS, Kim S, Kim YK, Seong SY. A multifunctional core-shell nanoparticle for dendritic cell-based cancer immunotherapy. Nat Nanotechnol 2011;6:675-82.

[280] Dong C, Flavell RA. Cell fate decision: T-helper 1 and 2 subsets in immune responses. Arthritis Res 2000;2:179-88.

[281] Fuse S, Zhang W, Usherwood EJ. Control of memory CD8+ T cell differentiation by CD80/CD86-CD28 costimulation and restoration by IL-2 during the recall response. J Immunol 2008;180:1148-57.

[282] Shahinian A, Pfeffer K, Lee KP, Kundig TM, Kishihara K, Wakeham A, Kawai K, Ohashi PS, Thompson CB, Mak TW. Differential T cell costimulatory requirements in CD28-deficient mice. Science 1993;261:609-12.

[283] Steinman RM, Hemmi H. Dendritic cells: translating innate to adaptive immunity. Curr Top Microbiol Immunol 2006;311:17-58.

[284] Bhatia S, Edidin M, Almo SC, Nathenson SG. B7-1 and B7-2: similar costimulatory ligands with different biochemical, oligomeric and signaling properties. Immunol Lett 2006;104:70-5.

[285] Wolf SF, Lee K, Swiniarski H, O'Toole M, Sturmhoefel K. Cytokines and cancer immunotherapy. Immunol Invest 2000;29:143-6.

[286] Chen BA, Jin N, Wang J, Ding J, Gao C, Cheng J, Xia G, Gao F, Zhou Y, Chen Y, Zhou G, Li X, Zhang Y, Tang M, Wang X. The effect of magnetic nanoparticles of Fe(3)O(4) on immune function in normal ICR mice. Int J Nanomedicine 2010;5:593-9.

[287] Jurkic LM, Cepanec I, Pavelic SK, Pavelic K. Biological and therapeutic effects of ortho-silicic acid and some ortho-silicic acid-releasing compounds: New perspectives for therapy. Nutr Metab (Lond) 2013;10:2.

[288] Look M, Saltzman WM, Craft J, Fahmy TM. The nanomaterial-dependent modulation of dendritic cells and its potential influence on therapeutic immunosuppression in lupus. Biomaterials 2014;35:1089-95.

[289] Shahbazi MA, Shrestha N, Mäkilä E, Araújo F, Correia A, Ramos T, Sarmento B, Salonen J, Hirvonen J, Santos HA. A prospective cancer chemo-immunotherapy approach mediated by synergistic CD326 targeted porous silicon nanovectors. Nano Res.

[290] Weiner LM, Dhodapkar MV, Ferrone S. Monoclonal antibodies for cancer immunotherapy. Lancet 2009;373:1033-40.

[291] Iannello A, Ahmad A. Role of antibody-dependent cell-mediated cytotoxicity in the efficacy of therapeutic anti-cancer monoclonal antibodies. Cancer Metastasis Rev 2005;24:487-99.

[292] van Sorge NM, van der Pol WL, van de Winkel JG. FcgammaR polymorphisms: Implications for function, disease susceptibility and immunotherapy. Tissue Antigens 2003;61:189-202.

[293] Smith KA. Interleukin-2: inception, impact, and implications. Science 1988;240:1169-76.

[294] Strome SE, Sausville EA, Mann D. A mechanistic perspective of monoclonal antibodies in cancer therapy beyond target-related effects. Oncologist 2007;12:1084-95.

[295] Kawaguchi Y, Kono K, Mimura K, Sugai H, Akaike H, Fujii H. Cetuximab induce antibody-dependent cellular cytotoxicity against EGFR-expressing esophageal squamous cell carcinoma. Int J Cancer 2007;120:781-7.

[296] Kwon IK, Lee SC, Han B, Park K. Analysis on the current status of targeted drug delivery to tumors. J Control Release 2012;164:108-14.

[297] Shen J, Sun H, Meng Q, Yin Q, Zhang Z, Yu H, Li Y. Simultaneous Inhibition of Tumor Growth and Angiogenesis for Resistant Hepatocellular Carcinoma by Co-delivery of Sorafenib and Survivin Small Hairpin RNA. Mol Pharm 2014.

[298] El-Dakdouki MH, Pure E, Huang X. Development of drug loaded nanoparticles for tumor targeting. Part 1: Synthesis, characterization, and biological evaluation in 2D cell cultures. Nanoscale 2013;5:3895-903.

[299] Chan CL, Majzoub RN, Shirazi RS, Ewert KK, Chen YJ, Liang KS, Safinya CR. Endosomal escape and transfection efficiency of PEGylated cationic liposome-DNA complexes prepared with an acid-labile PEG-lipid. Biomaterials 2012;33:4928-35.

[300] Ke JH, Young TH. Multilayered polyplexes with the endosomal buffering polycation in the core and the cell uptake-favorable polycation in the outer layer for enhanced gene delivery. Biomaterials 2010;31:9366-72.

[301] Rennert R, Wespe C, Beck-Sickinger AG, Neundorf I. Developing novel hCT derived cell-penetrating peptides with improved metabolic stability. Biochim Biophys Acta 2006;1758:347-54.

[302] Haas AK, Maisel D, Adelmann J, von Schwerin C, Kahnt I, Brinkmann U. Human-protein-derived peptides for intracellular delivery of biomolecules. Biochem J 2012;442:583-93.

[303] Bhattacharyya S, Wang H, Ducheyne P. Polymer-coated mesoporous silica nanoparticles for the controlled release of macromolecules. Acta Biomater 2012;8:3429-35.

[304] Aggarwal P, Hall JB, McLeland CB, Dobrovolskaia MA, McNeil SE. Nanoparticle interaction with plasma proteins as it relates to particle biodistribution, biocompatibility and therapeutic efficacy. Adv Drug Deliv Rev 2009;61:428-37.

[305] Xie J, Xu C, Kohler N, Hou Y, Sun S. Controlled PEGylation of Monodisperse Fe3O4 Nanoparticles for Reduced Non-Specific Uptake by Macrophage Cells. Adv Mater 2007;19:3163-6.

[306] Xia T, Kovochich M, Liong M, Meng H, Kabehie S, George S, Zink JI, Nel AE. Polyethyleneimine coating enhances the cellular uptake of mesoporous silica nanoparticles and allows safe delivery of siRNA and DNA constructs. ACS Nano 2009;3:3273-86.

[307] Ayala V, Herrera AP, Latorre-Esteves M, Torres-Lugo M, Rinaldi C. Effect of surface charge on the colloidal stability and in vitro uptake of carboxymethyl dextran-coated iron oxide nanoparticles. J Nanopart Res 2013;15:1-14.

[308] French RA, Jacobson AR, Kim B, Isley SL, Penn RL, Baveye PC. Influence of ionic strength, pH, and cation valence on aggregation kinetics of titanium dioxide nanoparticles. Environ Sci Technol 2009;43:1354-9.

[309] Tu J, Wang T, Shi W, Wu G, Tian X, Wang Y, Ge D, Ren L. Multifunctional ZnPc-loaded mesoporous silica nanoparticles for enhancement of photodynamic therapy efficacy by endolysosomal escape. Biomaterials 2012;33:7903-14.

[310] Takemoto H, Miyata K, Hattori S, Ishii T, Suma T, Uchida S, Nishiyama N, Kataoka K. Acidic pH-responsive siRNA conjugate for reversible carrier stability and accelerated endosomal escape with reduced IFNalpha-associated immune response. Angew Chem Int Ed Engl 2013;52:6218-21.

[311] Rozema DB, Ekena K, Lewis DL, Loomis AG, Wolff JA. Endosomolysis by masking of a membrane-active agent (EMMA) for cytoplasmic release of macromolecules. Bioconjug Chem 2003;14:51-7.

[312] Ahmed M, Narain R. Cell line dependent uptake and transfection efficiencies of PEI-anionic glycopolymer systems. Biomaterials 2013;34:4368-76.

[313] Alexander C. Temperature- and pH-responsive smart polymers for gene delivery. Expert Opin Drug Deliv 2006;3:573-81.

[314] Shahbazi MA, Almeida PV, Mäkilä EM, Kaasalainen MH, Salonen JJ, Hirvonen JT, Santos HA. Augmented cellular trafficking and endosomal escape of porous silicon nanoparticles via zwitterionic bilayer polymer surface engineering. Biomaterials 2014;35:7488-500.

[315] Appelhans D, Komber H, Quadir MA, Richter S, Schwarz S, van der Vlist J, Aigner A, Muller M, Loos K, Seidel J, Arndt KF, Haag R, Voit B. Hyperbranched PEI with various oligosaccharide architectures: synthesis, characterization, ATP complexation, and cellular uptake properties. Biomacromolecules 2009;10:1114-24.

[316] Aravindan L, Bicknell KA, Brooks G, Khutoryanskiy VV, Williams AC. Effect of acyl chain length on transfection efficiency and toxicity of polyethylenimine. Int J Pharm 2009;378:201-10.

[317] Florea BI, Meaney C, Junginger HE, Borchard G. Transfection efficiency and toxicity of polyethylenimine in differentiated Calu-3 and nondifferentiated COS-1 cell cultures. AAPS PharmSci 2002;4:E12.

[318] Shahbazi MA, Almeida PV, Mäkilä E, Correia A, Ferreira MP, Kaasalainen M, Salonen J, Hirvonen J, Santos HA. Poly(methyl vinyl ether-alt-maleic acid)-functionalized porous silicon nanoparticles for enhanced stability and cellular internalization. Macromol Rapid Commun 2014;35:624-9.

[319] Shahbazi MA, Hamidi M. The impact of preparation parameters on typical attributes of chitosan-heparin nanohydrogels: particle size, loading efficiency, and drug release. Drug Dev Ind Pharm 2012.

[320] Shahbazi MA, Hamidi M, Mohammadi-Samani S. Preparation, optimization, and in-vitro/in-vivo/ex-vivo characterization of chitosan-heparin nanoparticles: drug-induced gelation. J Pharm Pharmacol 2013;65:1118-33.

[321] Barros S, Mencia N, Rodriguez L, Oleaga C, Santos C, Noe V, Ciudad CJ. The redox state of cytochrome c modulates resistance to methotrexate in human MCF7 breast cancer cells. PLoS One 2013;8:e63276.

[322] McInnes SJ, Irani Y, Williams KA, Voelcker NH. Controlled drug delivery from composites of nanostructured porous silicon and poly(L-lactide). Nanomedicine (Lond) 2012;7:995-1016.

[323] Tian H, Cronstein BN. Understanding the mechanisms of action of methotrexate: implications for the treatment of rheumatoid arthritis. Bull NYU Hosp Jt Dis 2007;65:168-73.

[324] Genestier L, Paillot R, Quemeneur L, Izeradjene K, Revillard JP. Mechanisms of action of methotrexate. Immunopharmacology 2000;47:247-57.